

# **Airborne Transmission of Influenza A Virus in Indoor Environments**

Wan Yang

Dissertation submitted to the faculty of the Virginia Polytechnic Institute and State University  
in partial fulfillment of the requirements for the degree of

**Doctor of Philosophy  
In  
Civil and Environmental Engineering**

*Committee*

Linsey C. Marr

John C. Little

Amy J. Pruden-Bagchi

Elankumaran Subbiah

March 30, 2012  
Blacksburg, Virginia

Keywords: influenza A virus; airborne transmission; relative humidity; size distribution;  
bioaerosol

Copyright © 2012 Wan Yang

# Airborne Transmission of Influenza A Virus in Indoor Environments

Wan Yang

## ABSTRACT

Despite formidable advances in virology and medicine in recent decades, we know remarkably little about the dynamics of the influenza virus in the environment during transmission between hosts. There is still controversy over the relative importance of various transmission routes, and the seasonality of influenza remains unexplained. This work focuses on developing new knowledge about influenza transmission via the airborne route and the virus' inter-host dynamics in droplets and aerosols.

We measured airborne concentrations of influenza A viruses (IAVs) and size distributions of their carrier aerosols in a health center, a daycare center, and airplanes. Results indicate that the majority of viruses are associated with aerosols smaller than 2.5  $\mu\text{m}$  and that concentrations are sufficient to induce infection.

We further modeled the fate and transport of IAV-laden droplets expelled from a cough into a room, as a function of relative humidity (RH) and droplet size. The model shows that airborne concentrations of infectious IAV vary with RH through its influence on virus inactivation and droplet size, which shrinks due to evaporation. IAVs associated with large droplets are removed mostly by settling, while those associated with aerosols smaller than 5  $\mu\text{m}$  are removed mainly by ventilation and inactivation.

To investigate the relationship between RH and influenza transmission further, we measured the viability of IAV in droplets at varying RHs. Results suggest that there exist three regimes defined by RH: physiological conditions ( $\sim 100\%$  RH) with high viability, concentrated conditions ( $\sim 50\%$  to  $\sim 99\%$  RH) with lower viability, and dry conditions ( $< \sim 50\%$  RH) with high viability. A droplet's extent of evaporation, which is determined by RH, affects solute concentrations in the droplet, and these appear to influence viability.

This research considerably advances the current understanding of the dynamics of the influenza virus while it is airborne and provides an explanation for influenza's seasonality. Increased influenza activity in winter in temperate regions could be due to greater potential

for IAV carrier aerosols to remain airborne and higher viability of IAV at low RH. In tropical regions, transmission could be enhanced due to better survival of IAV at extremely high RH.

## Acknowledgements

Along the way, I am indebted to a great number of people. Foremost, I would like to thank my advisor, Linsey, for being such a great advisor, mentor, and friend, for inspiring me to this research, for giving me great freedom to explore the topic, for having faith in me, for her guidance to the development of my career, and for her encouragement during my dull moments.

This work would not have been finished without the great support from my dissertation committee. I appreciate the time and efforts they have taken and I am grateful for their constructive advice that improved this work. Particularly, I must thank Dr. Pruden for allowing me to work in her lab, a great place to start with. My gratitude also goes to Dr. Subbiah who accommodated me in his lab, provided me with experimental training, and offered great inputs to this research.

Research is fun, in the meantime painful and sometimes even frustrating. My fellow lab-mates and friends shared my joys, and offered help or moral support when I was in trouble. I am grateful for being part of AirVT; the passion of each groupie for his/her research inspires me. I am particularly indebted to Dr. Sandeep Kumar, who trained me to do the cell experiments and has been such a great go-to person whenever I need help. I thank the fellows in Dr. Pruden's and Dr. Subbiah's labs, Yanjun, Hong, Krista, Mona, Dr. Wang, Jagadees, and others, for sharing lab space with me and for offering advice and help. I appreciate the technical assistance of Julie Petruska and Jody Smiley. A big thanks goes to Furong, my neighbor, for many rides to the lab on weekends. The completion of this work was also due in part to all of my dear friends here at Tech, without whose moral support I would not go this far.

Finally, my special thanks go to my beloved family, my parents and two sisters. My father always puts our education in the first place, and encourages us to pursue our passion. My mother takes good care of us all the time. My sisters' constant encouragement gets me through those stressful moments. My family is my ultimate strength: I know they are always there for me no matter where I am and what happen.

## Attributions

Dr. Linsey Marr (Department of Civil and Environmental Engineering, Virginia Tech) is the research advisor and committee chair. Dr. Marr is the co-author of Chapters 2, 3, and 4. She contributed to the experimental design, data analysis, and co-wrote the manuscripts. She also reviewed other parts of this dissertation. Additionally, Dr. Marr provided much of the financial support for the work presented in this dissertation through a National Science Foundation grant (CBET-0547107).

Dr. Elankumaran Subbiah (Department of Biomedical Sciences and Pathobiology, Virginia-Maryland Regional College of Veterinary Medicine, Virginia Tech) is on the dissertation committee. Dr. Subbiah is the co-author of Chapters 2 and 4. He provided lab space and partial financial support for this work, provided viruses and reagents, contributed to the experimental design, and commented on the manuscripts.

## Table of Contents

ABSTRACT.....	ii
Acknowledgements.....	1
Attributions.....	2
Table of Contents.....	3
List of Figures.....	7
List of Tables.....	9
Executive Summary.....	10
1 Introduction.....	18
1.1 Biological background of influenza viruses.....	19
1.1.1 Types of influenza viruses.....	19
1.1.2 Characteristics of influenza A virus: Morphology, viral structure, and genome structure.....	19
1.1.3 Detection methods.....	21
1.2 Transmission routes.....	21
1.2.1 Direct contact route.....	22
1.2.2 Indirect contact route.....	22
1.2.3 Droplet transmission.....	23
1.2.4 Airborne transmission.....	23
1.3 Influenza virus in the air.....	25
1.3.1 Size distribution and aerosol dynamics.....	25
1.3.2 Detecting IAV in air.....	26
1.4 Environmental factors affecting the transmission of influenza viruses.....	27
1.4.1 Temperature.....	27
1.4.2 Humidity.....	28
1.4.3 Solar radiation.....	29
1.5 Objectives.....	31
TABLES AND FIGURES.....	33
References.....	36

2	Concentrations and Size Distributions of Airborne Influenza A Viruses Measured Indoors at a Health Center, a Daycare, and on Aeroplanes .....	45
	Abstract .....	45
2.1	Introduction .....	46
2.2	Materials and methods.....	47
2.2.1	Reference Viruses .....	47
2.2.2	Detection of viral genome.....	47
2.2.3	Virus spike recovery experiments .....	50
2.2.4	Field sample collection .....	50
2.3	Results .....	52
2.3.1	qRT-PCR.....	52
2.3.2	Virus spike recovery experiments .....	52
2.3.3	Concentrations of airborne IAVs .....	52
2.3.4	Virus-laden particle size distribution .....	53
2.3.5	Indoor influenza virus emission and deposition flux by modeling.....	53
2.4	Discussion .....	54
2.4.1	IAV concentrations and size distributions in indoor facilities .....	54
2.4.2	Risk of airborne IAV infection.....	57
2.5	Conclusions .....	58
	TABLES AND FIGURES .....	60
	References .....	62
3	Dynamics of Airborne Influenza A Viruses Indoors and Dependence on Humidity .....	65
	Abstract .....	65
3.1	Introduction .....	67
3.2	Results .....	68
3.2.1	Initial size distribution of droplets expelled from a cough .....	68
3.2.2	Respiratory droplet size transformation.....	69
3.2.3	Inactivation of airborne IAVs.....	69
3.2.4	Evolution of infectious IAV distribution after a cough.....	69
3.2.5	Humidity dependency and removal mechanisms .....	71

3.3 Discussion .....	72
3.3.1 Removal of infectious IAVs .....	72
3.3.2 IAV viability, seasonality, and humidity dependency .....	73
3.3.3 Model limitations .....	75
3.4 Methods .....	76
3.4.1 Equations for generating the initial respiratory droplet size distributions .....	76
3.4.2 Model for calculating equilibrium respiratory droplet size .....	77
3.4.3 Virus inactivation rate .....	78
3.4.4 Concentration of infectious IAVs indoors .....	78
3.4.5 Removal efficiency of settling, ventilation, and inactivation .....	79
TABLES AND FIGURES .....	81
References .....	87
4 Relationship between Humidity and Influenza A Viability in Droplets and Implications for Influenza's Seasonality .....	91
Abstract .....	91
4.1 Introduction .....	93
4.2 Materials and Methods .....	94
4.2.1 Cells and Virus .....	94
4.2.2 Mucus specimen .....	94
4.2.3 Control of RH in a desiccator .....	94
4.2.4 Exposure of IAV in droplets to various RH .....	95
4.2.5 Calculation of viral decay .....	95
4.3 Results .....	96
4.3.1 IAV viability in model media v. RH .....	96
4.3.2 IAV viability in mucus v. RH .....	97
4.3.3 Relationship between viral decay and salt concentrations .....	97
4.3.4 Efflorescence .....	97
4.4 Discussion .....	98
4.4.1 Hypothesis to explain the relationship between RH and viability in laboratory studies .....	98

4.4.2	Explanation of discordant findings in literature.....	99
4.4.3	Implications for influenza's occurrence patterns .....	100
4.4.4	Limitation and directions for future study .....	101
4.5	Conclusions .....	102
TABLES AND FIGURES .....		103
Supplemental Material .....		105
References .....		107
5	Conclusions.....	111
5.1	Summary of results.....	111
5.2	Implications .....	112
5.3	Recommendations for future study .....	113
5.3.1	Expand the detection of airborne IAV in more inter-host environments .....	113
5.3.2	Simulate the dynamics of airborne IAV with multiple modeling techniques .....	114
5.3.3	Explore how RH affects IAV viability at the molecular level .....	114
5.3.4	Study the airborne transmission route for IAV holistically.....	115
References .....		117

## List of Figures

Figure 1.1 Transmission electron micrograph of influenza A virus, late passage. [Public domain] Source: Dr. Erskine Palmer, Centers for Disease Control and Prevention Public Health Image Library, image #280 .....	34
Figure 1.2 Structure of influenza A virus. [Fair use] Source: S.J. Flint, L.W. Enquist, V.R. Racaniello, and A.M. Skalka. Principles of virology: Molecular biology, pathogenesis, and control of animal viruses, 2 <sup>nd</sup> edition. pp 815 .....	34
Figure 1.3 Relationship between transmission rate and relative humidity (RH). Data adapted from Refs. [6-7] .....	35
Figure 2.1 Airborne IAV particle size distributions in each positive sample (yy/mm/dd and location shown at top). Aerosol samples were collected over 6-8 h in each location using a cascade impactor with cut-point diameters of 0.25, 0.5, 1.0, and 2.5 $\mu\text{m}$ . The y-axis indicates the percentage of total virus genome copies found in each size range. In seven of the eight cases, the majority of viruses were associated with fine particles smaller than 2.5 $\mu\text{m}$ , that can remain suspended for hours, but there were no obvious trends in size distributions across different samples.....	61
Figure 3.1 Log-probability plot of droplet size distribution from a cough, adapted from Duguid [20]. $D_i$ is the initial droplet size in $\mu\text{m}$ , and $z$ is the corresponding quantile of a normal distribution with the same cumulative probability.....	84
Figure 3.2 IAV inactivation rate versus RH. IAV inactivation rates ( $k$ ) for each RH over 1 h were calculated based on experimental data adapted from Harper [12]......	84
Figure 3.3 Evolution of infectious airborne IAV concentrations and size distributions. Time series of airborne, infectious IAV concentrations following a cough into residential (A) and public (B) settings at 10-90% RH. The horizontal dashed line indicates 99.9% removal. Evolution over time of airborne, infectious IAV size distribution following a cough into residential (C) and public (D) settings at 50% RH. ....	85
Figure 3.4 IAV size distributions. Infectious IAV size distributions at various RHs in residential (A) and public (B) settings with a volume of 50 $\text{m}^3$ and a height of 2.5 m, 10 min after a cough. ....	85

Figure 3.5 IAV removal mechanisms. Infectious IAV removal efficiencies due to settling, ventilation, and inactivation in residential (A) and public (B) settings at different RHs. Removal efficiency of settling, ventilation, and inactivation as a function of droplet size in residential (C) and public (D) settings at 50% RH. Removal efficiencies are shown for each mechanism independently and do not sum to 100% because in actuality, more than one mechanism may act on the same virus/droplet. ....86

Figure 4.1 Relationship between IAV viability and RH in (A) media with mainly salts, (B) media with salts plus proteins, and (C) mucus. Error bars denote standard deviations. .... 104

Figure 4.2 Viral decay over 3 h versus NaCl concentration in droplets consisting of four types of media. .... 104

Figure 4.3 Hypothesized relationship between IAV viability and RH in (A) droplets containing salts only and (B) droplets containing salts plus proteins. .... 104

Supplemental Material, Figure 4.1 Crystals of the four media: (A) PBS, (B) PBS+FCS, (C) DMEM, (D) DMEM+FCS. Light microscope, 100X magnified; scale bar = 20  $\mu\text{m}$ . .... 106

## List of Tables

Table 1.1 Impacts of temperature and relative humidity on influenza A virus <sup>a</sup> .....	33
Table 2.1 Primers and probes of influenza A virus .....	60
Table 2.2 Virus recovery efficiency from polytetrafluoroethylene (PTFE) filters and control solutions (virus solution in PBS and virus solution only) spiked with $2.4 \pm 0.1 \times 10^7$ genome copies. Samples were incubated for 2 h and then analyzed by qRT-PCR. Recovery efficiencies were significantly less than 100% with both filters. ....	60
Table 3.1 Prior studies of respiratory droplet size distributions .....	81
Table 3.2 Respiratory droplet size transformation .....	82
Table 3.3 Inactivation of airborne IAVs at 20-24.5 °C over 1 h .....	83
Table 4.1 Media used in studies of influenza A virus viability versus RH .....	103

## Executive Summary

Annual influenza epidemics in the US result in an average of 610,660 life-years lost, 3.1 million hospitalization days, and 31.4 million outpatient visits, for a total economic burden of \$87.1 billion per year [1]. Seasonal influenza is caused by the influenza A virus (IAV). The disease can be transmitted via contact (either directly or indirectly), large droplets at close range, or smaller aerosols. While the disease and the virus have been studied at length, the routes of transmission and their relative importance remain poorly understood. In particular, the significance of transmission by fine aerosols is still under debate [2-6].

Through studies involving various animal models including mice [7-8], ferrets [9-10], and guinea pigs [3; 11-12], aerosol transmission has been proven to be possible. Laboratory studies suggest that the aerosol route could be a very efficient pathway for spreading the virus [13] and that it could be dominant under certain circumstances [3; 5; 14-16]. However, direct proof of aerosol transmission between humans remains sparse. We know remarkably little about the airborne concentrations and inter-host dynamics of the influenza virus.

Influenza A has a clear seasonal pattern in temperate regions; incidence is high in winter and low in summer [17-18]. The underlying cause for this pattern remains controversial. The literature identifies numerous factors that may influence influenza's seasonality: environmental conditions such as temperature, humidity, and solar radiation; immune function; school schedules; and human mobility patterns and contact rates [19-21]. Among these, the leading contenders are humidity and temperature [11; 22-23], and in indoor environments, where people spend ~90% of their time, humidity is the more variable factor, as indoor temperature usually falls around 20°C.

Humidity has been found to be associated with the incidence of influenza; low wintertime humidity coincides with the surge of influenza in temperate regions [22; 24]. Laboratory studies indicating better survival of the influenza virus at low relative humidity (RH, <50%) [22; 25-27] further support the correlation between low humidity and high transmission rates. Nevertheless, the precise mechanisms by which humidity might influence IAV viability and transmissibility via the aerosol route have not been elucidated. In addition, the apparent increase in influenza activity in tropical regions during the rainy season when

humidity is maximal contradicts the perception that low humidity drives the surge of influenza [19].

These questions form the core of this dissertation work. We begin by reviewing current knowledge about the transmission routes and dynamics of influenza and the potential environmental factors that contribute to the spread of the virus in Chapter 1. We then identify the important questions that remain unsolved.

### **Distribution of airborne IAV in indoor environments (Chapter 2)**

In this chapter, we describe the concentrations of airborne IAVs and size distributions of their carrier aerosols in indoor environments. We collected aerosol samples in a health center, a daycare center, and onboard three cross-country flights. Half of the samples (8/16) were confirmed to contain IAV genomes. More than half of the IAV genomes were found to be associated with aerosols smaller than 2.5  $\mu\text{m}$  in diameter, which can remain suspended in air for hours. Concentrations of IAV in the positive samples ranged from 5800 to 37000 genome copies  $\text{m}^{-3}$  air. The inhalation dose of IAV at average concentrations over 1 h is estimated to be  $30 \pm 18$  median tissue culture infective dose ( $\text{TCID}_{50}$ ), a dose adequate to induce infection [13].

### **Dynamics of airborne influenza A virus indoors and dependence on humidity (Chapter 3)**

In this chapter, we present a model for assessing the fate and transport of airborne IAV. When released from the respiratory tract, where RH is 100%, droplets experience rapid evaporation and shrinkage upon encountering the ambient atmosphere. Evaporation is driven by the difference in vapor pressure between the droplet's surface and ambient air. Through application of a theoretically based model of droplet transformation, we infer that droplets shrink to 40-50% of their initial diameters at an indoor RH of 10-90%. We further incorporate these results with a physical mass balance model to track the evolution of IAV emitted from a cough into a room. The predicted concentration of infectious IAV in air is 2.4 times higher at 10% RH than at 90% RH after 10 min in a residential setting, and this ratio grows over time. We show that gravitational settling is important for removal of large droplets containing large amounts of IAV, while ventilation and inactivation are relatively more important for removal of IAV associated with aerosols smaller than 5  $\mu\text{m}$ . The inactivation rate increases linearly with RH; at the highest RH, inactivation can remove up to 28% of IAVs in 10 min.

Through this modeling work, we gain a mechanistic understanding of the aerosol transmission route. We show that humidity is an important variable in aerosol transmission of IAV because it can induce transformation in the size distribution of droplets through evaporation, and it can also affect the inactivation rate of IAV. Our results indicate that maintaining a high indoor RH and ventilation rate may help reduce the chances of IAV infection.

#### **Relationship between humidity and viability of influenza A virus in droplets and implications for influenza's seasonality (Chapter 4)**

In this chapter, we explore the relationship of RH and IAV viability and its implication for the seasonality of influenza. We measured the viability of IAV in droplets consisting of various model media, chosen to isolate the effects of different solutes found in respiratory fluid, as well as in human respiratory mucus, at RH ranging from 17% to 99%. Viability was highest when RH was either close to 100% or below the efflorescence RH (ERH) of the droplet (<~50%), the point at which salts crystallize and all water is lost. At ~50-84% RH, viability decreased with decreasing RH in droplets composed of saline solutions with no or negligible proteins and was minimal at an RH just above the ERH; in droplets supplemented with proteins, viability did not change with decreasing RH, probably due to protection provided by proteins. Additionally, viral decay was shown to increase linearly with salt concentration in saline solutions but not when they were supplemented with proteins. The relationship in mucus was similar to that in model media supplemented with proteins, but the change in viability with varying RH was more dramatic at ~50-84% RH.

Based on results shown in this chapter, we postulate that there are three regimes governing viability of IAV in droplets, defined by ambient RH: (1) physiological conditions (~99 to 100% RH), where solute concentrations remain at levels harmless to IAV and viability is maintained, (2) concentrated conditions (~50 to ~99% RH), where evaporation leads to elevated salt concentrations that may be harmful to the virus, and (3) dry conditions (<50% RH), where solutes crystallize, all water is lost, and IAV viability is maintained. This hypothesis is supported by results from our study and those reported in the literature [22; 25-27]. It provides a mechanistic explanation for the relationships observed in model media

and also sheds light on the interaction of IAV with its microenvironment during transmission between hosts.

Furthermore, these results could help explain transmission patterns of influenza. In temperate regions, wintertime heating reduces RH in the indoor environment to low levels, usually <40% [28-29]. At such an RH, vigorous evaporation of respiratory droplets not only helps preserve the viability of IAV emitted by infected hosts but also enables the resulting aerosols to remain aloft longer because of their smaller size and lower settling velocities [30]. Thus, transmission of influenza in temperate regions could be enhanced in winter primarily via the aerosol route. In tropical regions, high temperature may suppress transmission through the aerosol route [11; 31]. But during rainy seasons, temperatures are lower and RH is close to 100%. Under such conditions, droplets do not shrink as much, only to 93% of their original diameters at 99% RH, and 76% at 98% RH [30], and they would be removed more quickly from air by gravitational settling. However, submicron aerosols, such as those exhaled in human breath [32] would remain aloft, and thanks to the relatively lower temperature and suitable RH for survival, transmission by these aerosols might still be effective. In addition, the contact transmission route may be enhanced because it is insensitive to temperature [15; 31] and IAV is well preserved at ~100% RH, as shown in our study.

### **Conclusions and future work**

We conclude that the airborne route is important for the transmission of influenza and that its efficiency is regulated by humidity. Humidity mediates influenza transmission through effects on both the size distribution of virus carrier aerosols and the viability of IAV. There appear to be three regimes of IAV viability in droplets, defined by humidity: physiological conditions (~100% RH) with high viability, concentrated conditions (~50% to near 100% RH) with lower viability, and dry conditions (<~50% RH) with high viability. The relationship between IAV viability and RH could help explain influenza's seasonality and global transmission patterns.

Future studies should expand the database on influenza virus concentrations in the inter-host environment and pursue the mechanisms by which RH mediates IAV viability at a molecular level. Quantification of influenza virus concentrations in additional indoor settings, such as offices and residences and even outdoors, is needed to develop a more complete

understanding of the risk of airborne transmission. More sophisticated modeling methods such as computational fluid dynamics (CFD) could be applied to study the dynamics of airborne IAV. Additionally, future studies on airborne transmission need to take into account the interplay of the virus, the virus carrier aerosol (size and composition), environmental factors including but not limited to humidity, and the host's immunocompetence holistically.

## References

1. Molinari, N.-A. M., Ortega-Sanchez, I. R., Messonnier, M. L., Thompson, W. W., Wortley, P. M., Weintraub, E., et al. (2007). The annual impact of seasonal influenza in the US: Measuring disease burden and costs. *Vaccine*, *25*(27), 5086-5096.
2. Brankston, G., Gitterman, L., Hirji, Z., Lemieux, C., & Gardam, M. (2007). Transmission of influenza A in human beings. *Lancet Infect Dis*, *7*, 257-265.
3. Mubareka, S., Lowen, A. C., Steel, J., Coates, A. L., Garcia-Sastre, A., & Palese, P. (2009). Transmission of influenza virus via aerosols and fomites in the guinea pig model. *J. Infect. Dis.*, *199*(6), 858-865.
4. Spicknall, I. H., Koopman, J. S., Nicas, M., Pujol, J. M., Li, S., & Eisenberg, J. N. (2010). Informing optimal environmental influenza interventions: How the host, agent, and environment alter dominant routes of transmission. *PLoS Comput Biol*, *6*(10), e1000969.
5. Tellier, R. (2009). Aerosol transmission of influenza A virus: A review of new studies. *J. R. Soc. Interface*, *6*(suppl 6), S783-S790.
6. Nicas, M., & Jones, R. M. (2009). Relative contributions of four exposure pathways to influenza infection risk. *Risk Anal.*, *29*(9), 1292-1303.
7. Schulman, J. L., & Kilbourne, E. D. (1962). Airborne transmission of influenza virus infection in mice. *Nature*, *195*, 1129-1130.
8. Schulman, J. L. (1967). Experimental transmission of influenza virus infection in mice. Iv. Relationship of transmissibility of different strains of virus and recovery of airborne virus in the environment of infector mice. *J. Exp. Med.*, *125*(3), 479-488.
9. Gustin, K. M., Belser, J. A., Wadford, D. A., Pearce, M. B., Katz, J. M., Tumpey, T. M., et al. (2011). Influenza virus aerosol exposure and analytical system for ferrets. *Proc Natl Acad Sci USA*, *108*(20), 8432-8437.
10. Munster, V. J., de Wit, E., van den Brand, J. M. A., Herfst, S., Schrauwen, E. J. A., Bestebroer, T. M., et al. (2009). Pathogenesis and transmission of swine-origin 2009 A(H1N1) influenza virus in ferrets. *Science*, *325*(5939), 481-483.
11. Lowen, A. C., Mubareka, S., Steel, J., & Palese, P. (2007). Influenza virus transmission is dependent on relative humidity and temperature. *PLoS Pathog*, *3*(10), e151.

12. Lowen, A. C., Mubareka, S., Tumpey, T. M., Garc ía-Sastre, A., & Palese, P. (2006). The guinea pig as a transmission model for human influenza viruses. *Proc Natl Acad Sci USA*, *103*(26), 9988-9992.
13. Alford, R. H., Kasel, J. A., Gerone, P. J., & Knight, V. (1966). Human influenza resulting from aerosol inhalation. *Proc. Soc. Exp. Biol. Med.*, *122*(3), 800-804.
14. Atkinson, M. P., & Wein, L. M. (2008). Quantifying the routes of transmission for pandemic influenza. *Bulletin of Mathematical Biology*, *70*(3), 820-867.
15. Lowen, A., & Palese, P. (2009). Transmission of influenza virus in temperate zones is predominantly by aerosol, in the tropics by contact: A hypothesis. *PLoS Curr*, *1*, RRN1002.
16. Stilianakis, N. I., & Drossinos, Y. (2010). Dynamics of infectious disease transmission by inhalable respiratory droplets. *J. R. Soc. Interface*, *7*(50), 1355-1366.
17. Viboud, C., Bjrnsstad, O. N., Smith, D. L., Simonsen, L., Miller, M. A., & B.T, G. (2006). Synchrony, waves, and spatial hierarchies in the spread of influenza. *Science*, *312*(5772), 447-451.
18. Alonso, W. J., Viboud, C., Simonsen, L., Hirano, E. W., Daufenbach, L. Z., & Miller, M. A. (2007). Seasonality of influenza in Brazil: A traveling wave from the Amazon to the subtropics. *Am. J. Epidemiol.*, *165*(12), 1434-1442.
19. Tamerius, J., Nelson, M., Zhou, S., Viboud, C., Miller, M., & Alonso, W. (2011). Global influenza seasonality: Reconciling patterns across temperate and tropical regions. *Environ. Health Perspect.*, *119*(4), 439-445.
20. Lipsitch, M., & Viboud, C. (2009). Influenza seasonality: Lifting the fog. *Proc. Natl. Acad. Sci. U. S. A.*, *106*(10), 3645-3646.
21. Lofgren, E., Fefferman, N. H., Naumov, Y. N., Gorski, J., & Naumova, E. N. (2007). Influenza seasonality: Underlying causes and modeling theories. *J. Virol.*, *81*(11), 5429-5436.
22. Hemmes, J. H., Winkler, K. C., & Kool, S. M. (1960). Virus survival as a seasonal factor in influenza and poliomyelitis. *Nature*, *188*, 430-431.
23. Steel, J., Palese, P., & Lowen, A. C. (2011). Transmission of a 2009 pandemic influenza virus shows a sensitivity to temperature and humidity similar to that of an H3N2

- seasonal strain. *J. Virol.*, 85(3), 1400-1402.
24. Shaman, J., Pitzer, V. E., Viboud, C., Grenfell, B. T., & Lipsitch, M. (2010). Absolute humidity and the seasonal onset of influenza in the continental United States. *PLoS Biol*, 8(2), e1000316.
  25. Harper, G. J. (1961). Airborne micro-organisms: Survival tests with four viruses. *J Hyg*, 59, 479-486.
  26. Schaffer, F. L., Soergel, M. E., & Straube, D. C. (1976). Survival of airborne influenza virus: Effects of propagating host, relative humidity, and composition of spray fluids. *Arch. Virol*, 51(4), 263-273.
  27. Shechmeister, I. L. (1950). Studies on the experimental epidemiology of respiratory infections: III. Certain aspects of the behavior of type A influenza virus as an air-borne cloud. *J. Infect. Dis.*, 87(2), 128-132.
  28. Engvall, K., Wickman, P., & Norbäck, D. (2005). Sick building syndrome and perceived indoor environment in relation to energy saving by reduced ventilation flow during heating season: A 1 year intervention study in dwellings. *Indoor Air*, 15(2), 120-126.
  29. Yang, W., Elankumaran, S., & Marr, L. C. (2011). Concentrations and size distributions of airborne influenza A viruses measured indoors at a health centre, a day-care centre, and on aeroplanes. *J R Soc Interface*, 8(61), 1176-1184.
  30. Yang, W., & Marr, L. C. (2011). Dynamics of airborne influenza A viruses indoors and dependence on humidity. *PLoS ONE*, 6(6), e21481.
  31. Lowen, A. C., Steel, J., Mubareka, S., & Palese, P. (2008). High temperature (30 °C) blocks aerosol but not contact transmission of influenza virus. *J. Virol.*, 82(11), 5650-5652.
  32. Fabian, P., McDevitt, J. J., DeHaan, W. H., Fung, R. O. P., Cowling, B. J., Chan, K. H., et al. (2008). Influenza virus in human exhaled breath: An observational study. *PLoS ONE*, 3(7), e2691.

## 1 Introduction

Despite great advances in modern vaccination and medication, influenza and pneumonia are still among the ten leading causes of death, particularly among persons 65 years of age and over [1]. The CDC has estimated an average death count associated with seasonal influenza of around 30,000 per year over the period of 1976-2007 [2]. Also, it is estimated that annual influenza epidemics result in an average of 610,660 life-years lost, 3.1 million hospitalization days, 31.4 million outpatient visits, and a total economic burden of \$87.1 billion per year [3]. Gaining a better understanding of how the disease is transmitted is therefore paramount to the prevention of it.

Influenza is caused by infection with influenza viruses. The influenza A virus (IAV) was first isolated in 1933. Since then it has been intensively studied. The emerging highly pathogenic influenza virus strains such as avian A/H5N1 strain and the 2009 pandemic have triggered a new surge of interest in the transmission of influenza. Intriguing topics include its transmission routes [4-7], the relative importance of and factors influencing each route [8-10], the disease's transmission patterns around the world [11-14], the underlying cause for its seasonal oscillations in temperate regions [15-17], and modeling the transmission dynamics [18-21].

Four transmission modes for influenza have been identified, but the importance of any one mode versus another is still controversial. The four modes are (1) direct contact with an infected individual, (2) indirect contact via fomites that are contaminated with the virus, (3) inhalation of large droplets expelled by an infected individual and transported over a short distance, and (4) inhalation of small aerosols either directly expelled from infected individuals or left behind by evaporation of large droplets (i.e., droplet nuclei), also known as the aerosol mode. Two recent literature reviews on this subject reach completely different conclusions. Tellier [22] contends that aerosol transmission can be an important mode, based on studies on experimental influenza infection (by aerosol exposure in mouse and squirrel monkey models, and human volunteers) and epidemiological observations. However, another review by Brankston and colleagues [23] concludes that airborne transmission is unlikely to be of significance in most clinical settings. They argued that results from animal transmission

studies cannot be extrapolated to humans, and they also questioned the relevance of transmission experiments using artificially generated aerosols to natural infections.

Another interesting topic is influenza's global transmission pattern. In temperate regions, influenza incidence peaks in the winter across the world [11; 14; 24], while in tropical regions, high incidence has been observed during the rainy season [12; 25]. Possible driving forces for the disease's seasonality include humidity (either relative [6; 24] or absolute humidity [17]), temperature [7], solar radiation [26-27], human behaviors [14; 28], and seasonal fluctuation in host immunocompetence [29]. However, despite nearly a century of investigation, a clear mechanism for the disease's seasonal pattern remains lacking [13; 30-31].

## **1.1 Biological background of influenza viruses**

### **1.1.1 Types of influenza viruses**

There are three types of influenza viruses: A, B, and C. Influenza A viruses (IAV) can infect people, birds, pigs, horses, seals, whales, and other animals, with wild birds as their natural hosts. IAV can be further divided into subtypes based on its surface glycoproteins: hemagglutinin (HA) and neuraminidase (NA). Many different combinations of HA and NA proteins are possible. The subtypes that currently circulate in humans include H1N1, H1N2, and H3N2. Other subtypes are found mostly in other animal species. Influenza B viruses are normally found only in humans; they can cause human epidemics, but have never caused pandemics. Influenza C viruses cause mild illness in humans and pigs and do not cause epidemics or pandemics. In this study, we focus on IAV that can cause widespread seasonal infections and pandemics.

### **1.1.2 Characteristics of influenza A virus: Morphology, viral structure, and genome structure**

IAV is an enveloped virus with eight segmented RNA strands. The virion (i.e., the infectious virus particle) is roughly spherical with a diameter of 80-120 nm (Figure 1.1). The structure of IAV is shown schematically in Figure 1.2.

The virus envelope is a lipid membrane derived from the host cell; thus, it is similar to the membrane of the host cell or cellular compartment. Consequently, the virus envelope may differ depending on its host species (e.g., human, chicken, horse, etc.), which may partly

account for the variation in survival for viruses of different origins [32]. Furthermore, the envelope may be a major determinant for a virus' survival capability. A broad generalization is that enveloped viruses are less stable in the environment than non-enveloped ones and they survive better at lower relative humidity [33].

Three important proteins, HA, NA, and M2 are embedded in the envelope. HA is the protein that facilitates the attachment of the virion onto a cell, which is critical for its entry to the host cell. NA is an enzyme that can cleave the receptor on the cell (sialic acid) and subsequently release viral progeny from the cell and allow for their spread to new cells or new hosts. Consequently, HA and NA are important for the immune response against the virus; antibodies against these two proteins may protect against infection. The NA protein is the target of the antiviral drugs, Relenza and Tamiflu [34-35]. The M2 protein is an ion channel that can actively pump protons from the endosome into the interior of the virion, which in turn lowers the pH in the interior of the virion. Low pH (<5) is necessary for the fusion of the virus into the cell. The antivirals amantadine and rimantadine function by blocking the M2 ion channel [36-38]. Therefore, any factor that can damage HA, NA, and/or M2 can compromise the infectivity of the virus. The questions are which factors in the environment are capable of this and how.

The envelope and its three integral membrane proteins HA, NA, and M2 overlay a matrix of M1 protein (Figure 1.2). The M1 protein confers the rigidity of the envelope and greatly determines the morphology of the virion. It is also noteworthy that the gene coding this protein is very conservative despite the constant mutation in other genes. Thus, the M1 gene is commonly used as a target in polymerase chain reaction (PCR) techniques.

The IAV genome comprises eight segmented negative-sense RNA, which means that the polarity of these RNAs is the opposite that of the messenger RNA (mRNA) and thus they cannot replicate directly. Negative-sense RNA is usually associated with nucleoprotein and organized into a nucleocapsid, which is very stable and resistant to RNases, enzymes that destroy RNAs [39]. This to some extent explains why the viral genome usually persists longer than its infectivity. The nature of a segmented RNA genome makes it possible to exchange entire RNA molecules between different strains, i.e., reassortment. In cells co-infected with two different influenza virus strains (for instance, in a pig), the eight genome

segments of each virus replicate, and when new progeny viruses are assembled, they can pack RNA segments from either parental virus, which is a common way of producing new subtypes. The novel 2009 A/H1N1 virus may have been generated in this way [40].

### **1.1.3 Detection methods**

Many methods are available for detecting influenza viruses. Some methods detect the virion by observing replication of the virus in an appropriate host, such as cells, embryonated eggs, or animals. Commonly used methods include plaque assay and end-point dilution assay. Plaque assay measures virus titer, or the concentration of the virus in a sample, by visualization of plaque forming units (PFU). The end-point dilution assay measures cytopathogenic effects (CPE) caused by infection of serial virus dilutions and expresses the titer as 50% infective dose ( $ID_{50}$ ), or 50% tissue culture infective dose ( $TCID_{50}$ ) per mL. These methods can determine the infectivity of IAV, but they usually take a long time (3-7 days), require well trained personnel, and demand special laboratories and equipment.

Electron microscopy (EM) can be used to obtain direct images of virus particles, and if a sample contains only one type of virus, the number of virus particles can be counted under EM by comparison to a known concentration of latex beads mixed with the sample. Detection by EM is fast, but it cannot discriminate between active and inactive viruses, and EM is still prohibitively expensive and time-consuming for routine application.

The HA glycoprotein can bind to N-acetylneuraminic acid-containing glycoproteins on red blood cells and cause them to aggregate and form a visible lattice. This property can be utilized to detect influenza viruses. Such methods include hemagglutination assay and hemagglutination inhibition assay (HI). These methods are rapid (about 30 min) and semi-quantitative, but are not sufficiently sensitive to detect samples with low virus titers.

Reverse transcriptase-polymerase chain reaction (RT-PCR) has been universally used for detecting influenza viruses. It is sensitive, rapid, and relatively inexpensive. In addition, quantitative RT-PCR (qRT-PCR) can readily quantify the number of genome copies in a sample. However, RT-PCR does not provide information on the viability of the virus.

## **1.2 Transmission routes**

The influenza virus may be transmitted among humans through four pathways: (1) direct contact, (2) indirect contact, (3) large droplet, and (4) aerosols. The contribution of each

mode to the overall transmission of influenza remains unknown.

### **1.2.1 Direct contact route**

Direct contact transmission occurs via direct physical contact between infected and susceptible individuals. People can contract influenza when they come in contact with the secretions of a sick person and then inoculate themselves by touching their mouth, nose or eyes. Cunney and colleagues [41] reported an outbreak of influenza A in a neonatal intensive care unit and identified pregnancy with twins as an independent risk factor for the outbreak. They attributed the increase in infection among twins to transmission facilitated by parental contact. It was suspected that parents of twins were likely to handle both siblings during a single visit to the unit and might fail to wash their hands or change gowns between contacts with each child.

### **1.2.2 Indirect contact route**

For the indirect contact route, transmission occurs by the passive transfer of virus to a susceptible host from contaminated surfaces or objects. Such contaminated objects are termed fomites. An investigation of an influenza outbreak [42] in a nursing home reported an association of higher attack rates in bedfast patients (5 out of 11 bedfast (45%) versus 6 out of 28 other patients (21%),  $p=0.10$ ) and in tube-fed or frequently suctioned patients (9 out of 24 tube-fed (38%) versus 2 out of 15 other residents (13%),  $p=0.08$ ), as well as clustered onsets in four patients without other opportunities for exposure to a common source. Retracing the evolution of the outbreak showed that designated medication or tube feeding nurses (confirmed to be naïve) went from resident to resident, routinely having ungloved contact with oral secretions in patient-to-patient sequences. The nurses' activities were consistent with the transmission patterns and probably the case cluster. This evidence suggested the outbreak might be mediated by staff via either contaminated hands or fomites.

Studies on the survival of influenza virus on fomites also support the premise of this transmission route. Bean et al. [43] studied the survival of influenza A and influenza B viruses on various surfaces and found that both viruses survived for 24-48 h on hard, nonporous surfaces such as stainless steel and plastic, and for <8-12 h on cloth, paper, and tissues. They also found that influenza virus could survive on hands for up to 5 min after transfer from the environmental surfaces. A recent study by Thomas et al. [44] showed that

IAV could survive up to 3 days on a banknote when inoculated at high concentrations, and the virus could persist longer in the presence of respiratory mucus (up to 17 days). Boone and Gerba [45] detected influenza virus on over 50% of the fomites tested in homes and day care centers during an influenza season. Another recent experiment [46] used human subjects to study the transmission between experimentally infected volunteers (donors) and naive individuals (recipients); they tested surfaces in the environment of the donors and 19% (9 out of 48 samples) were confirmed to contain influenza virus RNA. Infection can occur when fomites contact mucous membranes of our mouth, nose, or eyes.

### **1.2.3 Droplet transmission**

Droplet-mediated transmission occurs via large droplets (many authors adopt a minimum size cut-off of 5  $\mu\text{m}$ ) generated from the respiratory tract of infected individuals during coughing, sneezing, or talking. Due to their relatively larger sizes, these droplets would settle to the ground quickly after being expelled. Thereby they can only cause infection in hosts in close vicinity by depositing on their nasal or oral mucosa. A rule of thumb is that they can travel up to 1 m, or 3 feet [47], horizontally before settling down. A retrospective cohort investigation [48] identified large droplets as the cause for an outbreak within a tour group during the 2009 pandemic. Thirty percent of the tour group (9 out of 30) contracted the pandemic influenza after sharing a 1-h flight with the index case-patient. Investigation showed that all the patients had talked with the index case-patient (not a member of the tour group), who sat within two rows of them, while none of the members who had not talked with the index case-patient became ill.

### **1.2.4 Airborne transmission**

Airborne transmission, or aerosol transmission, occurs via virus-laden aerosols, usually considered to be smaller than 5  $\mu\text{m}$  [47]. As aforementioned, this mode of transmission is still a subject of debate, as direct proof of airborne transmission between humans remains sparse. Most studies on aerosol transmission were conducted with animal models, such as mice [49-50], ferrets [51-52], and guinea pigs [6; 53]. Lowen et al. [53] used a guinea pig model to show that influenza virus can be transmitted from infected guinea pigs to naive ones housed in different cages placed 91 cm away, indicating airborne transmission.

The Alaska Airlines outbreak [15] has often been presented as evidence of airborne

influenza transmission [16]: a jet with 54 persons aboard was delayed on the ground for 3 h (during which the airplane ventilation system was inoperative), and 72 per cent of the passengers who stayed on the airplane were infected by a passenger sick with influenza within 72 h. Opponents, on the other hand, contended that close-range transmission via large droplets or direct contact is more likely since passengers were not confined during the outbreak and malfunction of the ventilation system would restrict effective airborne transmission [4].

A laboratory study in human volunteers showed that inhalation of aerosolized influenza virus strain A2 at a dose as low as 1 TCID<sub>50</sub> resulted in infection with typical clinical symptoms of influenza [54]. The diameters of the aerosols were 1–3 µm. A particularly interesting finding of this study is, as pointed out by the authors, that much lower doses of virus were sufficient to produce typical clinical influenza when administered by the aerosol route than by nasopharyngeal inoculation (80,000-180,000 TCID<sub>50</sub>). This suggests that the aerosol route could be a very effective pathway for spreading the virus.

Another interesting study conducted by Dick and colleagues [55] on rhinovirus transmission affords some clue for the airborne route of influenza virus. The study examined transmission of rhinovirus type 16 via aerosols (loosely including both large and small droplets), direct contact, or indirect contact between human volunteers. Laboratory-infected men (donors) and susceptible men (recipients) were asked to play cards together for 12 h. Half of the recipient group were restrained from touching their faces so that the virus could only be transmitted through aerosols, while the other half were unrestrained so that transmission could occur through any one of the three routes. In three experiments, the infection rate of restrained recipients was 56% (10 out of 18), compared to 67% for the unrestrained recipients (12 of 18); these two rates were not significantly different. Although this study involved rhinovirus rather than influenza virus and differences may exist between the two, it clearly demonstrates that aerosols are capable of transmitting virus.

However, it should be pointed out that the 5-µm size cut-off is somewhat arbitrary [22]. There is no exact particle size cut-off at which pathogen transmission changes from exclusively large droplet to airborne, or vice versa. It is also important to distinguish between the initial size and the final size following water evaporation when studying bioaerosols

generated by human subjects. Droplets can shrink within seconds after release into the ambient air, resulting in what are termed droplet nuclei with only around half of their original diameter [56]. This will be further discussed in Chapter 3.

### **1.3 Influenza virus in the air**

#### **1.3.1 Size distribution and aerosol dynamics**

Influenza virus can be emitted from infected individuals when they cough, sneeze, talk, and breathe [57-58]. The virus is associated with droplets of various sizes. The size distribution of droplets expelled varies greatly depending on the origin of emission (mouth versus nose), the activity leading to emission (coughing, sneezing, talking, or breathing), and individuals' biological and physical characteristics (age, gender, body weight, etc.) [59]. Thus, the geometric size, size range, and droplet number could vary greatly. Droplets emitted from coughs are generally larger, ranging from 1 to 2000  $\mu\text{m}$  in diameter, with geometric means ranging from 0.5 to 97  $\mu\text{m}$ , depending on the study; the number of droplets emitted is in the hundreds to thousands, much less than that from sneezing [59-65]. A sneeze can generate up to one million droplets, and they tend to be smaller (95% of them less than 100  $\mu\text{m}$  in diameter) [65]. Speaking emits droplets of size similar to those from coughing [62; 64-65]. Droplets in exhaled breath are mostly less than 5  $\mu\text{m}$ , and about 87% of them are less than 1  $\mu\text{m}$  [57]. These studies are reviewed and summarized in Table 3.1 in Chapter 3.

When released from the respiratory tract, where relative humidity (RH) is 100%, droplets experience rapid evaporation and shrinkage upon encountering the ambient atmosphere. Evaporation is driven by the difference in vapor pressure between the droplet's surface and ambient air. As the droplet shrinks, the decreasing radius of curvature causes an increase in its vapor pressure, while the competing effect of rising solute concentrations in the droplet causes a reduction in its vapor pressure. Evaporation ceases when the vapor pressure at the droplet surface equals that of ambient air (i.e., humidity). Thus, humidity controls the extent of droplet evaporation.

Another factor governing the final size of a droplet is the composition of the droplet. Respiratory fluid is a complex combination of water (~95%), inorganic salts (~1%), and various glycoproteins and lipids [66-68]. These solutes altogether affect the vapor pressure at the droplet's surface. Various models have been developed to estimate the final size of a

droplet. Some models simply used saline solutions (e.g., NaCl solution) to simulate respiratory droplets [62; 69]. More complicated models have taken into account both composition and ambient humidity [56; 70-71]. Results of these models consistently indicate that droplets emitted from the human respiratory tract would shrink by around half after release. This process is completed within 1 second for small droplets ( $<20\ \mu\text{m}$ ) [56]. We estimated the size transformation of respiratory droplets at different RH conditions in Chapter 3.

The final size of a droplet is important, as it largely determines the droplet's physical behavior (settling velocity, diffusion, penetration into airways, etc.) in the air and thus the fate and transport of airborne IAV. First of all, the size of droplet determines whether a virus-laden droplet will remain suspended in air long enough to be inhaled, and where within the respiratory system it will deposit. In aerosol science, Stokes' law indicates that the settling velocity of a droplet scales with its diameter squared; thus the smaller the droplet, the much longer it can remain suspended. A droplet  $1\ \mu\text{m}$  in diameter can remain aloft for hours while one  $10\ \mu\text{m}$  in diameter falls to the ground within minutes. Secondly, the ability of a droplet to penetrate and deposit in different regions within the respiratory system varies with its size [72-73]. It can be shown through model calculations that droplets  $6.1\ \mu\text{m}$ ,  $2.7\ \mu\text{m}$ ,  $1.4\ \mu\text{m}$ , and  $4.7\ \mu\text{m}$  in diameter are the ones that deposit most efficiently in the head airways (87.4%), the tracheobronchial region (6.1%), the alveolar region (12.8%), and the whole respiratory tract (94.8%), respectively [72]. Finally, it is still unclear which part of the respiratory system is the most susceptible target for influenza infection. Thus, it is possible that droplet size influences the efficiency of aerosol transmission not only through affecting the number of airborne viruses, but also through controlling the efficiency of initiating an infection at the most susceptible region within the respiratory system. Such influences are worth investigating in depth.

### **1.3.2 Detecting IAV in air**

Although methods including those mentioned in section 1.1.3 are available for clinical and laboratory samples, the detection of IAV in the air remains challenging. When virus-laden aerosols are released from infected hosts, they are quickly diluted by ambient air to extremely low concentrations [74]. Additional challenges come from the potential inactivation during

the aerosol sampling process, and inhibition of detection methods by airborne contaminants [75-76]. Consequently, there are still very few measurements of influenza viruses in the air. Even fewer have determined the size of influenza virus-laden particles.

Most studies are based on qRT-PCR. Blachere et al. (2009) [77] measured airborne influenza viruses in a health center; the concentrations ranged from 460 to 16,278 TCID<sub>50</sub>-equivalent RNA particles for an entire sample, and over 50% of the total genome copies were detected in droplets smaller than 4  $\mu\text{m}$ . Lindsley et al. [78], in a more detailed study in the same clinic, detected  $1.2 \pm 4.4$  pg RNA  $\text{m}^{-3}$  in examination rooms,  $1.1 \pm 3.0$  pg RNA  $\text{m}^{-3}$  in procedure rooms, and  $0.3 \pm 4.3$  pg RNA  $\text{m}^{-3}$  in a waiting room. Another study by Chen et al. [79] detected IAV from ambient air in open fields; the concentrations were thus much lower than detected indoors, only up to hundreds of genome copies per  $\text{m}^3$  in positive samples; and the study related the increase in IAV concentrations to long-distance transport of dust storms from Asia.

In this dissertation work, we measured concentrations of IAVs and size distributions of their carrier aerosols in a health center, a daycare center, and onboard aircraft [80]. Results are presented in Chapter 2.

#### **1.4 Environmental factors affecting the transmission of influenza viruses**

In the 6<sup>th</sup> International Symposium on Aerobiology (Netherlands, 1973), an aerovirologist compared the investigation of virus transmission to investigating the death of a rabbit who happened to run by an apple tree and get hit by a falling apple. The aerovirologist then remarked that it is impossible to figure out how an individual virus hits an individual host, but hopefully we could find out the odds that it could happen [81]. Probably with the same hope, researchers have been trying to find out the potential environmental factors that could impact the transmission of influenza virus and possibly induce the disease's seasonal oscillation. Possible environmental factors that have been identified include temperature, humidity, solar radiation, and air pollutants such as nitrogen oxides and ozone [33; 82].

##### **1.4.1 Temperature**

Most viruses are sensitive to temperature; viruses usually can survive for hours at 37  $^{\circ}\text{C}$ , for days at 4  $^{\circ}\text{C}$ , and for months to years at below -70  $^{\circ}\text{C}$ . Studies on influenza viruses indicate a similar pattern [83-84]. Harper [85] conducted intensive experiments on the impacts of

temperature and relative humidity (RH) using the PR8 strain, in which three temperature levels (7-8 °C, 20.5-24 °C, and 32 °C, respectively) and three RH levels (20-25%, 49-51%, and 81-82%, respectively) were tested. Table 1.1 shows the decay rates, indicated by “slope,” calculated on the basis of his results. The analysis shows that IAV favors lower temperature and that the adverse effect of high temperature escalates with increasing RH. Other studies on the influence of temperature report consistent results: higher viability and higher transmission rates at lower temperature (5-30 °C) [6].

It should be noted that (1) some of these experiments were done with influenza viruses of various origins (e.g., mouse, swine) besides human, and (2) even when human strains were used, they were propagated in embryonated eggs or different types of animal tissue cells. Therefore, these experiments have certain limitations. One question is whether human strains can replicate with similar efficiency in cell cultures. Under- or over- estimation could ensue due to variability in the efficiency of a strain to replicate in a certain host [86]. Another uncertainty lies in whether laboratory-propagated strains behave similarly to human strains under natural conditions. A study by Mitchell and Guerin [32] compared the survival of human, avian, swine, and equine IAVs in aerosols. It was found that equine and avian strains survived much longer in the airborne state (24-36 h) than did human strains (9-18 h); these results indicate that IAV’s survival varies depending on its origins. Body temperatures of animals differ from species to species: 42 °C for chickens, 38 °C for horses, 39.0 °C for pigs, and 39.8 °C for piglets. Assuming the original host body temperature is optimal for the corresponding influenza virus strain, then, would strains that originally infect hosts with higher body temperatures be more resistant to higher temperatures, and thus be able to survive longer? Another problem is that, as the virus’s envelope is taken from the host cells, properties of the envelope may vary with its host, leading to possible alteration of response to environmental factors such as temperature and humidity. Whether these differences will affect the experimental results necessitates further investigation.

#### **1.4.2 Humidity**

Humidity has been found to be associated with the incidence of influenza A [16; 87-88]. The surge in influenza epidemics in temperate populations is usually observed in winter, when humidity is lower [21; 88-89]. This connection is further supported by laboratory studies

indicating that the virus survives better under low-RH conditions [24; 85-86; 90].

RH is defined as the actual water vapor pressure over the saturation vapor pressure of the air. Using a guinea pig model, Lowen et al. [6-7] demonstrated that airborne IAV transmission was dependent on RH and temperature and that higher temperature (30 °C) blocked airborne transmission (Figure 1.3c). Based on their data, the airborne transmission rate can be shown to be inversely correlated to RH at a given temperature ( $p=0.0020$  at 5 °C and 0.0168 at 20 °C, Figure 1.3a & b). In indoor environments, where people spend ~90% of their time, temperature falls in a narrow range around 20 °C. RH thus is expected to be a controlling factor in the disease's transmission, as shown in Figure 1.3b.

Using data reported by Harper [85], we calculated inactivation rates for IAV at room temperature to be 0.0031-0.028  $\log_{10} \text{ min}^{-1}$  at 20-81% RH, with higher inactivation rate at higher RH [91]. Hemmes [24], similarly reported  $0.0073 \pm 0.0031 \log_{10} \text{ min}^{-1}$  at 15-40% RH and  $0.091 \pm 0.024 \log_{10} \text{ min}^{-1}$  at 50-90% RH. These two studies both showed a monotonic relationship between IAV viability and RH. In contrast, studies by Shechmeister [90] and Schaffer et al. [86] found a bimodal relationship, showing higher inactivation rates at medium but not high RHs. Thus laboratory studies on the relationship with RH were discordant at medium and high RH (~50% to ~90%), and reasons for the disagreement remain unclear [13].

Two additional questions remain unanswered. Firstly, increasing evidence indicates that influenza incidence is higher during the rainy season in tropical regions [12; 25; 92]. If the virus is unstable under higher-RH conditions as shown in previous studies [24; 85-86; 90], then how would influenza incidence increase when RH is maximal? Secondly, it is still unclear how ambient RH affects a virus encased in an airborne respiratory droplet [17]. These questions will be explored in Chapter 4.

### **1.4.3 Solar radiation**

Effects of solar radiation on the transmission of influenza may due to two aspects: the survival of the influenza virus and the susceptibility of the human host.

Ultraviolet (UV) radiation, especially UVB (medium wave, 280–315 nm) and UVC (short wave, 100–280 nm), has been recognized as a potent virucidal factor, mainly by inducing formation of pyrimidine dimers and consequently damage to DNA/RNA. A UV

lamp that can generate wavelengths around 254 nm is commonly used to disinfect ambient air in many places, such as hospitals and food factories. However, is the natural solar radiation reaching the earth's surface (98.7% is blocked by the ozone layer) strong enough to effectively kill influenza virus in the air, considering that its power is much less than that of a UV lamp? And, if the solar radiation is indeed capable of killing the virus, is its seasonal fluctuation the leading factor for the disease's seasonality?

Sagripanti and Lytle [26] estimated the intensity of solar UV and calculated its inactivation effect on IAV in several cities located in mid-latitude regions (25.8°N–47.6°N) during different times of the year. The inactivation rates were reported to be 3.8–7.5  $\log_{10} \text{d}^{-1}$  (summer), 0.9–5.0  $\log_{10} \text{d}^{-1}$  (spring), 1.6–6.1  $\log_{10} \text{d}^{-1}$  (fall), and 0.1–1.9  $\log_{10} \text{d}^{-1}$  (winter) for four seasons, respectively. Apparently, there is a seasonal variation with the weakest intensity in winter coincident with the peak of influenza incidence. The authors thereby concluded that solar UV radiation has a far stronger effect than RH or temperature on the inactivation of IAV in the environment and that inactivation by solar UV radiation plays a role in the disease's seasonality. However, their conclusion seems to be based on an erroneous reading of the data provided in Hemmes et al. [24], as pointed out by Weber and Stilianakis [93]. Hemmes et al. reported inactivation rates of influenza virus at  $0.091 \pm 0.024 \log_{10} \text{min}^{-1}$  (i.e.,  $131.04 \pm 34.56 \log_{10} \text{d}^{-1}$ ) at 50-90% RH and  $0.0073 \pm 0.0031 \log_{10} \text{min}^{-1}$  (i.e.,  $10.50 \pm 4.46 \log_{10} \text{d}^{-1}$ ) at 15-40% RH. The variation in inactivation between high and low RH is up to 12.5 fold, which is already calculated on a logarithmic base. Yet Sagripanti and Lytle [26] applied a logarithmic transformation to the 12.5-fold variation again and claimed that it only corresponded to 1.1  $\log_{10}$ , and they seemed to mistake the units for inactivation rate as  $\log_{10} \text{d}^{-1}$ . Therefore, upon reconsideration of the effects of solar UV radiation and RH, the influence of solar UV radiation on IAV inactivation appears relatively trivial.

Another impact of solar radiation may lie in its ability to moderate human immunity. Cannell et al. [29; 94] hypothesized that seasonal changes in UVB intensity induce fluctuations in vitamin D levels in human body, a powerful innate immunity stimulus which in turn regulates the innate immunity and hence the human susceptibility to the influenza virus. They cited a study by Hyppönen and Power [95] which demonstrates a seasonal fluctuation in vitamin D levels with a winter trough. Since humans obtain most vitamin D

from sun exposure rather than diet, such an oscillation is probably triggered by seasonal variations in solar radiation. In addition, they referred to data provided by a post-hoc analysis of questionnaire responses gathered from a 3-year randomized controlled trial [96] to show that vitamin D has a significant effect on influenza incidence. Aloia et al. [96-97] conducted the experiment aimed initially to test the influence of vitamin D<sub>3</sub> on bone loss. In the experiment, 208 post-menopausal African American women were equally divided to two groups (placebo-controlled group and vitamin D group) to receive either a placebo or vitamin D<sub>3</sub> (20 µg d<sup>-1</sup> in the first two years and 50 µg d<sup>-1</sup> in the third year). In the post-hoc analysis, they found that only 8 patients in the vitamin D group reported getting a cold or influenza, in comparison to 26 in the placebo group. The placebo group had cold or influenza symptoms mostly in the winter, while the vitamin D group had symptoms throughout the year when they were given vitamin D<sub>3</sub> at a dose of 20 µg d<sup>-1</sup>. Only one subject had a cold or influenza when they were given vitamin D<sub>3</sub> at a dose of 50 µg d<sup>-1</sup>. Although this experiment appears to directly prove the effect of vitamin D on influenza contraction, it should be noted that there are several pitfalls of these data. (1) Since it was not designed specifically for investigating the effect of vitamin D on influenza infection, the data on viral upper respiratory infection (URI) symptoms were collected in an insensitive and imprecise way, as pointed out by the authors [97]. Only 39 reports of viral URI symptoms were collected in the 3-year trial, which is much less than expected. (2) The participants were interviewed every 6 months, and whether they had a flu or cold was only inquired after they responded negatively to the question “Have you been well?” Judging from the long time span, indirect inquiry, and relatively high age of the participants (50~75 years old), it is highly possible that they did not consider having a flu or cold as not “being well” or simply forgot they had a flu or cold. (3) This experiment focused on black women with ages ranging from 50 to 75 years, which is clearly race and age biased. Whether this effect, if there is one, would apply to other race and age groups warrants further investigation.

### **1.5 Objectives**

The previous sections review the current knowledge on the transmission of IAV, as well as questions that remain unclear. The ones of particular interest to this dissertation work are: (1) the prevalence of IAV in air; (2) the dynamics of IAV in the indoor environment during

transmission between hosts; (3) potential environmental effectors in the airborne transmission of IAV and their governing mechanisms. The overall objective of this work is to investigate the feasibility and mechanisms of the airborne transmission of influenza A in indoor environments. Specific research objectives are to:

1) Measure the concentrations of airborne IAVs and size distributions of their carrier aerosols in public places with high risk of transmission, such as hospitals and daycare facilities, to investigate the feasibility of airborne transmission of influenza A in these indoor environments;

2) Model the fate and transport of the IAV carrier aerosols in indoor environments to study the dynamics of IAV and determine what factors affect its transmission;

3) Quantify the variation of IAV viability with RH and concentrations of solutes in the droplet to study the mechanisms by which humidity affects the transmission of IAV.

## TABLES AND FIGURES

**Table 1.1 Impacts of temperature and relative humidity on influenza A virus<sup>a</sup>**

RH (%)	Temp. (°C)	Percentage viable at given times (h)							Statistics		
		0	1/12	1/2	1	4	6	23	Correlation coeff <sup>c</sup>	Slope (%h <sup>-1</sup> ) <sup>d</sup>	Intercept <sup>e</sup>
	7-8	88	87	80	78	68	63	61	-0.76	-1.01	79.99
20-25	20.5-24.0	75	77	65	64	74	66	22	-0.94	-2.16	73.95
	32	87	70	56	45	18	17	1.3	-0.75	-2.85	56.11
	7-8	66	49	75	61	39	42	19	-0.84	-1.91	59.59
49-51	20.5-24.0	84	62	49	29	6.4	4.2	- <sup>b</sup>	-0.87	-11.11	60.56
	32	98	45	22	13	2.7	0.7	-	-0.67	-9.95	49.45
	7-8	126	120	71	70	39	35	3	-0.78	-4.23	87.20
81-82	20.5-24.0	67	55	22	13	6.4	5	-	-0.73	-7.80	43.12
	32	91	50	15	6.6	-	-	-	-0.87	-73.14	69.60

<sup>a</sup>Data adapted from ref. [85];

<sup>b</sup>No quantitative data given in the paper;

<sup>c</sup>Correlation of percentage viable and time, calculated;

<sup>d</sup>Slope of the linear regression of percentage viable versus time, calculated; greater slope indicates faster inactivation;

<sup>e</sup>Intercept of the linear regression of percentage viable versus time, calculated.

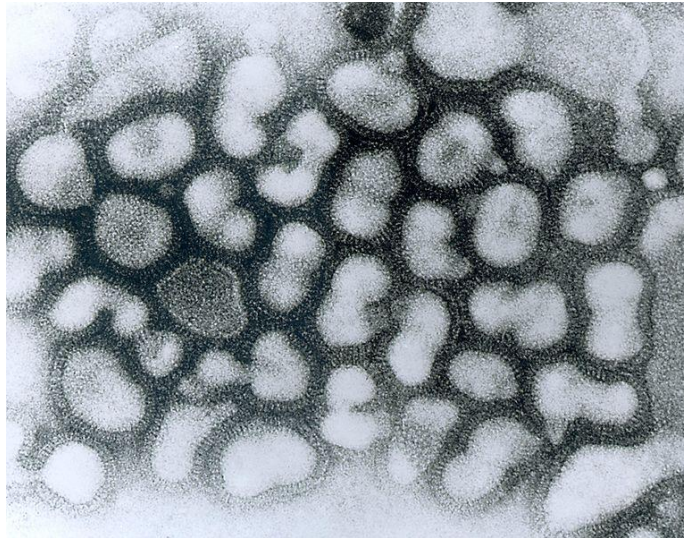


**Figure 1.1** Transmission electron micrograph of influenza A virus, late passage. [Public domain] Source: Dr. Erskine Palmer, Centers for Disease Control and Prevention Public Health Image Library, image #280

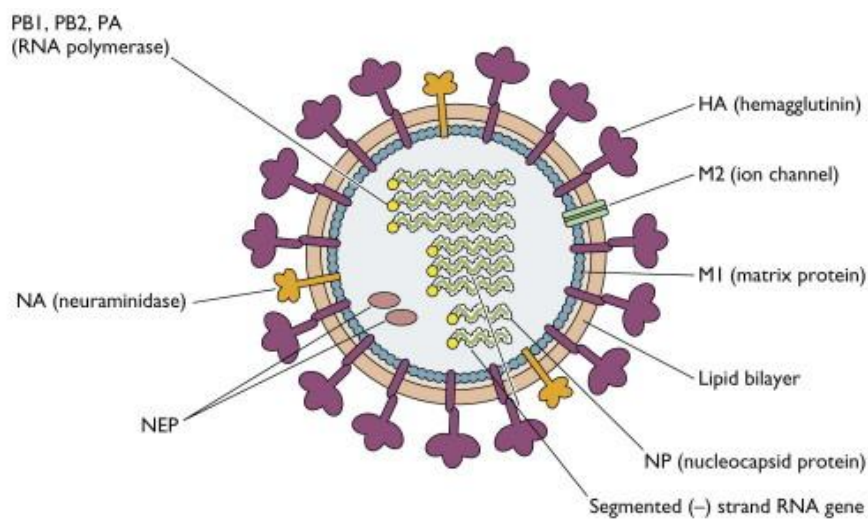


**Figure 1.2** Structure of influenza A virus. [Fair use] Source: S.J. Flint, L.W. Enquist, V.R. Racaniello, and A.M. Skalka. Principles of virology: Molecular biology, pathogenesis, and control of animal viruses, 2<sup>nd</sup> edition. pp 815

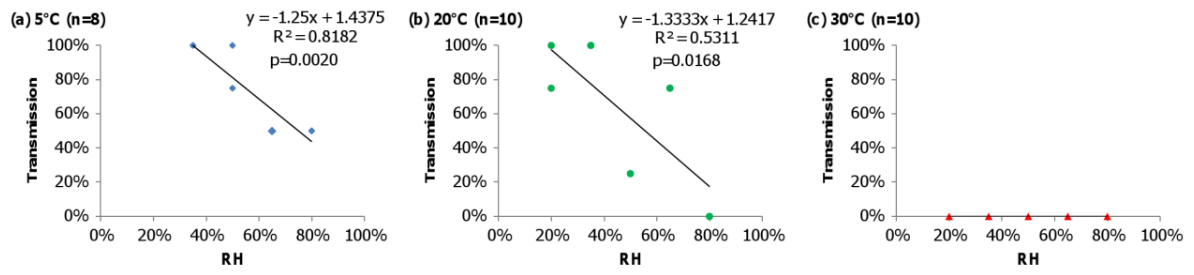


**Figure 1.3 Relationship between transmission rate and relative humidity (RH). Data adapted from Refs. [6-7]**

## References

1. Xu, J., Kochanek, K., Murphy, S., & Tejada-Vera, B. (2010). *Deaths: Final data for 2007*: Centers for Disease Control and Prevention.
2. Centers for Disease Control and Prevention. (2010). Estimates of deaths associated with seasonal influenza --- United States, 1976-2007. *Morbidity and Mortality Weekly Report*, 59(33), 1057-1062.
3. Molinari, N.-A. M., Ortega-Sanchez, I. R., Messonnier, M. L., Thompson, W. W., Wortley, P. M., Weintraub, E., et al. (2007). The annual impact of seasonal influenza in the US: Measuring disease burden and costs. *Vaccine*, 25(27), 5086-5096.
4. MacInnes, H., Zhou, Y., Gouveia, K., Cromwell, J., Lowery, K., Layton, R. C., et al. (2011). Transmission of aerosolized seasonal H1N1 influenza A to ferrets. *PLoS ONE*, 6(9), e24448.
5. Lakdawala, S. S., Lamirande, E. W., Suguitan, A. L., Jr., Wang, W., Santos, C. P., Vogel, L., et al. (2011). Eurasian-origin gene segments contribute to the transmissibility, aerosol release, and morphology of the 2009 pandemic H1N1 influenza virus. *PLoS Pathog*, 7(12), e1002443.
6. Lowen, A. C., Mubareka, S., Steel, J., & Palese, P. (2007). Influenza virus transmission is dependent on relative humidity and temperature. *PLoS Pathog*, 3(10), e151.
7. Lowen, A. C., Steel, J., Mubareka, S., & Palese, P. (2008). High temperature (30 °C) blocks aerosol but not contact transmission of influenza virus. *J. Virol.*, 82(11), 5650-5652.
8. Nicas, M., & Jones, R. M. (2009). Relative contributions of four exposure pathways to influenza infection risk. *Risk Anal.*, 29(9), 1292-1303.
9. Spicknall, I. H., Koopman, J. S., Nicas, M., Pujol, J. M., Li, S., & Eisenberg, J. N. (2010). Informing optimal environmental influenza interventions: How the host, agent, and environment alter dominant routes of transmission. *PLoS Comput Biol*, 6(10), e1000969.
10. Cauchemez, S., Bhattarai, A., Marchbanks, T. L., Fagan, R. P., Ostroff, S., Ferguson, N. M., et al. (2011). Role of social networks in shaping disease transmission during a community outbreak of 2009 H1N1 pandemic influenza. *Proc Natl Acad Sci USA*.
11. Alonso, W. J., Viboud, C., Simonsen, L., Hirano, E. W., Daufenbach, L. Z., & Miller, M.

- A. (2007). Seasonality of influenza in Brazil: A traveling wave from the Amazon to the subtropics. *Am. J. Epidemiol.*, *165*(12), 1434-1442.
12. Moura, F. E., Perdigao, A. C., & Siqueira, M. M. (2009). Seasonality of influenza in the tropics: A distinct pattern in northeastern Brazil. *Am. J. Trop. Med. Hyg.*, *81*(1), 180-183.
  13. Tamerius, J., Nelson, M., Zhou, S., Viboud, C., Miller, M., & Alonso, W. (2011). Global influenza seasonality: Reconciling patterns across temperate and tropical regions. *Environ. Health Perspect.*, *119*(4), 439-445.
  14. Viboud, C., Bjrnsstad, O. N., Smith, D. L., Simonsen, L., Miller, M. A., & B.T, G. (2006). Synchrony, waves, and spatial hierarchies in the spread of influenza. *Science*, *312*(5772), 447-451.
  15. Dushoff, J., Plotkin, J. B., Levin, S. A., & Earn, D. J. D. (2004). Dynamical resonance can account for seasonality of influenza epidemics. *Proc. Natl. Acad. Sci. U. S. A.*, *101*(48), 16915-16916.
  16. Shaman, J., Goldstein, E., & Lipsitch, M. (2011). Absolute humidity and pandemic versus epidemic influenza. *Am. J. Epidemiol.*, *173*(2), 127-135.
  17. Shaman, J., & Kohn, M. (2009). Absolute humidity modulates influenza survival, transmission, and seasonality. *Proc Natl Acad Sci USA*, *106*(9), 3243-3248.
  18. Russell, C. A., Jones, T. C., Barr, I. G., Cox, N. J., Garten, R. J., Gregory, V., et al. (2008). The global circulation of seasonal influenza A (H3N2) viruses. *Science*, *320*(5874), 340-346.
  19. Goldstein, E., Cobey, S., Takahashi, S., Miller, J. C., & Lipsitch, M. (2011). Predicting the epidemic sizes of influenza A/H1N1, A/H3N2, and B: A statistical method. *PLoS Med*, *8*(7), e1001051.
  20. Kenah, E., Chao, D. L., Matrajt, L., Halloran, M. E., & Longini, I. M., Jr. (2011). The global transmission and control of influenza. *PLoS ONE*, *6*(5), e19515.
  21. Soebiyanto, R. P., Adimi, F., & Kiang, R. K. (2010). Modeling and predicting seasonal influenza transmission in warm regions using climatological parameters. *PLoS ONE*, *5*(3).
  22. Tellier, R. (2006). Review of aerosol transmission of influenza A virus. *Emerg. Infect. Dis.*,

- 12(11), 1657-1662.
23. Brankston, G., Gitterman, L., Hirji, Z., Lemieux, C., & Gardam, M. (2007). Transmission of influenza A in human beings. *Lancet Infect Dis*, 7, 257-265.
  24. Hemmes, J. H., Winkler, K. C., & Kool, S. M. (1960). Virus survival as a seasonal factor in influenza and poliomyelitis. *Nature*, 188, 430-431.
  25. Dosseh, A., Ndiaye, K., Spiegel, A., Sagna, M., & Mathiot, C. (2000). Epidemiological and virological influenza survey in Dakar, Senegal: 1996-1998. *Am. J. Trop. Med. Hyg.*, 62(5), 639-643.
  26. Sagripanti, J.-L., & Lytle, C. D. (2007). Inactivation of influenza virus by solar radiation. *Photochem. Photobiol.*, 83, 1278-1282.
  27. Hope-Simpson, R. E., & Golubev, D. B. (1987). A new concept of the epidemic process of influenza A virus. *Epidemiol. Infect.*, 99(1), 5-54.
  28. Cauchemez, S., Valleron, A.-J., Boelle, P.-Y., Flahault, A., & Ferguson, N. M. (2008). Estimating the impact of school closure on influenza transmission from sentinel data. *Nature*, 452(7188), 750-754.
  29. Cannell, J. J., Zaslhoff, M., Garland, C. F., Scragg, R., & Giovannucci, E. (2008). On the epidemiology of influenza. *Virol J*, 5, 29.
  30. Lofgren, E., Fefferman, N. H., Naumov, Y. N., Gorski, J., & Naumova, E. N. (2007). Influenza seasonality: Underlying causes and modeling theories. *J. Virol.*, 81(11), 5429-5436.
  31. Lipsitch, M., & Viboud, C. (2009). Influenza seasonality: Lifting the fog. *Proc. Natl. Acad. Sci. U. S. A.*, 106(10), 3645-3646.
  32. Mitchell, C. A., & Guerin, L. F. (1972). Influenza A of human, swine, equine and avian origin: Comparison of survival in aerosol form. *Can. J. Comp. Med.*, 36(1), 9-11.
  33. Weber, T. P., & Stilianakis, N. I. (2008). Inactivation of influenza A viruses in the environment and modes of transmission: A critical review. *J. Infect.*, 57(5), 361-373.
  34. von Itzstein, M., Wu, W. Y., Kok, G. B., Pegg, M. S., Dyason, J. C., Jin, B., et al. (1993). Rational design of potent sialidase-based inhibitors of influenza virus replication. *Nature*, 363(6428), 418-423.
  35. Kim, C. U., Lew, W., Williams, M. A., Liu, H., Zhang, L., Swaminathan, S., et al. (1997).

- Influenza neuraminidase inhibitors possessing a novel hydrophobic interaction in the enzyme active site: Design, synthesis, and structural analysis of carbocyclic sialic acid analogues with potent anti-influenza activity. *J. Am. Chem. Soc.*, 119(4), 681-690.
36. Wang, C., Takeuchi, K., Pinto, L. H., & Lamb, R. A. (1993). Ion channel activity of influenza A virus m2 protein: Characterization of the amantadine block. *J. Virol.*, 67(9), 5585-5594.
37. Pinto, L. H., Holsinger, L. J., & Lamb, R. A. (1992). Influenza virus m2 protein has ion channel activity. *Cell*, 69(3), 517-528.
38. Bright, R. A., Shay, D. K., Shu, B., Cox, N. J., & Klimov, A. I. (2006). Adamantane resistance among influenza A viruses isolated early during the 2005-2006 influenza season in the United States. *JAMA: The Journal of the American Medical Association*, 295(8), 891-894.
39. S.J. Flint, L. W. E., V.R. Racaniello, and A.M. Skalka. (2004). *Principles of virology, Molecular biology, pathogenesis, and control of animal viruses, 2nd edition. RNA virus genome replication and mRNA production*, 183-214.
40. Trifonov, V., Khiabani, H., & Rabadan, R. (2009). Geographic dependence, surveillance, and origins of the 2009 influenza A (H1N1) virus. *N. Engl. J. Med.*, 361(2), 115-119.
41. Cunney, R. J., Bialachowski, A., Thornley, D., Smaill, F. M., & Pennie, R. A. (2000). An outbreak of influenza A in a neonatal intensive care unit. *Infect. Control Hosp. Epidemiol.*, 21(7), 449-454.
42. Morens, D. M., & Rash, V. M. (1995). Lessons from a nursing home outbreak of influenza A. *Infect. Control Hosp. Epidemiol.*, 16(5), 275-280.
43. Bean, B., Moore, B. M., Sterner, B., Peterson, L. R., Gerding, D. N., & Balfour Jr, H. H. (1982). Survival of influenza viruses on environmental surfaces. *J. Infect. Dis.*, 146(1), 47-51.
44. Thomas, Y., Vogel, G., Wunderli, W., Suter, P., Witschi, M., Koch, D., et al. (2008). Survival of influenza virus on banknotes. *Appl. Environ. Microbiol.*, 74(10), 3002-3007.
45. Boone, S. A., & Gerba, C. P. (2005). The occurrence of influenza A virus on household

- and day care center fomites. *J. Infect.*, 51(2), 103-109.
46. Killingley, B., Enstone, J. E., Greator, J., Gilbert, A. S., Lambkin-Williams, R., Cauchemez, S., et al. (2012). Use of a human influenza challenge model to assess person-to-person transmission: Proof-of-concept study. *J. Infect. Dis.*, 205(1), 35-43.
  47. Schulster, L. M., Chinn, R. Y. W., Arduino, M. J., Carpenter, J., Donlan, R., Ashford, D., et al. (2004). *Guidelines for environmental infection control in health-care facilities. Recommendations from CDC and the healthcare infection control practices advisory committee (hicpac)*. Chicago IL: American Society for Healthcare Engineering/American Hospital Association.
  48. Han, K., Zhu, X., He, F., Liu, L., Zhang, L., Ma, H., et al. (2009). Lack of airborne transmission during outbreak of pandemic (H1N1) 2009 among tour group members, china, june 2009. *Emerg. Infect. Dis.*, 15(10), 1578-1581.
  49. Schulman, J. L., & Kilbourne, E. D. (1962). Airborne transmission of influenza virus infection in mice. *Nature*, 195, 1129-1130.
  50. Schulman, J. L. (1967). Experimental transmission of influenza virus infection in mice. Iv. Relationship of transmissibility of different strains of virus and recovery of airborne virus in the environment of infector mice. *J. Exp. Med.*, 125(3), 479-488.
  51. Maines, T. R., Jayaraman, A., Belser, J. A., Wadford, D. A., Pappas, C., Zeng, H., et al. (2009). Transmission and pathogenesis of swine-origin 2009 A(H1N1) influenza viruses in ferrets and mice. *Science*, 325(5939), 484-487.
  52. Van Hoeven, N., Pappas, C., Belser, J. A., Maines, T. R., Zeng, H., Garc á-Sastre, A., et al. (2009). Human HA and polymerase subunit PB2 proteins confer transmission of an avian influenza virus through the air. *Proc Natl Acad Sci USA*, 106(9), 3366-3371.
  53. Lowen, A. C., Mubareka, S., Tumpey, T. M., Garc á-Sastre, A., & Palese, P. (2006). The guinea pig as a transmission model for human influenza viruses. *Proc Natl Acad Sci USA*, 103(26), 9988-9992.
  54. Alford, R. H., Kasel, J. A., Gerone, P. J., & Knight, V. (1966). Human influenza resulting from aerosol inhalation. *Proc. Soc. Exp. Biol. Med.*, 122(3), 800-804.
  55. Dick, E. C., Jennings, L. C., Mink, K. A., Wartgow, C. D., & Inhorn, S. L. (1987). Aerosol transmission of rhinovirus colds. *J. Infect. Dis.*, 156(3), 442-448.

56. Nicas, M., Nazaroff, W. W., & Hubbard, A. (2005). Toward understanding the risk of secondary airborne infection: Emission of respirable pathogens. *J Occup Environ Hyg*, 2(3), 143-154.
57. Fabian, P., McDevitt, J. J., DeHaan, W. H., Fung, R. O. P., Cowling, B. J., Chan, K. H., et al. (2008). Influenza virus in human exhaled breath: An observational study. *PLoS ONE*, 3(7), e2691.
58. Lindsley, W. G., Blachere, F. M., Thewlis, R. E., Vishnu, A., Davis, K. A., Cao, G., et al. (2010). Measurements of airborne influenza virus in aerosol particles from human coughs. *PLoS ONE*, 5(11), e15100.
59. Yang, S., Lee, G. W. M., Chen, C.-M., Wu, C.-C., & Yu, K.-P. (2007). The size and concentration of droplets generated by coughing in human subjects. *J. Aerosol Med.*, 20(4), 484-494.
60. Loudon, R. G., & Roberts, R. M. (1967). Droplet expulsion from the respiratory tract. *Am. Rev. Respir. Dis.*, 95(3), 435-442.
61. Papineni, R. S., & Rosenthal, F. S. (1997). The size distribution of droplets in the exhaled breath of healthy human subjects. *J. Aerosol Med.*, 10(2), 105-116.
62. Chao, C. Y. H., Wan, M. P., Morawska, L., Johnson, G. R., Ristovski, Z. D., Hargreaves, M., et al. (2009). Characterization of expiration air jets and droplet size distributions immediately at the mouth opening. *J. Aerosol Sci*, 40(2), 122-133.
63. Morawska, L., Johnson, G. R., Ristovski, Z. D., Hargreaves, M., Mengersen, K., Corbett, S., et al. (2009). Size distribution and sites of origin of droplets expelled from the human respiratory tract during expiratory activities. *J. Aerosol Sci*, 40(3), 256-269.
64. Xie, X., Li, Y., Sun, H., & Liu, L. (2009). Exhaled droplets due to talking and coughing. *J. R. Soc. Interface*, 6(Suppl 6), S703-S714.
65. Duguid, J. P. (1946). The size and the duration of air-carriage of respiratory droplets and droplet-nuclei. *J Hyg*, 44(6), 471-479.
66. Raphael, G. D., Jeney, E. V., Baraniuk, J. N., Kim, I., Meredith, S. D., & Kaliner, M. A. (1989). Pathophysiology of rhinitis. Lactoferrin and lysozyme in nasal secretions. *J. Clin. Invest.*, 84(5), 1528-1535.
67. Effros, R. M., Hoagland, K. W., Bosbous, M., Castillo, D., Foss, B., Dunning, M., et al.

- (2002). Dilution of respiratory solutes in exhaled condensates. *Am. J. Respir. Crit. Care Med.*, 165(5), 663-669.
68. Bansil, R., & Turner, B. S. (2006). Mucin structure, aggregation, physiological functions and biomedical applications. *Curr. Opin. Colloid Interface Sci.*, 11(2-3), 164-170.
69. Xie, X., Li, Y., Chwang, A. T. Y., Ho, P. L., & Seto, W. H. (2007). How far droplets can move in indoor environments--revisiting the wells evaporation--falling curve. *Indoor Air*, 17(3), 211-225.
70. Redrow, J., Mao, S., Celik, I., Posada, J. A., & Feng, Z.-g. (2011). Modeling the evaporation and dispersion of airborne sputum droplets expelled from a human cough. *Building and Environment*, 46(10), 2042-2051.
71. Parienta, D., Morawska, L., Johnson, G. R., Ristovski, Z. D., Hargreaves, M., Mengersen, K., et al. (2011). Theoretical analysis of the motion and evaporation of exhaled respiratory droplets of mixed composition. *J. Aerosol Sci*, 42(1), 1-10.
72. Hinds, W. C. (1999). Respiratory deposition *Aerosol technology* (2nd ed., pp. 233-259). New York: John Wiley & Sons, Inc.
73. Oberdorster, G., Oberdorster, E., & Oberdorster, J. (2005). Nanotoxicology: An emerging discipline evolving from studies of ultrafine particles. *Environ. Health Perspect.*, 113(7), 823-839.
74. Fabian, P., McDevitt, J. J., Lee, W.-M., Houseman, E. A., & Milton, D. K. (2009). An optimized method to detect influenza virus and human rhinovirus from exhaled breath and the airborne environment. *J. Environ. Monit.*, 11(2), 314-317.
75. Fabian, P., McDevitt, J. J., Houseman, E. A., & Milton, D. K. (2009). Airborne influenza virus detection with four aerosol samplers using molecular and infectivity assays: Considerations for a new infectious virus aerosol sampler. *Indoor Air*, 19(5), 433-441.
76. Tellier, R. (2009). Aerosol transmission of influenza A virus: A review of new studies. *J R Soc Interface*, 6 Suppl 6, S783-790.
77. Blachere, F. M., Lindsley, W. G., Pearce, T. A., Anderson, S. E., Fisher, M., Khakoo, R., et al. (2009). Measurement of airborne influenza virus in a hospital emergency department. *Clin. Infect. Dis.*, 48(4), 438-440.
78. Lindsley, W. G., Blachere, F. M., Davis, K. A., Pearce, T. A., Fisher, M. A., Khakoo, R., et

- al. (2010). Distribution of airborne influenza virus and respiratory syncytial virus in an urgent care medical clinic. *Clin. Infect. Dis.*, 50(5), 693-698.
79. Chen, P.-S., Tsai, F. T., Lin, C. K., Yang, C.-Y., Chan, C.-C., Young, C.-Y., et al. (2010). Ambient influenza and avian influenza virus during dust storm days and background days. *Environ. Health Perspect.*, 118(9).
80. Yang, W., Elankumaran, S., & Marr, L. C. (2011). Concentrations and size distributions of airborne influenza A viruses measured indoors at a health centre, a day-care centre, and on aeroplanes. *J R Soc Interface*, 8(61), 1176-1184.
81. Hers, J. F. P., & Winkler, K. C. (1973). *Airborne transmission and airborne infection: Concepts and methods presented at the vith [i.E. Ivth] international symposium on aerobiology*. New York-Toronto: John Wiley & Sons.
82. Wong, C. M., Yang, L., Thach, T. Q., Chau, P. Y. K., Chan, K. P., Thomas, G. N., et al. (2009). Modification by influenza on health effects of air pollution in Hong Kong. *Environ. Health Perspect.*, 117(2), 248-253.
83. Brown, J. D., Goekjian, G., Poulson, R., Valeika, S., & Stallknecht, D. E. (2009). Avian influenza virus in water: Infectivity is dependent on pH, salinity and temperature. *Vet. Microbiol.*, 136(1-2), 20-26.
84. Davidson, I., Nagar, S., Haddas, R., Ben-Shabat, M., Golender, N., Lapin, E., et al. (2010). Avian influenza virus H9N2 survival at different temperatures and phs. *Avian Dis.*, 54(s1), 725-728.
85. Harper, G. J. (1961). Airborne micro-organisms: Survival tests with four viruses. *J Hyg*, 59, 479-486.
86. Schaffer, F. L., Soergel, M. E., & Straube, D. C. (1976). Survival of airborne influenza virus: Effects of propagating host, relative humidity, and composition of spray fluids. *Arch. Virol*, 51(4), 263-273.
87. Chan, P. K. S., Mok, H. Y., Lee, T. C., Chu, I. M. T., Lam, W. Y., & Sung, J. J. Y. (2009). Seasonal influenza activity in Hong Kong and its association with meteorological variations. *J. Med. Virol.*, 81(10), 1797-1806.
88. Tang, J. W., Lai, F. Y. L., Nymadawa, P., Deng, Y. M., Ratnamohan, M., Petric, M., et al. (2010). Comparison of the incidence of influenza in relation to climate factors during

- 2000-2007 in five countries. *J. Med. Virol.*, 82(11), 1958-1965.
89. Shaman, J., Pitzer, V. E., Viboud, C., Grenfell, B. T., & Lipsitch, M. (2010). Absolute humidity and the seasonal onset of influenza in the continental United States. *PLoS Biol*, 8(2), e1000316.
90. Shechmeister, I. L. (1950). Studies on the experimental epidemiology of respiratory infections: III. Certain aspects of the behavior of type A influenza virus as an air-borne cloud. *J. Infect. Dis.*, 87(2), 128-132.
91. Yang, W., & Marr, L. C. (2011). Dynamics of airborne influenza A viruses indoors and dependence on humidity. *PLoS ONE*, 6(6), e21481.
92. Shek, L. P., & Lee, B. W. (2003). Epidemiology and seasonality of respiratory tract virus infections in the tropics. *Paediatr Respir Rev*, 4(2), 105-111.
93. Weber, T. P., & Stilianakis, N. I. (2008). A note on the inactivation of influenza A viruses by solar radiation, relative humidity and temperature. *Photochem. Photobiol.*, 84(6), 1601-1602; author reply 1603-1604.
94. Cannell, J. J., Vieth, R., Umhau, J. C., Holick, M. F., Grant, W. B., Madronich, S., et al. (2006). Epidemic influenza and vitamin D. *Epidemiol. Infect.*, 134(06), 1129-1140.
95. Hypponen, E., & Power, C. (2007). Hypovitaminosis D in british adults at age 45 y: Nationwide cohort study of dietary and lifestyle predictors. *Am. J. Clin. Nutr.*, 85(3), 860-868.
96. Aloia, J. F., Talwar, S. A., Pollack, S., & Yeh, J. (2005). A randomized controlled trial of vitamin D3 supplementation in african american women. *Arch. Intern. Med.*, 165(14), 1618-1623.
97. Aloia, J. F., & LI-NG, M. (2007). Correspondence. *Epidemiol. Infect.*, 135(07), 1095-1098.

## 2 Concentrations and Size Distributions of Airborne Influenza A Viruses Measured Indoors at a Health Center, a Daycare, and on Aeroplanes\*

Wan Yang<sup>1</sup>, Subbiah Elankumaran<sup>2</sup>, Linsey C. Marr<sup>1,\*</sup>

<sup>1</sup>Department of Civil and Environmental Engineering, Virginia Tech, 418 Durham Hall, Blacksburg, Virginia 24061, USA

<sup>2</sup>Department of Biomedical Sciences and Pathobiology, Virginia-Maryland College of Veterinary Medicine, Virginia Tech, 1981 Kraft Drive, Blacksburg, Virginia 24060, USA

### Abstract

The relative importance of the aerosol transmission route for influenza remains contentious. To determine the potential for influenza to spread via the aerosol route, we measured the size distribution of airborne influenza A viruses (IAVs). We collected size-segregated aerosol samples during the 2009-2010 flu season in a health center, a daycare facility, and onboard airplanes. Filter extracts were analyzed using quantitative reverse transcriptase polymerase chain reaction (qRT-PCR). Half of the 16 samples were positive, and their total virus concentrations ranged from 5800 to 37000 genome copies  $\text{m}^{-3}$ . On average, 64% of the viral genome copies were associated with fine particles smaller than 2.5  $\mu\text{m}$ , which can remain suspended for hours. Modeling of virus concentrations indoors suggested a source strength of  $1.6 \pm 1.2 \times 10^5$  genome copies  $\text{m}^{-3}$  air  $\text{h}^{-1}$  and a deposition flux onto surfaces of  $13 \pm 7$  genome copies  $\text{m}^{-2}$   $\text{h}^{-1}$  by Brownian motion. Over 1 h, the inhalation dose was estimated to be  $30 \pm 18$  median tissue culture infectious dose ( $\text{TCID}_{50}$ ), adequate to induce infection. These results provide quantitative support for the idea that the aerosol route could be an important mode of influenza transmission.

Key words: influenza; bioaerosol; size distribution; aerosol transmission; emissions; deposition

---

\*Published, allowed to reproduce in this dissertation. Yang, W., Elankumaran, S., & Marr, L. C. (2011). Concentrations and size distributions of airborne influenza A viruses measured indoors at a health centre, a day-care centre, and on aeroplanes. *J R Soc Interface*, 8(61), 1176-1184.

## 2.1 Introduction

Influenza A viruses (IAVs) are transmitted through direct contact, indirect contact, large respiratory droplets, and droplet nuclei (aerosols) that are left behind by the evaporation of larger droplets. The relative importance of each of these routes remains contentious. The aerosol transmission route has been particularly controversial since there is scant direct proof of infection mediated by virus-laden aerosols, partly due to the difficulties in studies involving human subjects and partly due to the challenges in detecting IAVs in ambient air [1-3].

Virus-laden aerosols may be released into air when infected people cough, sneeze, talk, or breathe; however, the aerosols are quickly diluted by ambient air to extremely low concentrations [4]. In addition, the relatively insensitive culture methods to detect viruses, potential inactivation during aerosol sampling, and inhibition of detection methods by airborne contaminants present challenges to the measurement of airborne IAVs [3; 5]. Consequently, despite the rapid development of detection methods for IAVs in clinical and laboratory settings, there are still very few measurements of them in the airborne environment. Even fewer studies have determined the size of influenza-laden particles, which is important because it determines how long particles will remain suspended in air before being removed by gravitational settling or Brownian diffusion, and where they will deposit in the respiratory system.

Quantitative reverse transcriptase polymerase chain reaction (qRT-PCR), based on the detection of viral RNA, affords a sensitive and rapid approach for quantifying low levels of viruses. Chen *et al.* [6] applied this method to detect IAVs in a live poultry market, but their sampling method did not discriminate by particle size. Using qRT-PCR, Blachere *et al.* [7] measured aerosolized influenza viruses in a hospital emergency department for 6 days. Eighty-one air samples were collected with a modified National Institute for Occupational Safety and Health two-stage cyclone sampler that separated the aerosols into  $>4 \mu\text{m}$ ,  $1\text{--}4 \mu\text{m}$ , and  $<1 \mu\text{m}$  fractions, and IAV RNA was detected in 11 of the samples. They found that 46%, 49%, and 4% of the IAVs were collected in each of the size ranges, respectively. A more extensive follow-up study [8] reported that IAVs were detected on 10 out of 11 days, with 17%

out of 385 samples confirmed to contain IAV RNA. Of the detected IAV RNA, 42% was associated with particles  $\leq 4.1 \mu\text{m}$ .

Public places with a susceptible population and/or a high population density, such as hospitals, daycare centers, and airplanes, may harbor high concentrations of pathogens. Of 218 surfaces (toys, diaper changing areas, toilet seat tops, etc.) tested in 14 different daycare centers, Boone & Gerba [9] detected influenza viruses on 23% and 53% of the samples during fall and spring, respectively. Infected individuals on an airplane may spread the influenza virus to other passengers [10]. The Alaska Airlines outbreak [11] has been presented as proof of airborne influenza transmission: a jet with 54 persons aboard was delayed on the ground for 3 h (during which the airplane ventilation system was inoperative), and 72% of the passengers who stayed on the airplane were infected by an influenza-contracted passenger within 72 hours.

To evaluate the prevalence of airborne IAVs in high-risk, public spaces, we collected aerosol samples from a health center, a daycare facility, and onboard three commercial passenger airplane flights during the 2009-2010 flu season. Particles were divided into five size fractions, and IAVs in each were analyzed using qRT-PCR. The indoor influenza virus emission strength, the deposition flux onto the wall surfaces, and risk for airborne infection were then estimated using our experimental data.

## **2.2 Materials and methods**

### **2.2.1 Reference Viruses**

Reference strains of influenza A were from our collection at the Department of Biomedical Sciences and Pathology, Center for Molecular Medicine and Infectious Disease at Virginia Tech. Prototype strains utilized to develop the qPCR method were A/PR/8/34 (H1N1) and A/swine/Minnesota/1145/2007 (H3N2). These two strains were used to construct and test the qRT-PCR concentration standards.

### **2.2.2 Detection of viral genome**

*Viral genomic RNA extraction.* Influenza virus RNA collected on the filters was extracted using a Trizol-chloroform-based method modified from a protocol reported elsewhere [12-13]. Briefly, the filter was rolled and put into a 2-mL microcentrifuge tube containing 250  $\mu\text{L}$  of phosphate buffered saline (PBS) supplemented with 20  $\mu\text{g}$  of glycogen (Ambion,

TX, USA), 15 µg of glycoblue (Ambion, TX, USA), and 50 ng of human genomic DNA (Cat. No. 636401, Clontech Laboratories, Inc., CA, USA). A volume of 750 µL of Trizol LS (Invitrogen, CA, USA) was added, and the sample was vortexed thoroughly and incubated at room temperature for 10 min. The sample was then briefly centrifuged, and the supernatant was transferred to a 1.5-mL microcentrifuge tube, to which 230 µL of chloroform was added (Sigma-Aldrich, MO, USA). The sample was briefly vortexed, incubated at room temperature for 5 min, and then centrifuged at 2100×g for 5 min. The colorless upper aqueous phase was carefully transferred to a new 1.5-mL tube containing 600 µL of isopropanol (Sigma-Aldrich, MO, USA) for RNA precipitation for 1 h. Then the RNA was pelleted by centrifuging for 12 min at 20000×g and was washed with 600 µL of 75% ethanol. The RNA was finally dissolved in 20 µL of diethylpyrocarbonate (DEPC)-treated water (Sigma-Aldrich, MO, USA) and immediately converted to complementary DNA (cDNA) or stored at -80 °C until use.

*Reverse transcription.* Complementary DNA was generated with a TaqMan Reverse Transcription Reagents Kit (N8080234, Applied Biosystems, USA) according to the manufacturer's instructions. A 20-µL reaction mixture was made with a final concentration of 1X TaqMan RT buffer, 5.5 mM of Mg<sup>2+</sup>, 500 µM of each dNTP, 2.5 µM of RT random hexamer primers, 0.4 U µL<sup>-1</sup> of RNase inhibitor, and 1.25 U µL<sup>-1</sup> of MultiScribe Reverse Transcriptase, plus 7.7 µL of RNA. Complementary DNA synthesis was carried out on a thermal cycler (1000-Series Thermal Cycling Platform, Bio-Rad, USA) at 25 °C for 10 min, 48 °C for 30 min, and 95 °C for 5 min.

*Quantifying standard and standard curve preparation.* The cDNA standard solution was constructed by ligation of the targeted gene fragment in a pCR2.1-TOPO® vector according to the instructions of the TOPO TA Cloning® Kit (Invitrogen, USA). Two sets of IAV primers, one reported by Ward *et al.* [14] and the other by van Elden *et al.* [15], are widely used to detect the M1 protein gene of IAVs [6; 14; 16]. The primers by Ward *et al.* [14] have proven to be applicable for the currently circulating A (H3N2), seasonal A (H1N1), and pandemic A (H1N1) strains [17-18]. The genomic regions amplified by these two sets of primers are partially overlapping (Table 2.1). We used the forward primer reported by Ward *et al.* (2004) and the reverse primer reported by van Elden *et al.* [15] to amplify a segment

that spans both genomic regions. The amplicon obtained for cloning was a 262-bp segment by RT-PCR from stocks of A/swine/Minnesota/1145/2007 (H3N2). The ligation plasmids were transformed into competent *E. coli* cells, and recombinant bacteria were selected on kanamycin-containing LB agar. Positive inserts were amplified by M13 primers embedded within the pCR2.1-TOPO® vector according to the manufacturer's protocol. The resulting PCR products were sequenced and confirmed to be the target IAV gene fragment. The PCR products were quantified by a Molecular Imager® Gel Doc™ XR system (Bio-Rad, USA) and were used as the cDNA standard for qPCR. A standard stock solution was prepared at a concentration of  $10^{10}$  genome copies  $\mu\text{L}^{-1}$ . It was tested and confirmed to quantify successfully both the H3N2 and the H1N1 influenza virus strains.

The calibration curve was generated using serial 10-fold dilutions of the standard solution from  $10^7$  to 10 genome copies  $\mu\text{L}^{-1}$  in triplicate. A standard curve was generated each time that field samples were quantified, and the amount of influenza A virus genome in field samples was determined according to the linear regression of cycle threshold ( $C_t$ ) values against the known log concentrations ( $C_0$ ). Autoclaved ultrapure water (NANOpure Ultrapure Water System, Barnstead/Thermolyne, IA, USA) was used as a qPCR negative control during each run.

*Quantitative PCR.* The qPCR assay was performed in 96-well reaction plates (MicroAmp Optical, Applied Biosystems, CA, USA) on a 7300 Real Time PCR System (Applied Biosystems, CA, USA). Two sets of primers [14-15] were tested using a SYBR® Green PCR Master Mix Kit (Applied Biosystems, CA, USA). The qPCR mixture consisted of a final concentration of 1X SYBR® Green Master Mix, 200 nM of each primer, 5  $\mu\text{L}$  of cDNA, and autoclaved ultrapure water to bring the qPCR reaction volume to 25  $\mu\text{L}$ . Cycling conditions were 1 cycle of AmpliTaq Gold enzyme activation at 95 °C for 10 min, 40 cycles of denaturation of DNA at 95 °C for 15 s, and annealing and extension at 60 °C for 1 min. The amplification was followed by a melting curve analysis with a dissociation stage from 60 °C to 95 °C.

The standard and Ward's primers were further tested with a TaqMan® One-Step RT-PCR Master Mix Reagents Kit (Applied Biosystems, CA, USA), and the influenza A probe (6-FAM-5' TTT GTG TTC ACG CTC ACC GT 3'- Black Hole Quencher® 1) [14]

was used. One-step RT-PCR was performed in 25  $\mu\text{L}$  consisting of a final concentration of 1X Master Mix without UNG, 1X MultiScribe and RNase Inhibitor Mix (0.25 U  $\mu\text{L}^{-1}$  and 0.4 U  $\mu\text{L}^{-1}$ , respectively), 900 nM of each primer, and 225 nM of the influenza A probe, plus 3  $\mu\text{L}$  of viral RNA. The reaction mixture was held at 48  $^{\circ}\text{C}$  for 30 min for cDNA synthesis, 95  $^{\circ}\text{C}$  for 10 min for AmpliTaq Gold enzyme activation, and 40 two-step cycles followed (95  $^{\circ}\text{C}$  for 15 s for denaturation and 60  $^{\circ}\text{C}$  for 1 min for primer annealing and extension). All qPCR assays were run in triplicate.

### **2.2.3 Virus spike recovery experiments**

Virus spike recovery experiments were conducted to test the recovery efficiencies of the viral genome from the filters used to collect ambient particle samples and the PBS buffer used for RNA extraction. Two polytetrafluoroethylene (PTFE) filters, 25 mm and 37 mm in diameter (Cat. No. 225-1708 and 225-1709, SKC Inc., PA, USA), were used for sample collection. The H1N1 virus stock was diluted  $2 \times 10^{-2}$  with autoclaved ultrapure water and used as a spiking solution. Filters were spiked with 50  $\mu\text{L}$  of virus solution (2.5  $\mu\text{L}$  per droplet, 20 droplets total for the 25-mm filter, and 5  $\mu\text{L}$  per droplet, 10 droplets total for the 37-mm filter). Because the 37-mm filter was especially hydrophobic, the droplet volume had to be increased to 5  $\mu\text{L}$  for it to be taken up from a pipette. For the PBS buffer, 50  $\mu\text{L}$  of the virus solution was spiked into a 2-mL microcentrifuge tube containing 200  $\mu\text{L}$  of PBS buffer (referred to as “PBS-control” hereafter). To test for possible decay of the virus with time, 50  $\mu\text{L}$  of the virus solution was added into a 2-mL microcentrifuge tube without PBS (referred to as “decay-control” hereafter). All samples were placed in a biological safety cabinet for 2 h, allowing the virus solution droplets on the filters to dry out. The temperature in the cabinet was maintained at approximately 20  $^{\circ}\text{C}$ . Aliquots of 50  $\mu\text{L}$  of the same virus solution used for spiking were stored at 4  $^{\circ}\text{C}$  for quantification of the spiked amount. All samples were supplemented with PBS to a final volume of 250  $\mu\text{L}$  and subjected to viral RNA extraction as described above. All tests were conducted in duplicate.

### **2.2.4 Field sample collection**

*Sampling locations.* Samples were collected from a health center at Virginia Tech, a daycare center in Blacksburg, Virginia, and airplanes corresponding to three cross-county flights between Roanoke and San Francisco. The health center samples were collected from a

waiting room, which is a semi-open space about 8.5 m × 5 m. The mean indoor temperature ( $\pm$ SD) was 22.0 $\pm$ 1.0 °C, with a mean relative humidity of 34.5 $\pm$ 11.4%. Design room air exchange rates (AERs) were 8–12 air changes h<sup>-1</sup> (ACH). The daycare center samples were collected in two toddlers' room and a babies' room. Each of the toddlers' rooms is about 8 m × 4 m and holds 16 children plus four adults, and the babies' room is about 8 m × 3.5 m and holds 12 children and four adults. The mean indoor temperature in the toddlers' rooms was 22.8 $\pm$ 1.7 °C, with a mean relative humidity of 40.6 $\pm$ 5.1%. The mean indoor temperature in the babies' room was 25.1 $\pm$ 1.1 °C, with a mean relative humidity of 32.9 $\pm$ 2.0%. The mean temperature in the airplanes (between Roanoke and San Francisco with a layover) was 23.6 $\pm$ 3.1 °C, with a mean relative humidity of 27.1 $\pm$ 11.9%. The ventilation systems were operating properly during all sampling periods.

*Sample Collection.* A total of 16 samples were collected between 10 December 2009 and 22 April 2010, of which nine were collected from the health center, four from the daycare center, and three from airplanes. A cascade impactor (Sioutas Cascade Impactor, SKC Inc., PA, USA) and a pump running at 9 L min<sup>-1</sup> (Leland Legacy, SKC Inc., PA, USA) were used to collect the samples over 6–8 h. The impactor consists of four stages that allow the separation and collection of airborne particles in five size ranges: >2.5  $\mu$ m, 1.0–2.5  $\mu$ m, 0.5–1.0  $\mu$ m, 0.25–0.5  $\mu$ m, and <0.25  $\mu$ m. Particles larger than each cut-point were collected on 25-mm PTFE filters (Cat. No. 225-1708, SKC Inc., PA, USA); those smaller than the 0.25  $\mu$ m cut-point of the last stage were collected on a 37-mm PTFE after-filter (Cat. No. 225-1709, SKC Inc., PA, USA).

In the health center, the sampler was placed on a desk (~0.5 m high) around which patients sit while waiting; in the daycare center, the sampler was placed on a shelf (~1.0 m high); and on airplanes, it was placed near the seat pocket (<0.5 m high). Temperature and relative humidity were recorded every 2 min during sampling (OM-73, Omega Engineering, Inc., USA). After each sampling period, the impactor was washed with 10% bleach, cleaned with ultrapure water, and autoclaved (121 °C, 30 min). New filters were loaded into the impactor, left overnight before sampling, and used as device blank controls. Only those with results confirmed to have no detectable influenza virus RNA in the device blank controls were adopted.

## **2.3 Results**

### **2.3.1 qRT-PCR**

We tested two sets of influenza virus primers that have been widely cited in the literature [4; 6; 14-16]. Both sets of primers proved to be adequate; they were able to specifically amplify the target gene segments from the H1N1 and H3N2 strains, as indicated by the dissociation curve (data not shown). We tested the efficiency of primers to detect a field isolate of the H3N2 and pandemic H1N1 strains. Ward's primers achieved better qPCR efficiency (91% versus 61%) and a lower detection limit (100 genome copies per reaction versus 1000 genome copies per reaction) than did van Elden's. Hence, we used Ward's primers in subsequent experiments. TaqMan qRT-PCR showed that with Ward's primers, the detection limit was 10 genome copies per reaction, with an efficiency around 100% and  $R^2 > 0.99$  for our samples.

### **2.3.2 Virus spike recovery experiments**

According to qRT-PCR results, each spiked sample contained approximately  $2.4 \times 10^7$  genome copies of the H1N1 virus. The recovery efficiencies were calculated by dividing the amount of virus detected by the number spiked into each sample (filter, PBS-control, or decay-control). Results are reported in Table 2.2. The viral genome recovery efficiencies were 40.5% from the 25-mm filter ( $p=0.00011$ ), 62.0% from the 37-mm filter ( $p=0.0058$ ), 86.6% from the PBS-control samples ( $p=0.077$ ), and 91.2% from the decay-control samples ( $p=0.23$ ). The control experiments showed that PBS had no significant adverse effect on the viral genome, and the natural decay of virus genome was insignificant within a 2-h period. In contrast, the recovery efficiencies from the two filters were significantly less than 100%. During the RNA extraction step, only 800-900  $\mu\text{L}$  of Trizol lysate was retrieved for phase separation by chloroform, with 100-200  $\mu\text{L}$  of lysate retained by the filter. This loss accounts for a portion of the incomplete recovery from the filter.

### **2.3.3 Concentrations of airborne IAVs**

Between 10 December 2009 and 22 April 2010, we collected 16 samples, listed in Table 2.3. Half of the samples were confirmed to contain aerosolized IAVs: 33% of the health center samples (3/9), 75% of the daycare center samples (3/4), and 67% of the airplane samples (2/3). Concentrations in all of the field and laboratory blanks were below the detection limit.

In the samples containing detectable amounts of IAVs, the average concentration was  $1.6 \pm 0.9 \times 10^4$  genome copies  $\text{m}^{-3}$ .

### 2.3.4 Virus-laden particle size distribution

The cascade impactor separated particles into five size fractions:  $>2.5 \mu\text{m}$ ,  $1.0\text{-}2.5 \mu\text{m}$ ,  $0.5\text{-}1.0 \mu\text{m}$ ,  $0.25\text{-}0.5 \mu\text{m}$ , and  $<0.25 \mu\text{m}$ . The amounts of virus found in each fraction, summed over all samples, were 36%, 28%, 11%, 10%, and 15%, respectively. As shown in Figure 2.1, the virus-laden particle size distributions of the eight positive samples were diverse, and no obvious trend was observed. In some cases, the virus was relatively evenly distributed across the different particle sizes, while in others, it was found predominantly in the smallest and largest, or just the largest, size fractions.

### 2.3.5 Indoor influenza virus emission and deposition flux by modeling

*Indoor IAV emission rate.* To estimate the emission source strength of influenza A in airborne particles, we developed a mass-balance model. The model assumes that well-mixed, steady-state conditions apply at each sampling site: in a room of volume  $V$  ( $\text{m}^3$ ), air flows in and out through the heating, ventilating, and air-conditioning (HVAC) system with a flow rate of  $Q$  ( $\text{m}^3 \text{h}^{-1}$ ). Aerosolized viruses are generated by the occupants with an emission rate of  $E$  (genome copies  $\text{h}^{-1}$ ), disperse into ambient air, and become well mixed immediately upon release. Assuming that the virus concentration in the air entering the room is zero, the indoor virus concentration is maintained at  $C$  (genome copies  $\text{m}^{-3}$ ), and the outlet virus concentration is also  $C$ , we establish the mass balance for the modeled room:

$$\frac{dC}{dt}V = QC_{in} - QC_{out} + E = E - QC \quad (1)$$

where  $C$ ,  $C_{in}$ , and  $C_{out}$  are, respectively, the virus concentrations in the room, in the inflow, and in the outflow (genome copies  $\text{m}^{-3}$ ), and  $t$  is time (h).

At steady-state,

$$E_v = \frac{E}{V} = \frac{Q}{V}C = \lambda C \quad (2)$$

where  $E_v$  is the emission rate in genome copies  $\text{m}^{-3} \text{h}^{-1}$  and  $\lambda$  is the air exchange rate.

Typical AERs are 13 ACH in hospitals, 9 ACH in schools, and 4 ACH in commercial offices [19]. The AER in commercial aircraft is usually higher with a typical value of 15 ACH [20]. Therefore, we adopt an AER of  $10 \pm 5$  ACH to estimate the IAV emission rate in these

public places, and for a measured indoor virus concentration of  $1.6 \pm 0.9 \times 10^4$  genome copies  $\text{m}^{-3}$ , the emission rate  $E_v$  is  $1.6 \pm 1.2 \times 10^5$  genome copies  $\text{m}^{-3} \text{h}^{-1}$ .

*Influenza virus deposition on surfaces by Brownian motion.* Applying the well-mixed model, we assume the virus-laden particles are evenly distributed throughout the room, except in a thin boundary layer alongside each wall surface, across which the virus-laden particles diffuse by Brownian motion and finally deposit onto the surface. The deposition flux can be calculated according to Fick's law:

$$J_d = -D \frac{dC}{dx} \quad (3)$$

where  $J_d$  is the virus flux to the surface (genome copies  $\text{m}^{-2} \text{s}^{-1}$ ),  $D$  is the diffusion coefficient ( $\text{m}^2 \text{s}^{-1}$ ), and  $x$  is the distance to the wall (m). The diffusion coefficient can be calculated by the Einstein-Stokes equation:

$$D = \frac{kTC_c}{3\pi\mu d_p} \quad (4)$$

where  $k$  is the Boltzmann constant ( $1.38 \times 10^{-23} \text{ m}^2 \text{ kg s}^{-2} \text{ K}^{-1}$ ),  $T$  is temperature (K),  $\mu$  is the viscosity of air at standard conditions ( $1.81 \times 10^{-5} \text{ kg m}^{-1} \text{ s}^{-1}$ ),  $d_p$  is particle diameter (m), and  $C_c$  is the Cunningham slip correction factor [21]. The concentration gradient can be estimated as the ratio of the concentration in the core of the room to the thickness of the diffusion boundary layer, given by the modified Einstein equation:

$$x^2 = 2Dt \quad (5)$$

where  $t$  is the residence time of particles in the room, or 360 s in this case.

We sum over all particle sizes and use the midpoint diameter of each range, assuming a minimum of 0.1  $\mu\text{m}$  for the smallest one and maximum of 10  $\mu\text{m}$  for the largest one, to calculate the diffusion coefficients. Based on our measurements, the total diffusive flux of viruses to indoor surfaces is  $13 \pm 7$  genome copies  $\text{m}^{-2} \text{h}^{-1}$ . This flux is sufficiently small that it can be neglected in the previous mass-balance model used to estimate the virus emission rate.

## 2.4 Discussion

### 2.4.1 IAV concentrations and size distributions in indoor facilities

To our knowledge, there have been only a few studies on the presence of airborne IAVs in a health care environment, and no airborne IAV detection has been reported in daycare centers

or onboard passenger airplanes. Blachere *et al.* [7] reported airborne IAV concentrations in a health center ranging from 460 to 16,278 median tissue culture infectious dose (TCID<sub>50</sub>)-equivalent RNA particles for an entire sample. The sampling time and flow rate were 3-5 h and 3.5 L min<sup>-1</sup>, respectively, and if we assume a total sample volume of 840 L of air (4 h at 3.5 L min<sup>-1</sup>), then the corresponding concentrations were 5.5×10<sup>2</sup> to 1.9×10<sup>4</sup> TCID<sub>50</sub>-equivalent RNA particles m<sup>-3</sup>. Their PCR was calibrated in TCID<sub>50</sub> by using serial dilutions of a live-attenuated influenza virus quantified in TCID<sub>50</sub> mL<sup>-1</sup>. Lindsley *et al.* [8], in a more detailed study in the same clinic, detected 1.2±4.4 pg RNA m<sup>-3</sup> in examination rooms, 1.1±3.0 pg RNA m<sup>-3</sup> in procedure rooms, and 0.3±4.3 pg RNA m<sup>-3</sup> in a waiting room. These values can be converted to 5.0±18.5 TCID<sub>50</sub> m<sup>-3</sup>, 4.6±12.6 TCID<sub>50</sub> m<sup>-3</sup>, and 1.3±18.1 TCID<sub>50</sub> m<sup>-3</sup>, respectively, using the ratio of ~4.2 TCID<sub>50</sub> FluMist vaccine pg<sup>-1</sup> RNA reported in the study.

The ratio of viral particles to TCID<sub>50</sub> can vary greatly depend on types of viruses (even for strains of the same type), culture methods, and conditions (e.g., culturing cells, media, and harvest time). For influenza viruses, this ratio has been reported to be in the range of hundreds to thousands: Fabian *et al.* [13] established a ratio of 300 copies TCID<sub>50</sub><sup>-1</sup>; Ward *et al.* [14] determined that 1000 genome copies mL<sup>-1</sup> corresponded to 1 TCID<sub>50</sub> mL<sup>-1</sup>; and Poon *et al.* [22] estimated that 1 TCID<sub>50</sub> of A/California/04/2009 (H1N1) contained approximately 5000 copies of the M gene. In our experiment, 1 PFU of A/PR/8/34 (H1N1) stock was equivalent to 3 × 10<sup>3</sup> genome copies, or approximately 2.1 × 10<sup>3</sup> genome copies per TCID<sub>50</sub> according to the relationship between TCID<sub>50</sub> and PFU [23], and the ratio for the pandemic A/California/04/2009 (H1N1) strain was determined to be 452 ± 84 copies/TCID<sub>50</sub>. Based on this ratio (i.e., 452), our results from the health center correspond to airborne influenza virus concentrations of 12.8-81.9 TCID<sub>50</sub> m<sup>-3</sup>, 1-2 orders of magnitude lower than those observed by Blachere *et al.* [7] but slightly higher than those reported by Lindsley *et al.* [8]. With respect to size distributions, we found a larger fraction of total genome copies to be associated with fine particles: 80% with particles smaller than 2.5 μm versus 53% [7] and 42% [8] with particles smaller than 4.1 μm.

For the three positive samples from the daycare center, the total concentrations ranged from 1.6×10<sup>4</sup> to 3.7×10<sup>4</sup> genome copies m<sup>-3</sup>, half of which were associated with

particles  $>2.5 \mu\text{m}$  and the other half with smaller particles. The average concentration in the daycare center was nearly two times higher than that in the health center. Considering that children are the primary susceptible population of influenza, the difference is not surprising. In addition, the influenza particle size distributions in the daycare center differed from those in the health center: a larger portion of genome copies was found in particles  $>2.5 \mu\text{m}$  (50% versus 20%). This discrepancy could originate from the ways that viruses were released (from coughing, sneezing, talking, or breathing) and/or differences in the droplet size distribution of different age groups [24]. Viruses were likely released from latent subjects in the daycare center (children are sent home as soon as symptoms are apparent), whereas those released in the health center are assumed to come from symptomatic patients. Whether there are any differences between virus-laden particles released at different stages of infection and between hosts of different age warrants further investigation.

Virus concentrations of the two positive airplane samples were very similar ( $1.4 \times 10^4$  and  $1.1 \times 10^4$  genome copies  $\text{m}^{-3}$ ), and virus-laden particles were relatively evenly distributed across each size fraction (Figure 2.1e, f). It is possible that the diverse ages of airplane passengers evened out the difference observed in particular groups such as college students in the university health center and children in the daycare center.

Although this discussion has focused on the positive results, half of the samples were negative for IAVs. These negative results could be attributable to inhibitors to qRT-PCR, as observed by Chen *et al.* [6]. However, since the RNA extraction method adopted in this study has the potential to eliminate such inhibitions [4], it is more likely that in these instances, there were no infected individuals in the sampling locations or that concentrations were below the detection limit. The fact that the total virus concentration in the measurable samples ranged over a factor of only six, rather than orders of magnitude, seems surprising but could possibly be explained by the presence of only one or two infected individuals and similar AERs in each setting.

While the qPCR method is a powerful tool for determining the presence of viral genomic material, it does not indicate whether the virus is viable or not. Therefore, the results presented here are an upper limit on the concentration of viable viruses. On the other hand, the recovery efficiency of viruses spiked onto filters was roughly 50% across the two types of

filters used in this study, so the reported concentration of genome copies may be underrepresented by a factor of ~2. However, the true recovery efficiency is unknown because sample collection by impacting particles onto filters is not equivalent to spiking them onto filters from solution. Additionally, viral RNA may be subject to decay during extended sampling times. One important question to address in the future which could not be answered by qPCR is, “Are the viruses found across different sizes of particles equally viable, or are those in one size fraction more so?”

#### **2.4.2 Risk of airborne IAV infection**

Assuming a uniform airborne IAV concentration of  $1.6 \pm 0.9 \times 10^4$  copies  $\text{m}^{-3}$  air (corresponding to  $35.4 \pm 21.0$  TCID<sub>50</sub>  $\text{m}^{-3}$  air) and a adult breathing rate of  $20 \text{ m}^3 \text{ day}^{-1}$  [25], we estimate the inhalation doses during exposures of 1 h (for example, the duration of a clinical visit), 8 h (a workday), and 24 h to be  $30 \pm 18$ ,  $236 \pm 140$ , and  $708 \pm 419$  TCID<sub>50</sub>, respectively. Compared to the human infectious dose 50% (ID<sub>50</sub>) by aerosols of 0.6-3 TCID<sub>50</sub> [26], these doses are adequate to induce infection. In most instances, the measured concentration of airborne IAVs could be either over- or underestimated based on the sensitivity of the qRT-PCR assay. However, it is not our intent to imply that all the estimated amounts of airborne viral particles are infectious. Our results allow an accurate estimate of exposure to viral particles in air.

While illustrative, this calculation is subject to several limitations. First, the conversion from genome copies to TCID<sub>50</sub> is based on the ratio determined with the laboratory strain A/California/04/2009 (H1N1) rather than with samples from the field, where infectivity may decay due to environmental factors such as temperature, humidity, and UV radiation. Therefore, a more sensitive method that can determine the infectivity of IAVs is needed to assess the exposure risk more accurately.

Second, the exposure doses calculated above are cumulative over 1-24 h, while the ID<sub>50</sub> measured by Alford *et al.* [26] is based on inoculations completed within 1 min. In reality, viruses depositing within the respiratory tract will be cleared by mucociliary action instead of simply accumulating at the deposition sites [27]. Therefore, the exposure doses calculated in this study provide only the simplest estimation of the amount inhaled. Models taking into account particle deposition efficiency within the respiratory tract as well as host

defense mechanisms are needed to estimate the infection risk more accurately. The deposition efficiency of particles can range from less than 1% to nearly 100%, depending on particle size, density, airway geometry, and the individual's breathing pattern [21].

Third, the assumption of uniform concentrations throughout a room is complicated when accounting for true dispersion patterns from a point source and the existence of non-homogeneous ventilation.

Finally, only IAVs were measured in this study, so it did not account for infection risk due to the influenza B virus (IBV). However, according to the nationwide Weekly Influenza Surveillance by the U.S. World Health Organization (WHO) and National Respiratory and Enteric Virus Surveillance System (NREVSS) [28], the IBV accounted for only 0-3.3% of samples that tested positive for influenza viruses during the period 4 October 2009 to 10 April 2010. Therefore, underestimation due to exclusion of IBVs may be negligible.

On the other hand, the virus deposition flux to surfaces was estimated to be only  $13 \pm 7$  genome copies  $\text{m}^{-2} \text{h}^{-1}$ . Over an 8-h workday,  $106 \pm 60$  genome copies  $\text{m}^{-2}$  could accumulate on surfaces. This analysis suggests that all surfaces, not just those that come into direct contact with an infected host, can harbor influenza viruses, although they are not expected to survive beyond 2-3 days [29]. However, the amount deposited on surfaces via Brownian motion seems unlikely to produce infectious doses, as the surface-hand-nasal mucosa route requires transferring at least  $10^4$  TCID<sub>50</sub> from the surface [29]. This estimation does not account for deposition due to gravitational settling, which is important for larger particles and can result in higher deposition fluxes in the vicinity of emission.

## 2.5 Conclusions

The concentrations and size distributions of airborne influenza viruses were measured in a health center, a daycare facility, and airplanes by qRT-PCR. During the 2009-2010 flu season, 50% of the samples collected (8/16) contained influenza A viruses with concentrations ranging from 5800 to 37,000 genome copies  $\text{m}^{-3}$ . On average, 64% of virus-laden particles were found to be associated with particles smaller than 2.5  $\mu\text{m}$ , which can remain airborne for hours. Modeling of virus concentrations indoors suggests a source strength of  $1.6 \pm 1.2 \times 10^5$  genome copies  $\text{m}^3 \text{h}^{-1}$  and a deposition flux onto surfaces of  $13 \pm 7$  genome copies  $\text{m}^{-2} \text{h}^{-1}$ . Doses of  $30 \pm 18$ ,  $236 \pm 140$ , and  $708 \pm 419$  TCID<sub>50</sub> were estimated for 1-h, 8-h,

and 24-h exposures, respectively. As a whole, these results provide quantitative support for the possibility of airborne transmission of influenza.

### **Acknowledgments**

This material is based in part upon work supported by the National Science Foundation under Grant Number CBET-0547107. We thank A. Pruden for sharing laboratory space and equipment, J. Petruska for much assistance, K. Charoensiri of the university health center, and a daycare center in Blacksburg for allowing sampling in their facilities.

## TABLES AND FIGURES

**Table 2.1 Primers and probes of influenza A virus**

primer or probe	sequence	position <sup>a</sup>	reference
INFA-1	5' GGA CTG CAG CGT AGA CGC TT 3'	241-260	
INFA-2	5' CAT CCT GTT GTA TAT GAG GCC CAT 3'	406-429	
INFA-3	5' CAT TCT GTT GTA TAT GAG GCC CAT 3'	406-429	[15]
INFA probe	5' CTC AGT TAT TCT GCT GGT GCA CTT GCC A 3'	373-400	
senseA	5' AAG ACC AAT CCT GTC ACC TCT GA 3'	168-190	
antisenseA	5' CAA AGC GTC TAC GCT GCA GTC C 3'	241-262	[14]
influenza A probe	5' TTT GTG TTC ACG CTC ACC GT 3'	208-227	

<sup>a</sup>Aligned with A/PR/8/34(H1N1) segment 7 (M gene).

**Table 2.2 Virus recovery efficiency from polytetrafluoroethylene (PTFE) filters and control solutions (virus solution in PBS and virus solution only) spiked with  $2.4 \pm 0.1 \times 10^7$  genome copies. Samples were incubated for 2 h and then analyzed by qRT-PCR. Recovery efficiencies were significantly less than 100% with both filters.**

sample	amount of virus recovered		recovery efficiency
	(genome copies)		
	mean	s.d.	
25-mm filter	$9.6 \times 10^6$	$2.2 \times 10^6$	41%*
37-mm filter	$1.5 \times 10^7$	$3.1 \times 10^6$	62%*
PBS	$2.1 \times 10^7$	$2.4 \times 10^6$	87%
Virus solution only	$2.2 \times 10^7$	$2.6 \times 10^6$	91%

\*Recovery efficiency significantly less than 100%.

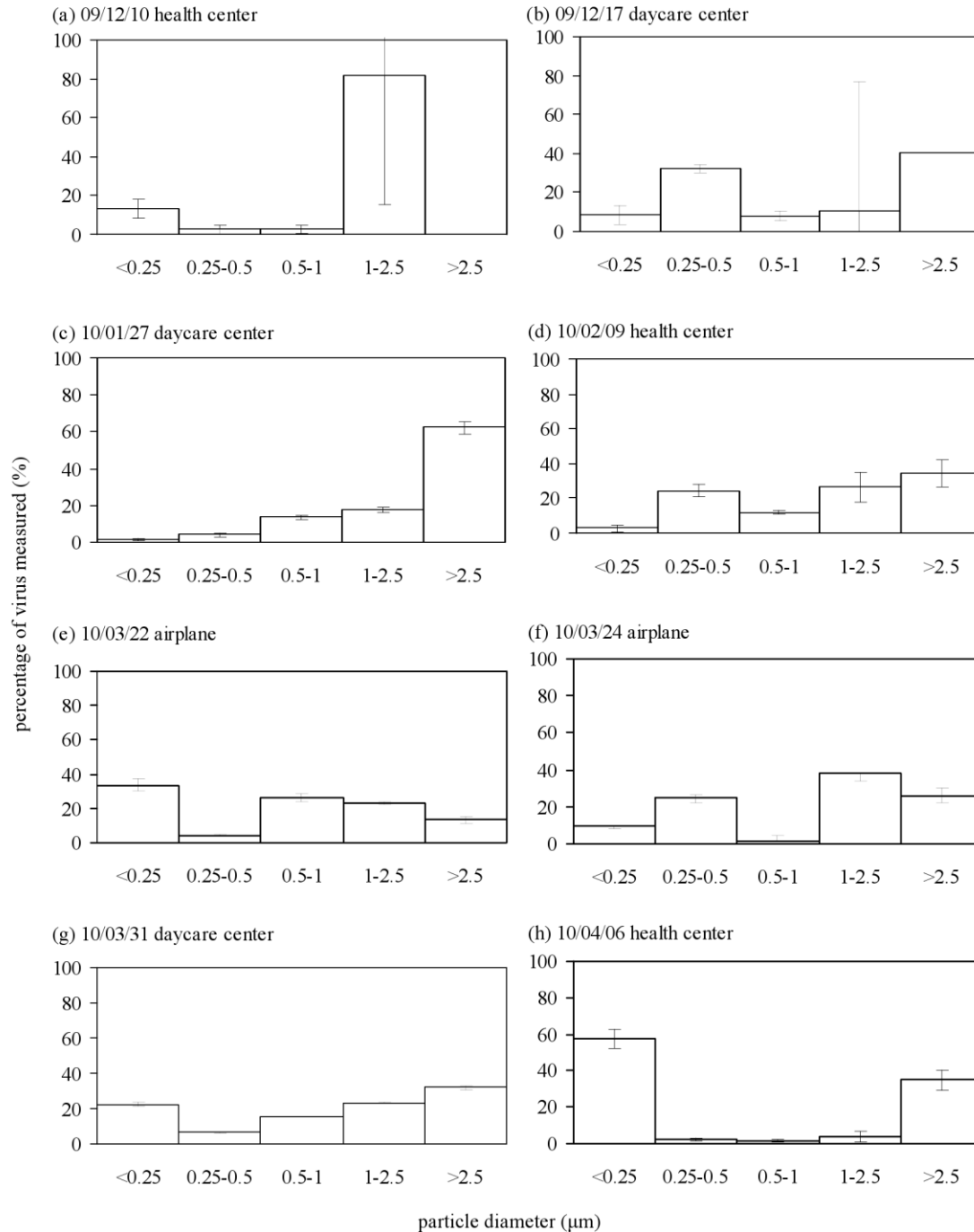


**Figure 2.1 Airborne IAV particle size distributions in each positive sample (yy/mm/dd and location shown at top). Aerosol samples were collected over 6-8 h in each location using a cascade impactor with cut-point diameters of 0.25, 0.5, 1.0, and 2.5  $\mu\text{m}$ . The y-axis indicates the percentage of total virus genome copies found in each size range. In seven of the eight cases, the majority of viruses were associated with fine particles smaller than 2.5  $\mu\text{m}$ , that can remain suspended for hours, but there were no obvious trends in size distributions across different samples.**

## References

1. Brankston, G., Gitterman, L., Hirji, Z., Lemieux, C., & Gardam, M. (2007). Transmission of influenza A in human beings. *Lancet Infect Dis*, *7*, 257-265.
2. Tellier, R. (2006). Review of aerosol transmission of influenza A virus. *Emerg. Infect. Dis.*, *12*(11), 1657-1662.
3. Tellier, R. (2009). Aerosol transmission of influenza A virus: A review of new studies. *J. R. Soc. Interface*, *6*(suppl 6), S783-S790.
4. Fabian, P., McDevitt, J. J., Lee, W.-M., Houseman, E. A., & Milton, D. K. (2009). An optimized method to detect influenza virus and human rhinovirus from exhaled breath and the airborne environment. *J. Environ. Monit.*, *11*(2), 314-317.
5. Fabian, P., McDevitt, J. J., Houseman, E. A., & Milton, D. K. (2009). Airborne influenza virus detection with four aerosol samplers using molecular and infectivity assays: Considerations for a new infectious virus aerosol sampler. *Indoor Air*, *19*(5), 433-441.
6. Chen, P.-S., Lin, C. K., Tsai, F. T., Yang, C.-Y., Lee, C.-H., Liao, Y.-S., et al. (2009). Quantification of airborne influenza and avian influenza virus in a wet poultry market using a filter/real-time qPCR method. *Aerosol Sci. Technol.*, *43*, 290-297.
7. Blachere, F. M., Lindsley, W. G., Pearce, T. A., Anderson, S. E., Fisher, M., Khakoo, R., et al. (2009). Measurement of airborne influenza virus in a hospital emergency department. *Clin. Infect. Dis.*, *48*(4), 438-440.
8. Lindsley, W. G., Blachere, F. M., Davis, K. A., Pearce, T. A., Fisher, M. A., Khakoo, R., et al. (2010). Distribution of airborne influenza virus and respiratory syncytial virus in an urgent care medical clinic. *Clin. Infect. Dis.*, *50*(5), 693-698.
9. Boone, S. A., & Gerba, C. P. (2005). The occurrence of influenza A virus on household and day care center fomites. *J. Infect.*, *51*(2), 103-109.
10. Wagner, B., Coburn, B., & Blower, S. (2009). Calculating the potential for within-flight transmission of influenza A (H1N1). *BMC Medicine*, *7*(1), 81.
11. Moser, M. R., Bender, T. R., Margolis, H. S., Noble, G. R., Kendal, A. P., & Ritter, D. G. (1979). An outbreak of influenza aboard A commercial airliner. *Am. J. Epidemiol.*, *110*(1), 1-6.
12. Lee, W.-M., Grindle, K., Pappas, T., Marshall, D. J., Moser, M. J., Beaty, E. L., et al.

- (2007). High-throughput, sensitive, and accurate multiplex PCR-microsphere flow cytometry system for large-scale comprehensive detection of respiratory viruses. *J. Clin. Microbiol.*, 45(8), 2626-2634.
13. Fabian, P., McDevitt, J. J., DeHaan, W. H., Fung, R. O. P., Cowling, B. J., Chan, K. H., et al. (2008). Influenza virus in human exhaled breath: An observational study. *PLoS ONE*, 3(7), e2691.
  14. Ward, C. L., Dempsey, M. H., Ring, C. J. A., Kempson, R. E., Zhang, L., Gor, D., et al. (2004). Design and performance testing of quantitative real time PCR assays for influenza A and B viral load measurement. *J. Clin. Virol.*, 29(3), 179-188.
  15. van Elden, L. J. R., Nijhuis, M., Schipper, P., Schuurman, R., & van Loon, A. M. (2001). Simultaneous detection of influenza viruses A and B using real-time quantitative PCR. *J. Clin. Microbiol.*, 39(1), 196-200.
  16. Munster, V. J., Baas, C., Lexmond, P., Bestebroer, T. M., Guldemeester, J., Beyer, W. E. P., et al. (2009). Practical considerations for high-throughput influenza A virus surveillance studies of wild birds by use of molecular diagnostic tests. *J. Clin. Microbiol.*, 47(3), 666-673.
  17. Yang, J.-R., Lo, J., Ho, Y.-L., Wu, H.-S., & Liu, M.-T. (2011). Pandemic H1N1 and seasonal H3N2 influenza infection in the human population show different distributions of viral loads, which substantially affect the performance of rapid influenza tests. *Virus Res.*, 155(1), 163-167.
  18. van der Vries, E., Jonges, M., Herfst, S., Maaskant, J., Van der Linden, A., Guldemeester, J., et al. (2010). Evaluation of a rapid molecular algorithm for detection of pandemic influenza A (H1N1) 2009 virus and screening for a key oseltamivir resistance (H275Y) substitution in neuraminidase. *J. Clin. Virol.*, 47(1), 34-37.
  19. Tompkins, J. A., White, J. A., Bozer, Y. A., & Tanchoco, J. M. A. (2010). *Facilities planning* (4th ed.): John Wiley & Sons, Inc.
  20. Mangili, A., & Gendreau, M. A. (2005). Transmission of infectious diseases during commercial air travel. *Lancet*, 365(9463), 989-996.
  21. Hinds, W. C. (1999). *Aerosol technology* (2nd ed., pp. 49). New York: Wiley.
  22. Poon, L. L., Chan, K. H., Smith, G. J., Leung, C. S., Guan, Y., Yuen, K. Y., et al. (2009).

- Molecular detection of a novel human influenza (H1N1) of pandemic potential by conventional and real-time quantitative RT-PCR assays. *Clin. Chem.*, 55(8), 1555-1558.
23. ATCC. (2009, 8/20/2009). Converting TCID<sub>50</sub> to plaque forming units (PFU) Retrieved July 1, 2010, from <http://www.atcc.org/CulturesandProducts/TechnicalSupport/FrequentlyAskedQuestions/tabid/469/Default.aspx>
24. Yang, S., Lee, G. W. M., Chen, C.-M., Wu, C.-C., & Yu, K.-P. (2007). The size and concentration of droplets generated by coughing in human subjects. *J. Aerosol Med.*, 20(4), 484-494.
25. U.S. EPA. (1994). *Methods for derivation of inhalation reference concentrations and application of inhalation dosimetry*.
26. Alford, R. H., Kasel, J. A., Gerone, P. J., & Knight, V. (1966). Human influenza resulting from aerosol inhalation. *Proc. Soc. Exp. Biol. Med.*, 122(3), 800-804.
27. Oberdorster, G. (1993). Lung dosimetry - pulmonary clearance of inhaled particles. *Aerosol Sci. Technol.*, 18(3), 279-289.
28. U.S. CDC. (2010, November 19, 2010). Seasonal influenza (flu) *Past Weekly Surveillance Reports* Retrieved November 23, 2010, from <http://www.cdc.gov/flu/weekly/pastreports.htm>
29. Bean, B., Moore, B. M., Sterner, B., Peterson, L. R., Gerding, D. N., & Balfour Jr, H. H. (1982). Survival of influenza viruses on environmental surfaces. *J. Infect. Dis.*, 146(1), 47-51.

### 3 Dynamics of Airborne Influenza A Viruses Indoors and Dependence on Humidity<sup>†</sup>

Wan Yang, Linsey C. Marr

Department of Civil and Environmental Engineering, Virginia Tech,  
Blacksburg, Virginia, United States of America

#### **Abstract**

There is mounting evidence that the aerosol transmission route plays a significant role in the spread of influenza in temperate regions and that the efficiency of this route depends on humidity. Nevertheless, the precise mechanisms by which humidity might influence transmissibility via the aerosol route have not been elucidated. We hypothesize that airborne concentrations of infectious influenza A viruses (IAVs) vary with humidity through its influence on virus inactivation rate and respiratory droplet size. To gain insight into the mechanisms by which humidity might influence aerosol transmission, we modeled the size distribution and dynamics of IAVs emitted from a cough in typical residential and public settings over a relative humidity (RH) range of 10-90%. The model incorporates the size transformation of virus-containing droplets due to evaporation and then removal by gravitational settling, ventilation, and virus inactivation. The predicted concentration of infectious IAVs in air is 2.4 times higher at 10% RH than at 90% RH after 10 min in a residential setting, and this ratio grows over time. Settling is important for removal of large droplets containing large amounts of IAVs, while ventilation and inactivation are relatively more important for removal of IAVs associated with droplets  $<5 \mu\text{m}$ . The inactivation rate increases linearly with RH; at the highest RH, inactivation can remove up to 28% of IAVs in 10 min. Humidity is an important variable in aerosol transmission of IAVs because it both induces droplet size transformation and affects IAV inactivation rates. Our model advances a mechanistic understanding of the aerosol transmission route, and results complement recent studies on the relationship between humidity and influenza's seasonality. Maintaining a high indoor RH and ventilation rate may help reduce chances of IAV infection.

---

<sup>†</sup>Published, open-access article. Yang, W., & Marr, L. C. (2011). Dynamics of airborne influenza A viruses indoors and dependence on humidity. PLoS ONE, 6(6), e21481.

**Funding:** This research was supported by the National Science Foundation under grant number CBET-0547107. No additional external funding was received for this study.

**Competing Interests:** The authors have declared that no competing interests exist.

### 3.1 Introduction

Influenza A has a clear seasonal pattern in temperate regions, yet the underlying cause for it remains controversial despite nearly a century of investigation. The literature identifies numerous factors that may influence influenza's seasonality: environmental conditions such as temperature, humidity, and ultraviolet radiation; immune function; school schedules; and human mobility patterns and contact rates [1]. Among these, the leading contenders are humidity and temperature [2-4], and in indoor environments, where people spend ~90% of their time, humidity is the more variable factor. Particularly in the developed world where heating, ventilation, and air conditioning systems (HVAC) are the norm, indoor temperature tends to fall in a narrower range, and thus its influence is limited. Recent studies using a guinea pig experimental model [3-4] indicate that low relative humidity (RH) favors aerosol transmission of influenza A viruses (IAVs), in which they are transmitted by small respiratory droplets expelled from infected hosts. Nevertheless, the precise mechanisms by which humidity might influence influenza viability and transmissibility via the aerosol route have not been elucidated.

Humidity may affect airborne IAV transmission via two important variables. The first is droplet size. When released from the respiratory tract (assumed to have 100% RH), droplets experience rapid evaporation and shrinkage upon encountering the unsaturated ambient atmosphere. The ultimate size of a droplet depends on ambient humidity, and size determines aerodynamic behavior and whether the droplet will settle to the ground quickly or remain suspended in the air long enough to possibly cause a secondary infection. Previous studies on evaporation of respiratory droplets usually used water or simple saline solutions (e.g., NaCl) to simulate respiratory fluid [5-6]. However, respiratory fluid is a complicated combination of water, salts, and various organic compounds [7-8] that affect the thermodynamics of evaporation, compared to pure water or saline solutions. The equilibrium droplet size is affected by surface curvature and solute effects, the combination of which is described by Köhler theory [9]. While the vapor pressure is enhanced over curved versus flat surfaces, it is reduced by the presence of solutes. These competing effects are magnified at smaller droplet diameters and determine the equilibrium size at a particular RH.

The second variable that is sensitive to humidity is IAV viability [2; 10-13]. Hemmes et al. [2] linked influenza's seasonality to the seasonal oscillation of RH indoors, based on their experiment on death-rate variation versus RH. Shaman and Kohn [14], on the other hand, concluded that absolute humidity (AH) rather than RH modulates influenza seasonality through constraint on viability, but whether AH or RH is controlling is under debate. For our

purposes, differentiating between the two is not possible because this work focuses on a narrow range of typical indoor temperatures. Finally, it is possible that the two variables—final droplet size and viability—are linked, if evaporation and subsequent concentration of solutes in respiratory droplets affects IAV viability in aerosols.

Elucidating the causes of influenza’s seasonality will require improved comprehension of transmission mechanisms, especially the aerosol route. To advance a mechanistic understanding of the role of humidity in aerosol transmission, we model the change in size of respiratory droplets and IAV inactivation at RHs ranging from 10% to 90%. Based on these results, we further model the dynamics of droplets emitted from a cough in an indoor environment and illustrate the evolution of infectious IAV concentrations and size distributions, considering removal by gravitational settling, ventilation, and viral inactivation. We are thus able to determine the magnitude by which humidity affects airborne concentrations of infectious IAVs.

## 3.2 Results

### 3.2.1 Initial size distribution of droplets expelled from a cough

We located seven papers that reported the size distribution of droplets expelled while coughing, sneezing, and speaking [6; 15-20]. The droplet diameter geometric mean (GM), size range, and droplet number varied greatly among the different studies, as summarized in Table 3.1. Because ~80% of patients with influenza manifest symptoms of coughing [21], we focus on droplets emitted from coughing to demonstrate the dynamics of airborne IAVs. Droplet diameters as small as 0.3  $\mu\text{m}$  and as large as 2000  $\mu\text{m}$  have been observed from coughing, and the GMs in the studies ranged from 0.25  $\mu\text{m}$  to 96.6  $\mu\text{m}$ , depending on the experimental methods used (Table 3.1). Four of the studies reported GMs in a much narrower range of 8.4  $\mu\text{m}$  to 16.0  $\mu\text{m}$ . We adopted Duguid’s [20] results on the basis of reliability of the methods and care and thoroughness of the experimental design and analysis. Though the study dates to 1946, its results were similar to those of more contemporary work that use modern aerosol characterization equipment [6; 17]. Similar to Nicas et al. [22], we found that droplets between 1-100  $\mu\text{m}$  from coughing follow a log-normal size distribution. Eq. 1 describes the relationship:

$$z = 1.216 \ln D_i - 3.113 \quad (r^2 = 0.997) \quad [1]$$

where  $D_i$  is the initial droplet diameter in  $\mu\text{m}$ , and  $z$  is the corresponding quantile of a normal distribution with the same cumulative probability. According to this relationship, the size distribution of droplets emitted from coughing has a GM of 12.9  $\mu\text{m}$  and a geometric

standard deviation (GSD) of 2.3 (Figure 3.1).

### 3.2.2 Respiratory droplet size transformation

Equilibrium droplet size is attained nearly instantaneously upon release. A 20- $\mu\text{m}$  droplet shrinks to one-half of its original diameter in less than half a second at 20  $^{\circ}\text{C}$  [22]. Table 3.2 shows the equilibrium, or final, diameters ( $D_{eq}$ ) of droplets with  $D_i$  of 0.1, 1, and 10  $\mu\text{m}$  at 10-90% RH. These were calculated based on a model of droplet transformation that assumes separate solutes and volume additivity (SS-VA) [23]. Due to the Kelvin effect, evaporation of smaller droplets is enhanced, and the equilibrium diameters are smaller. The ratio  $D_{eq}/D_i$  is 0.490 at 90% RH for a respiratory droplet with  $D_i = 0.1 \mu\text{m}$ , versus 0.516 under the same conditions for a larger one with  $D_i = 10 \mu\text{m}$ . However, the Kelvin effect is negligible for droplets with  $D_i > 0.1 \mu\text{m}$ , and  $D_{eq}/D_i$  is independent of RH for droplets larger than 1  $\mu\text{m}$ .

Efflorescence or crystallization of NaCl, a major component of respiratory droplets, due to loss of water is expected to occur between 40-50% RH [24]. According to our results, between 10-40% RH,  $D_{eq}/D_i$  varies by only 3.7% (0.402-0.417); in comparison, between 50-90% RH, the ratio varies by 21.7% (0.424-0.516). Respiratory droplets lose almost all their water at low RHs. For comparison, we also calculated the  $D_{eq}/D_i$  ratios based on volume additivity using experimental data on dehydration of droplets containing NaCl [25] and on hydration of those containing a glycoprotein [26]. Differences between modeled and experimental results are less than 4% (Table 3.2).

### 3.2.3 Inactivation of airborne IAVs

The viability of IAVs decreases over time and is affected by environmental variables such as temperature, humidity, and UV radiation [12; 27]. The inactivation rate ( $k$ ), derived from experimental data on airborne IAVs [12], is linearly correlated with RH (Figure 3.2), following the relationship

$$k = 0.0438RH - 0.00629 \quad [2]$$

with an  $r^2$  of 0.977 and  $p$ -values for the model, intercept, and slope of 0.0015, 0.059, and 0.0015, respectively.

### 3.2.4 Evolution of infectious IAV distribution after a cough

The well-mixed indoor air model we developed for infectious IAVs accounts for removal by gravitational settling, ventilation, and viral inactivation. The concentration of infectious IAVs associated with droplets of a specific diameter  $D_{eq}$  in a room at time  $t$  is

$$C = C_0 \exp\left[-\left(\frac{v}{H} + \lambda + k\right)t\right] \quad [3]$$

where  $C_0$  is the initial concentration of infectious IAVs associated with droplets of size  $D_{eq}$  in

the room,  $v$  is the settling velocity,  $H$  is the height of the room,  $\lambda$  is the air exchange rate (AER) and assumes no recirculation, and  $k$  is the inactivation rate. The inactivation rate  $k$  depends on RH, according to Eq. 2, and the settling velocity  $v$  depends on  $D_{eq}$ , which also depends on RH. Eq. 3 can be integrated over all droplet sizes to obtain the total concentration of infectious IAVs in a room. We calculate results for AERs of 1 air change per hour (ACH) and 10 ACH, typical of residential and public settings, respectively [28-29]. For simplicity, we assumed that room heights are the same in residences and public settings such as offices, classrooms, and hospitals, where people aggregate and thus have a higher risk of infection. The equation is applicable for a single rectangular room, does not depend on the volume of the room, and does not account for air exchange between multiple rooms.

Figure 3.3 shows the evolution of IAV concentrations in time in terms of both the total number of infectious viruses (Figure 3.3A and 3.3B) and size distribution (Figure 3.3C and 3.3D). Only emitted droplets with  $D_i \leq 100 \mu\text{m}$  are considered, as larger ones will be removed by gravitational settling within seconds. Following a single cough in a well-mixed room, the concentration of infectious IAVs is initially  $1.8 \times 10^3 \# \text{m}^{-3}$  under the assumptions of this study. Figures 3A and 3B show that the total number of infectious IAVs falls rapidly with time and that the loss is greater at higher RH and in public versus residential settings. If one infected person is continuously shedding viruses by coughing 15 times per hour [30], then the concentration of IAVs will be  $\sim 2 \times 10^3 \# \text{m}^{-3}$  in a public setting. This concentration is similar in magnitude to those measured in hospitals, medical clinics, day care facilities, and airplanes [31-33]. Under conditions of higher RH, removal by settling is more effective because droplets shrink less, and inactivation is more rapid. Removal of 99.9% of the IAVs emitted requires much greater time in a residential versus public setting, indicating that ventilation is an important removal mechanism and that airborne IAVs can persist for longer times in settings with lower AERs.

Figure 3.3C and 3.3D show that, at 50% RH, emitted droplets shrink to about half of their original diameters due to evaporation. Evaporation happens almost instantaneously [22], so while the initial size distribution at 0 min extends out to  $100 \mu\text{m}$ , all subsequent ones end at  $42 \mu\text{m}$  ( $D_{eq}/D_i = 0.42$ ). This process greatly increases the fraction of IAVs that are associated with smaller droplets, since the virus concentration within a droplet increases by a factor of 8 ( $2^3$ ) as its diameter shrinks by half. For instance, compared to the initial droplets emitted at 0 min, which quickly reach their equilibrium diameters, the number of IAVs associated with equilibrium droplet sizes smaller than  $25 \mu\text{m}$  increases by a factor of 5.2 at 50% RH. Due to more rapid settling, IAVs associated with larger droplets are lost faster than are

those associated with smaller ones. Consequently, IAVs associated with smaller droplets become more dominant over time, as indicated by the shifting of the peak of  $\Delta C/\Delta D_{eq}$  to the left in Figure 3.3C and 3.3D. The diameter of droplets containing the most IAVs (i.e., the mode of the distribution) shifts from  $\sim 50 \mu\text{m}$  upon release to  $\sim 16 \mu\text{m}$  at 1 min,  $\sim 10 \mu\text{m}$  at 10 min, and  $\sim 5 \mu\text{m}$  at 60 min in residential settings; a similar trend is shown in Figure 3.3D for public settings.

### 3.2.5 Humidity dependency and removal mechanisms

Figure 3.4 shows the effect of RH on size distributions of infectious IAVs, 10 min after a cough in residential and public settings. For both cases, IAV concentrations decrease with increasing RH across all sizes, but the modes of the distributions remain around 9-10  $\mu\text{m}$ . The total IAV concentration (i.e., the area under each curve) decreases with increased RH. As a result, it takes twice as long to remove 99.9% of IAVs emitted at 10% RH than that at 90% RH in residential settings ( $>100$  min at 10% RH versus  $<50$  min at 90% RH, as shown in Figure 3.3A).

Humidity affects both settling, because of its dependence on size transformation, and inactivation of IAVs. The relative importance of these two effects can be illustrated by comparing the ratios of virus concentrations at 10% RH versus those at 90% RH at varying times. The ratios increase approximately exponentially with time: 2.4 at 10 min, 5.4 at 30 min, and 16.1 at 60 min. If only inactivation were considered, these factors would instead be 1.4, 2.7, and 7.3, respectively; and if only settling were considered, the corresponding factors would be 1.7, 2.0, and 2.2, respectively. These ratios are independent of the ventilation rate. The much narrower range of factors for settling than for inactivation (i.e., 1.7-2.2 versus 1.4-7.3) indicates that RH has a greater impact on inactivation, especially over long periods ( $>30$  min).

Figure 3.5 shows the effectiveness of each removal mechanism—settling, ventilation, and inactivation—independently as a function of RH (Figure 3.5A and 3.5B) and droplet size (Figure 3.5C and 3.5D), 10 min following a cough. Figure 3.5A shows that gravitational settling is the dominant removal mechanism in residential settings. Settling alone removes over 80% of airborne IAVs within 10 min, and its removal efficiency increases slightly with RH, from 87% to 92% across the range of RHs. In contrast, ventilation only removes 15% of total IAVs, regardless of RH. Removal efficiency by inactivation increases with RH, accounting for up to 28% at the highest RH. Figure 3.5B shows that ventilation and gravitational settling are both important in removing airborne IAVs from public settings with higher AERs. At an AER of 10 ACH with no recirculation, ventilation removes 81% of

airborne IAVs. Settling and inactivation are independent of ventilation rate and remove the same amounts of IAVs as in residential settings.

Removal efficiencies for IAVs vary as a function of droplet size for settling but not ventilation or inactivation. Figure 3.5C and 3.5D show removal efficiency versus equilibrium droplet diameter at 50% RH, 10 min following a cough, for each mechanism individually and all three together. Because settling velocity scales with diameter squared, removal efficiencies due to gravitational settling range from only 0.7% for droplets with  $D_{eq} = 1 \mu\text{m}$  to 51.2% for those with  $D_{eq} = 10 \mu\text{m}$  to >98.8% for those with  $D_{eq} > 25 \mu\text{m}$ . Ventilation is equally effective for all sizes, with removal efficiencies of 15% in residential settings (Figure 3.5C) and 81% in public settings (Figure 3.5D), depending on the AER.

Overall, gravitational settling is the main removal mechanism in both residential and public settings (Figure 3.5A and 3.5B). It removes a disproportionately large fraction of IAVs because it favors larger droplets, which contain far more IAVs, as their numbers are proportional to the initial droplet volume, or  $D_i^3$ . However, settling is ineffective at removing droplets  $< 5 \mu\text{m}$ , as shown in Figure 3.5C and 3.5D. Ventilation is important in public settings and particularly so for removal of smaller droplets ( $< 5 \mu\text{m}$ ) for which settling is inefficient. It accounts for ~50% of total removal of IAVs associated with droplets  $< 5 \mu\text{m}$  in residential settings (Figure 3.5C) and ~80% in public settings (Figure 3.5D). Inactivation increases with RH and is maximal at 28% at 90% RH, 10 min following a cough (Figure 3.5A and 3.5B). Although the removal efficiency by inactivation is relatively low, it is important when removal by ventilation and settling are both minor. For instance, in residential settings (Figure 3.5C), inactivation accounts for ~50% of total removal of IAVs associated with droplets  $< 5 \mu\text{m}$ .

### 3.3 Discussion

#### 3.3.1 Removal of infectious IAVs

Higher RH favors removal of infectious IAVs. Since larger droplets have greater settling velocities, higher RHs, at which  $D_{eq}/D_i$  is larger, thereby will accelerate the removal rate. Additionally, the inactivation rate of IAVs increases with increasing RH (Eq. 2). According to our model, the concentration of airborne IAVs resulting from a cough would be reduced by 10% if the RH increases from 35%, the mean indoor RH in heating season [30], to 50%, 10 min following the cough, and by 40% after 1 h in residential settings. These estimates agree in magnitude with those reported by Myatt et al. [30], whose model suggests that influenza virus survival decreases by 17.5-31.6% when indoor RH increases by 11-19% over 15 h. Hence, maintaining a reasonably high indoor RH (e.g., 50%) may accelerate the removal of

infectious IAVs and help prevent or reduce influenza infection.

The relative importance of the two mechanisms—droplet size transformation and inactivation—as a function of humidity is of interest. Shaman and Kohn [14] concluded that AH modulates influenza transmission by influencing the virus' survival rate, rather than by enhancing production of airborne droplet nuclei in low humidity conditions. We found that respiratory droplets would shrink to one-half of their original diameters at 90% RH, and to around two-fifths at 10% RH. It thus appears that changes in droplet size are dramatic at unsaturated RHs and that variations due to differences in RH are relatively trivial. Our analysis shows that removal by inactivation is more variable with RH than is removal by settling. This may explain why Shaman and Kohn [14] could find a statistically significant relationship between AH and influenza survival but not transmission. However, this does not suggest that droplet shrinkage in response to unsaturated RHs is not important for influenza transmission, only that it is not as obvious as the induced change in viability.

We have demonstrated the relative importance of the three removal mechanisms. Settling can remove over 80% of droplets emitted from a cough within 10 min; however, it is effective only for larger droplets and allows the smaller ones ( $<5 \mu\text{m}$ ) to remain suspended. In contrast, ventilation is able to remove all droplets regardless of size simply by air exchange. Therefore, higher AERs will facilitate the elimination of virus-containing droplets from indoor environments, especially to compensate for the inefficacy of settling in removing the small ones. This observation also justifies the requirement to maintain a high AER in public places (e.g., 12 ACH in hospital waiting areas [34]). Removal efficiencies due to virus inactivation are relatively small (i.e., 0-28% in 10 min, if only inactivation were considered). However these estimates are based on experimental data reported by Harper [12], which indicated lower inactivation rates of  $0.0031\text{-}0.028 \text{ min}^{-1}$  at 20-81% RH, compared to  $0.0073 \pm 0.0031 \text{ min}^{-1}$  at 15-40% RH and  $0.091 \pm 0.024 \text{ min}^{-1}$  at 50-90% RH, as reported by Hemmes [2]. If estimated Hemmes' data [2], the corresponding removal efficiencies would be larger: 7.0% at 15-40% RH and 59.8% at 50-90% RH. Virus inactivation may thereby play a more significant role depending on the actual inactivation rate.

### **3.3.2 IAV viability, seasonality, and humidity dependency**

Experimental and/or theoretical models have been constructed to predict the viability of airborne IAVs as a function of humidity [14; 35], but a widely accepted mechanistic explanation for the relationship is still lacking. Studies on the effect of humidity agree that IAVs survive better at lower RHs. However, Hemmes [2; 11] and Harper [12] found higher inactivation rates at both medium and high RHs, in contrast to Shechmeister [10] and

Schaffer et al. [13], who found higher inactivation rates at medium but not high RHs. This disparity may stem from the different compositions of media used in each experiment. All media contained salts (approximately 0.5-3%); however, those used in the former two experiments contained far more proteins than did those in the latter two. High concentrations of salts are found to be detrimental to avian IAVs [36]. As water in the droplets evaporates, solute concentrations increase and may consequently accelerate IAV inactivation. However, an NaCl droplet can suddenly lose all of its water and crystallize at the point of efflorescence (45-48% RH) [25], thus eliminating the negative effect of dissolved salts at low RHs. This effect is perceivable in Table 3.2, which shows that  $D_{eq}/D_i$  varies little when  $RH \leq 40\%$ . The combination of increasing salt concentrations followed by efflorescence as RH decreases may explain the trend observed by Shechmeister [10] and Schaffer et al. [13].

Additionally, a study on aerosol transmission between guinea pigs [3] indicated that transmission was inversely related to RH at 5 °C, although experiments at 20 °C showed a lower transmission rate at 50% RH than at 65% RH. As 0% transmission was observed at 80% RH, the inconsistent result at 50% or 65% RH may be due to the stochastic nature of infection. If higher transmission rates are due to higher viabilities, at least in part, these results appear to agree with the trend reported by Hemmes [2; 11] and Harper [12]. Given the similar constitution of droplets emitted from infected human and guinea pigs (i.e., salts plus proteins), it seems reasonable to believe that IAVs associated with droplets expelled from humans will be subject to higher inactivation at higher RHs.

The relationship between IAV viability and RH may be due to interactions among components of respiratory droplets (i.e., glycoproteins, salts, and water) and the virus that are sensitive to concentration, which depends on the extent of evaporation, which depends in turn on ambient humidity. Proteins may complicate the effect of salt ions on IAVs by interacting with the salt ions and counteracting their adverse effects. Studies have shown that IAVs remain infectious much longer in the presence of respiratory mucus [37-38]. Investigation into such interactions and the possible complexes formed in respiratory droplets in response to humidity variation at a molecular level is needed.

We speculate that the seasonality of influenza with its wintertime peak in temperate regions is stimulated by more vigorous evaporation of droplets at low RHs leading to higher suspended concentrations of IAVs, combined with the sensitivity of aerosolized IAVs' viability to RH. When RH is <90%, droplets shrink approximately in half, leaving associated IAVs that can remain suspended long enough to cause secondary infections. Our recent measurements of size-resolved airborne IAV concentrations support this assertion: 64% of the

IAV genomes detected in a daycare center, a health center, and airplanes were associated with fine particles  $<2.5 \mu\text{m}$  (15% in the  $0.25\text{--}0.5 \mu\text{m}$  fraction, 10% in the  $0.5\text{--}1.0 \mu\text{m}$  fraction, and 28% in the  $1.0\text{--}2.5 \mu\text{m}$  fraction) [33]. These particles can remain suspended for hours to days. Because of the many factors involved in infection, it is still not clear which size of droplets is most likely to transmit influenza, nor is it clear which region in human airways is most susceptible to influenza infection. However, if we simply consider deposition efficiency in human airways, the droplet size with the highest deposition efficiency ( $\sim 95\%$ ) in all regions of the airways combined is  $\sim 5 \mu\text{m}$ . For such droplets, deposition efficiency is  $\sim 10\%$  in the tracheobronchial and alveolar regions; the majority of the droplets deposit in the nasopharyngeal region. The droplet size with the highest deposition efficiency ( $\sim 17\%$ ) in the tracheobronchial and alveolar regions is  $\sim 2.5 \mu\text{m}$  [39]. Thus these smaller droplets have greater potential both to remain suspended and to deposit deeper into human airways.

At extremely high RHs, for example, close to 100% in tropical regions during the rainy season, the droplets do not shrink as much ( $D_{eq}/D_i = 0.927$  at 99% RH, and 0.755 at 98% RH, according to our calculations). Droplets thus settle more quickly, rendering the aerosol route relatively less important. However, due to less evaporation, salts and glycoproteins remain at concentrations closer to those found in the respiratory tract, and these concentrations are not detrimental to the virus. As suggested by Lowen et al. [40-41], other transmission routes (e.g., contact) may dominate in the tropics. They also proposed that the airborne route's sensitivity to RH and temperature contributes to seasonality in temperate regions while the contact route's insensitivity to the two variables contributes to year-round influenza in tropical regions. Our analysis supports this hypothesis.

### **3.3.3 Model limitations**

There are several limitations of our model. First, although the model used to predict equilibrium droplet sizes has been confirmed with experiments using NaCl-bovine serum albumin (BSA) particles [23], further verification with actual respiratory fluid is needed due to its complex composition. Furthermore, the composition of respiratory fluid depends on the emission site (nose or mouth) and source (upper or lower respiratory tract), as well as the stage of infection. Inflamed airways secrete larger amounts of mucus which consequently increase the dry mass of respiratory fluid [42]. Therefore, the equilibrium size of emitted droplets may be larger than presented here based on composition under healthy conditions. On the other hand, saliva has much lower concentrations of salts and glycoproteins [43-44], due to dilution by which droplets emitted from coughing may have lower dry mass.

Second, the model is based on limited data obtained from laboratory experiments. Not

only are Harper [12] and other studies of IAV viability in aerosolized droplets [10-11; 13] decades old, but none investigated inactivation rates as a function of droplet size. More accurate measurements concerning the influence of respiratory droplet size on IAV viability are needed to better predict the fate of airborne IAVs.

Third, we calculated the IAV concentration based on a well-mixed room model with no recirculation. This model assumes that droplets are instantaneously, continuously, and evenly distributed throughout the room. However, according to Lai and Cheng [45], it takes at least 270 s for 10- $\mu\text{m}$  droplets to mix thoroughly at 5 ACH. It may take even longer for the system to become well-mixed at lower AERs. More accurate calculations may be achieved by the use of computational fluid dynamics. Additionally, if recirculation accounts for a large fraction of the AER and if viruses are not removed in the HVAC system, then ventilation will play a relatively smaller role in virus removal compared to settling and inactivation.

Finally, this research demonstrates the evolution of IAV concentrations induced by a cough but not other activities, such as normal respiration, talking, and sneezing. Fabian et al. [46] determined that IAV RNA (i.e., potentially infectious IAVs) was emitted in exhaled breath from infected patients at a rate of  $<3.2$  to  $20$  RNA particles  $\text{min}^{-1}$ . These droplets were smaller than those associated with a cough; over 87% of them were  $<1$   $\mu\text{m}$  in diameter. Therefore, for IAVs exhaled during normal breathing, because of the smaller droplet size, airborne IAV concentrations would be lower and removal would rely more on ventilation and inactivation than gravitational settling. IAVs may also be expelled during talking, although to our knowledge, no detailed experimental data on this phenomenon are currently available in the literature. The droplet size distribution for talking is similar to that for coughing (Table 3.1). Therefore, model results are expected to be similar for IAVs generated by talking in terms of removal efficiencies by different mechanisms. Sneezing is a far less common clinical manifestation of influenza than is coughing, which is manifested in  $\sim 80\%$  of patients [21; 46-48]. The main difference between sneezing and coughing is that the former generates far more droplets, especially smaller ones. Thus, IAV concentrations would be higher initially, and ventilation would play a larger role in removal.

### **3.4 Methods**

#### **3.4.1 Equations for generating the initial respiratory droplet size distributions**

From data on the size distribution of droplets expelled in a cough [20], we considered counts of droplets with  $D_i \leq 100$   $\mu\text{m}$ . The standard normal distribution  $z$ -value with the same cumulative probability as that for droplets with a diameter  $D_i$  was computed by the NORMSINV function in Excel 2007. The equation of the least-squares linear regression

between  $z$  and  $\ln D_i$  is shown in Eq. 1 and Figure 3.1.

The initial size distribution of droplets ( $\leq 100 \mu\text{m}$ ) from coughing was then generated by the NORMSDIST function in Excel 2007:

$$n_i = N \times (\text{NORMSDIST}(z_{i,upper}) - \text{NORMSDIST}(z_{i,lower})) \quad [4]$$

where  $n_i$  is the droplet count in the  $i$ th size bin (5- $\mu\text{m}$  step in this study),  $N$  is the total number of droplets  $\leq 100 \mu\text{m}$  (i.e., 4775 according to Duguid [20]), and  $z_{i,upper}$  and  $z_{i,lower}$  are the upper and lower  $z$  values of the  $i$ th size bin.

### 3.4.2 Model for calculating equilibrium respiratory droplet size

The equilibrium droplet sizes resulting from evaporation were estimated based on Köhler theory taking into account the two major constituents of respiratory fluid: inorganic salts and glycoproteins. Effros et al. [7] determined concentrations (mean  $\pm$  standard error) of the major electrolytes to be, respectively,  $91 \pm 8$  (Na),  $60 \pm 11$  (K), and  $102 \pm 17$  (Cl) mM, of glycoproteins to be  $76.3 \pm 18.2 \text{ g L}^{-1}$ , and of lactate to be  $44 \pm 17$  mM. We thereby assume respiratory fluid contains 150 mM ( $8.8 \text{ g L}^{-1}$ ) NaCl to represent the inorganic components and  $76 \text{ g L}^{-1}$  of total proteins (TP) to approximate the organic components, as done by Nicas et al. [22].

The SS-VA model derived by Mikhailov et al. [23] is based on the physiochemical properties (practical osmotic coefficients, molecular weights, and densities of the component solutes, etc.) of the droplet and the Kelvin effect. Their modeling results for particles with 90% BSA (dry mass fraction) fitted well with experimental data for dehydration of mixed NaCl-BSA particles. Given the similar composition of respiratory fluid (89.6% TP in dry mass) to their NaCl-BSA particles, we applied their SS-VA model to compute the equilibrium size for respiratory droplets.

The SS-VA model predicts the equilibrium RH with a specific droplet diameter ( $D_{eq}$ ) to be:

$$RH = \exp\left(\frac{4\sigma M_w}{\rho R T D_{eq}} - \frac{M_w}{\rho_w ((D_{eq} - D_{m,s})^3 - 1)} \sum_y \frac{v_y \Phi_y \rho_y x_{s,y}}{M_y}\right) \quad [5]$$

where,  $\sigma$  is the surface tension (approximated by that of water as done in Mikhailov et al. [23], i.e.,  $0.072 \text{ N m}^{-1}$ );  $M$  is the molar mass, the subscripts  $w$  and  $y$  refer to water and component  $y$  (either NaCl or TP), respectively, and  $M_w = 18 \text{ g mol}^{-1}$ ,  $M_{NaCl} = 58.4 \text{ g mol}^{-1}$ ,  $M_{TP} \approx M_{BSA} = 66.5 \times 10^3 \text{ g mol}^{-1}$ ;  $\rho$ ,  $\rho_w$ ,  $\rho_y$  are the densities of the entire droplet, water, and component  $y$  ( $\rho_{NaCl} = 2165 \text{ kg m}^{-3}$ ,  $\rho_{TP} \approx \rho_{BSA} = 1362 \text{ kg m}^{-3}$ ), respectively;  $R$  is the ideal gas constant;  $T$  is the absolute temperature (298 K in this study);  $D_{eq}$  is the equilibrium diameter of a droplet

residue at a given RH;  $D_{m,s}$  is the mass equivalent diameter of a particle consisting of the dry solutes;  $v_y$  is the stoichiometric dissociation number of component  $y$ ,  $v_{NaCl} = 2$ , and  $v_{TP} = v_{BSA} = 1$ ;  $\Phi_y$  is the molal or practical osmotic coefficient of component  $y$  describing the non-ideality of the solution; and  $x_{s,y}$  is the mass fraction of component  $y$  ( $x_{NaCl} = 0.104$  and  $x_{TP} = 0.896$  in this study). Given  $D_i$ , the mass equivalent diameter,  $D_{m,s}$  can be calculated and used as an input to further calculate  $D_{eq}$  with its equilibrium RH.

### 3.4.3 Virus inactivation rate

Harper [12] performed a detailed study on the viability of airborne IAVs over a wide range of both RH and temperature. In the experiment, droplets containing IAVs were generated with an atomizer and stored in a drum turning at 3 rpm, and results were corrected for physical loss by settling and other deposition mechanisms. We used his viability data at 20-24.5 °C, typical indoor temperatures, at RHs ranging from 20% to 81% to calculate inactivation rates as a function of RH (Table 3.3). Because the residence time of air indoors is typically 1-2 h at most, we considered viability data from the first 1 h of the experiment only.

We quantified viability by assuming that airborne IAVs undergo first-order inactivation upon emission, such that,

$$\frac{dN}{dt} = -kN \quad [6]$$

where  $N$  is the number of IAVs emitted,  $t$  is time, and the inactivation rate ( $k$ ) is

$$k = -\frac{\ln\left(\frac{N_t}{N_0}\right)}{t} = -\frac{\ln S_t}{t} \quad [7]$$

where  $N_0$  and  $N_t$  are the numbers of IAVs at  $t = 0$  and time  $t$ , and  $S_t$  is the survival rate, or viability (%) at time  $t$ . Accordingly, we computed  $k$  for each RH from the  $S_t$  data reported by Harper [12] using the SLOPE function in Excel 2007 (Table 3.3). The equation of the least-squares linear regression between  $k$  and  $RH$  is shown in Eq. 2.

### 3.4.4 Concentration of infectious IAVs indoors

The model for estimating the concentration of infectious IAVs assumes that they are emitted from a cough and instantaneously well-mixed within the whole indoor space such that IAV concentrations in the room and outlet air are the same. The IAVs are subjected to removal by ventilation, inactivation, and gravitational settling. Droplet size transformation is assumed complete at time zero, and  $D_{eq}$  was used for the calculation. Assuming the inlet air contains no IAVs, the change of IAV concentration with time is modeled as:

$$\frac{dC}{dt} = -\left(\frac{v}{H} + \lambda + k\right)C \quad [8]$$

where  $C$  is the infectious IAV concentration in the room and outflow ( $\# \text{ m}^{-3}$ );  $v$  is the gravitational settling velocity calculated by Stokes law based on  $D_{eq}$ ;  $H$  is assumed to be 2.5 m in this study;  $\lambda$  is the air exchange rate assuming no recirculation; and  $k$  is the inactivation rate given by Eq. 2.

At time zero, IAVs are released from a cough, and the initial concentration of IAVs associated with droplets in the  $i$ th size bin,  $C_{i,0}$  ( $\# \text{ m}^{-3}$ ) is

$$C_{i,0} = 0.778 \times 6.3 \times 10^{-3} \times \left( \frac{\pi}{24} \times \frac{D_{i,upper}^4 - D_{i,lower}^4}{D_{i,upper} - D_{i,lower}} \right) \left( \frac{n_i}{V} \right) \quad [9]$$

where 0.778 is the initial survival rate (i.e., the average survival rate at 1 s according to the results of Harper [12]);  $6.3 \times 10^{-3}$  is the IAV concentration in respiratory fluid ( $\# \mu\text{m}^{-3}$ ) obtained by assuming that the respiratory fluid contains the same concentration of IAV as in nasal washes of infected persons ( $6.3 \pm 0.3 \times 10^6$  median tissue culture infectious dose (TCID<sub>50</sub>) mL<sup>-1</sup> [49]) and that 1 TCID<sub>50</sub> equals 1000 virus particles [50]; the term in the first set of parentheses is the mean droplet volume for the bin;  $D_{i,upper}$  and  $D_{i,lower}$  are, respectively, the upper and lower diameters of the  $i$ th size bin ( $\mu\text{m}$ );  $n_i$  is the droplet count for the  $i$ th size bin given in Eq. 4, and  $V$  is the room volume (assumed to be 50 m<sup>3</sup>). The solution for  $C$  is given in Eq. 3.

### 3.4.5 Removal efficiency of settling, ventilation, and inactivation

Removal efficiency in this study refers to the percentage of IAVs removed by a certain mechanism (i.e., settling, ventilation, inactivation, or a combination of these three) at a given time and RH. In Figure 3.5, removal efficiencies of settling ( $E_{settlng}$ ), ventilation ( $E_{vent}$ ), and inactivation ( $E_{inactivation}$ ), and total removal efficiency ( $E_{total}$ ) are calculated by Eq. 10-13:

$$E_{settlng} = 1 - \exp\left(-\frac{v}{H} t\right) \quad [10]$$

$$E_{vent} = 1 - \exp(-\lambda t) \quad [11]$$

$$E_{inactivation} = 1 - \exp(-kt) \quad [12]$$

$$E_{total} = 1 - \exp\left[-\left(\frac{v}{H} + \lambda + k\right)t\right] \quad [13]$$

### Acknowledgments

We thank Dr. E. Subbiah for reviewing this work and offering insightful suggestions to improve it.

**Author Contributions**

Conceived and designed the experiments: WY LCM. Performed the experiments: WY.  
Analyzed the data: WY LCM. Wrote the paper: WY LCM.

## TABLES AND FIGURES

**Table 3.1 Prior studies of respiratory droplet size distributions**

Activity	Droplet size ( $\mu\text{m}$ )		Droplet number	Experimental conditions	Measurement methods	Adjustment for evaporation <sup>b</sup>	Reference
	GM (GSD) <sup>a</sup>	Range					
Cough	12.1 (2.6) <sup>c</sup>	1-2000	5000	NA	Microscope	Factor of 4	[20]
	16.0 (5.8) <sup>d</sup>	1->1471	466	NA	Bone paper and 0.45- $\mu\text{m}$ filter	As measured	[15]
	0.5 (1.7) <sup>e</sup>	<0.6-2.5	420	24 °C, 45%RH; 35 °C, 23%RH	Optical particle counter (OPC), electron microscope	As measured	[16; 22]
	8.4 (2.2)	NA	NA	95% RH	Aerodynamic particle sizer (APS), scanning mobility particle sizer, OPC	As measured, assumed to be the original size	[17]
	13.5 <sup>f</sup>	2-1000	NA	24.9 °C, 73.9% RH	Interferometric Mie imaging (>2 $\mu\text{m}$ ), particle image velocimetry	As measured	[6]
	1.8 <sup>g</sup>	0.3-20	NA	27 °C, 59.4% RH	Expiratory droplet investigation system, APS	As measured	[18]
	96.6 (2.4) <sup>h</sup>	0-1500	42	28 °C, 70% RH	Microscope, aerosol spectrometer	Factor of 3	[19]
Sneeze	8.2 (2.3) <sup>c</sup>	1-2000	$1 \times 10^6$	NA	Microscope	Factor of 4	[20]
	11.9 (2.8) <sup>c</sup>	1-1000	252	NA	Microscope	Factor of 4	[20]
Speak <sup>i</sup>	16 <sup>f</sup>	2-1000	NA	24.9 °C, 73.9% RH	Interferometric Mie imaging (>2 $\mu\text{m}$ ), particle image velocimetry	As measured	[6]
	62.1 (1.8) <sup>h</sup>	0-1000	253	28 °C, 70% RH	Microscope, aerosol spectrometer	Factor of 3	[19]

<sup>a</sup>Geometric mean (GM) and geometric standard deviation (GSD) calculated by methods presented in [51] or cited as reported in the original papers. <sup>b</sup>Whether droplet sizes were adjusted upward to account for evaporation or were reported as measured. <sup>c</sup>Calculated from data in Table 3 in [20]. <sup>d</sup>Calculated from data in Table 1 in [15]; droplet diameter upper end assumed to be 2000  $\mu\text{m}$ . <sup>e</sup>Calculated from data in Table IV in [22]. <sup>f</sup>No data on GSD reported. <sup>g</sup>Reported modal diameter. <sup>h</sup>Calculated from data in Table 2 in [19], only results from experiments without food dye were used. <sup>i</sup>Counting aloud from 1 to 100.

**Table 3.2 Respiratory droplet size transformation**

RH	Model-based $D_{eq}/D_i$ ratios <sup>a</sup>			Experimentally derived	Diff. <sup>c</sup>
	$D_i = 0.1 \mu\text{m}$	$D_i = 1 \mu\text{m}$	$D_i = 10 \mu\text{m}$	$D_{eq}/D_i$ ratios <sup>b</sup>	
10%	0.401	0.402	0.402	0.391	2.61%
20%	0.407	0.407	0.407	0.395	3.06%
30%	0.412	0.412	0.412	0.398	3.42%
40%	0.416	0.417	0.417	0.401	3.98%
50%	0.422	0.423	0.424	0.427	-0.90%
60%	0.429	0.431	0.432	0.437	-1.19%
70%	0.439	0.443	0.444	0.449	-1.20%
80%	0.456	0.464	0.465	0.464	0.02%
90%	0.490	0.513	0.516	0.502	2.63%

<sup>a</sup>Calculated according to the SS-VA model of Mikhailov et al. [23]. <sup>b</sup>Calculated based on volume additivity using experimental data from Tang et al. [25] and Bagger et al. [26].

<sup>c</sup>Difference between modeled and experimental  $D_{eq}/D_i$  ratios for  $D_i = 10 \mu\text{m}$ .

**Table 3.3 Inactivation of airborne IAVs at 20-24.5 °C over 1 h**

T (min)	Viability ( $S_t$ ) at different RHs <sup>a</sup>				
	20-22%	34-36%	50-51%	64-65%	81%
0.017 (1 s)	0.75	0.86	0.84	0.77	0.67
5	0.77	0.93	0.62	0.45	0.55
30	0.65	0.58	0.49	0.29	0.22
60	0.64	0.59	0.29	0.15	0.13
Inactivation rate					
RH <sup>b</sup>	21%	35%	51%	65%	81%
$k^c$	0.0031	0.0078	0.016	0.024	0.028
Intercept <sup>d</sup>	-0.28	-0.14	-0.27	-0.47	-0.48
$r^{2e}$	0.82	0.74	0.96	0.94	0.97

<sup>a</sup>Experimental data from Harper [12]. <sup>b</sup>Average RH. <sup>c</sup> $k$  = slope of  $\ln(S_t)$  versus  $t$ . <sup>d</sup>Intercept of the plot of  $\ln(S_t)$  versus  $t$ . <sup>e</sup> $r^2$  of the plot of  $\ln(S_t)$  versus  $t$ .

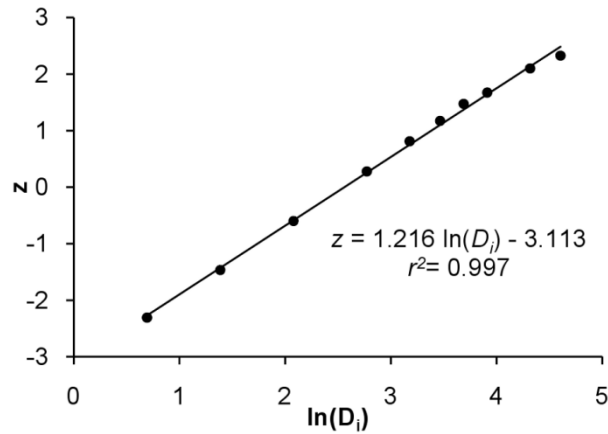


**Figure 3.1** Log-probability plot of droplet size distribution from a cough, adapted from Duguid [20].  $D_i$  is the initial droplet size in  $\mu\text{m}$ , and  $z$  is the corresponding quantile of a normal distribution with the same cumulative probability.

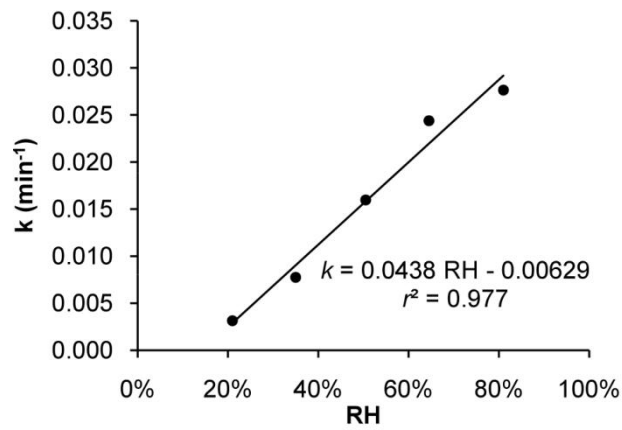


**Figure 3.2** IAV inactivation rate versus RH. IAV inactivation rates ( $k$ ) for each RH over 1 h were calculated based on experimental data adapted from Harper [12].

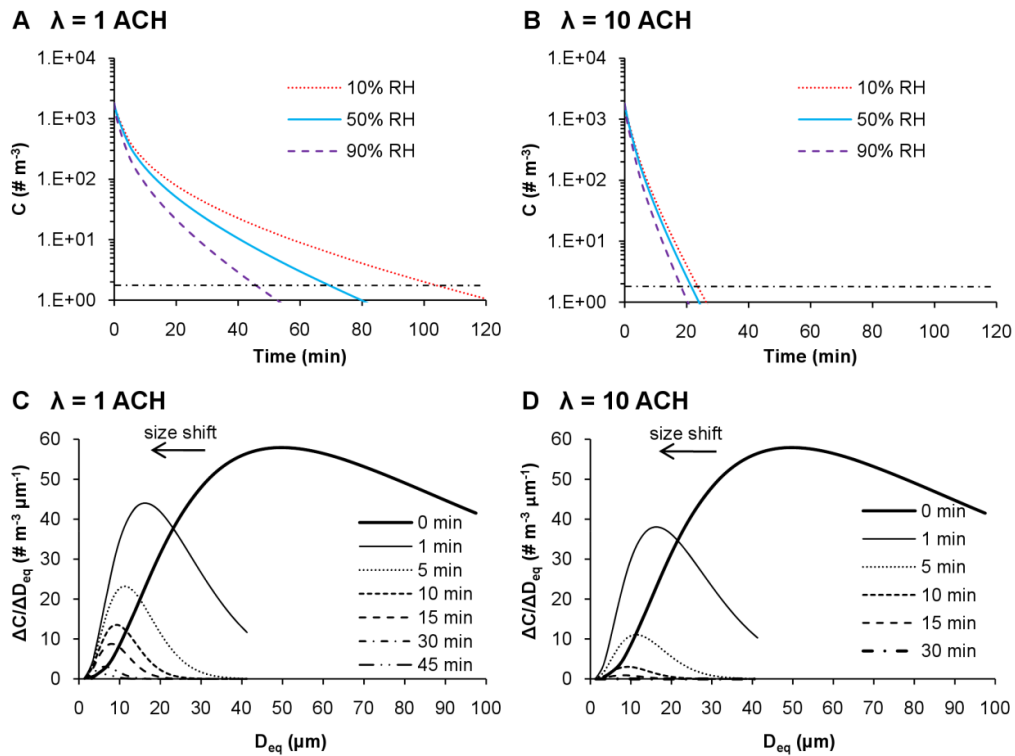


**Figure 3.3 Evolution of infectious airborne IAV concentrations and size distributions. Time series of airborne, infectious IAV concentrations following a cough into residential (A) and public (B) settings at 10-90% RH. The horizontal dashed line indicates 99.9% removal. Evolution over time of airborne, infectious IAV size distribution following a cough into residential (C) and public (D) settings at 50% RH.**

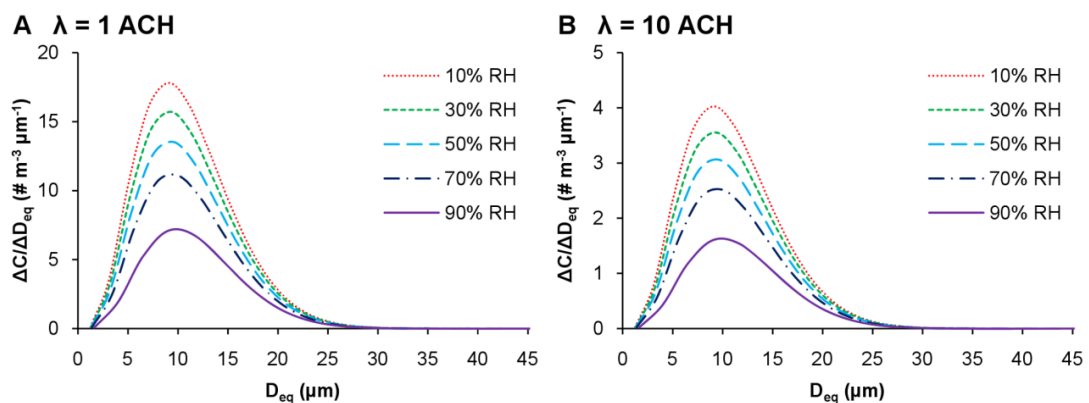


**Figure 3.4 IAV size distributions. Infectious IAV size distributions at various RHs in residential (A) and public (B) settings with a volume of 50 m<sup>3</sup> and a height of 2.5 m, 10 min after a cough.**

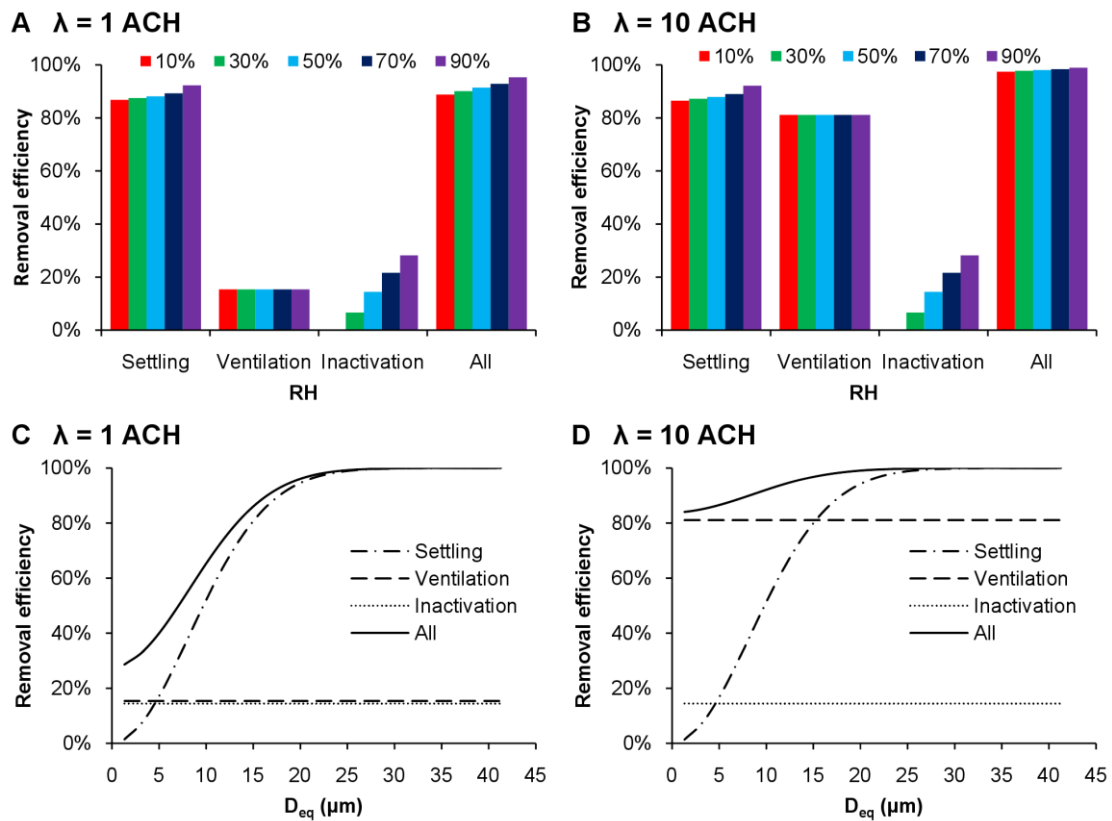


**Figure 3.5 IAV removal mechanisms. Infectious IAV removal efficiencies due to settling, ventilation, and inactivation in residential (A) and public (B) settings at different RHs. Removal efficiency of settling, ventilation, and inactivation as a function of droplet size in residential (C) and public (D) settings at 50% RH. Removal efficiencies are shown for each mechanism independently and do not sum to 100% because in actuality, more than one mechanism may act on the same virus/droplet.**

## References

1. Tamerius, J., Nelson, M., Zhou, S., Viboud, C., Miller, M., & Alonso, W. (2011). Global influenza seasonality: Reconciling patterns across temperate and tropical regions. *Environ. Health Perspect.*, *119*(4), 439-445.
2. Hemmes, J. H., Winkler, K. C., & Kool, S. M. (1960). Virus survival as a seasonal factor in influenza and poliomyelitis. *Nature*, *188*, 430-431.
3. Lowen, A. C., Mubareka, S., Steel, J., & Palese, P. (2007). Influenza virus transmission is dependent on relative humidity and temperature. *PLoS Pathog*, *3*(10), e151.
4. Steel, J., Palese, P., & Lowen, A. C. (2011). Transmission of a 2009 pandemic influenza virus shows a sensitivity to temperature and humidity similar to that of an H3N2 seasonal strain. *J. Virol.*, *85*(3), 1400-1402.
5. Xie, X., Li, Y., Chwang, A. T. Y., Ho, P. L., & Seto, W. H. (2007). How far droplets can move in indoor environments--revisiting the wells evaporation--falling curve. *Indoor Air*, *17*(3), 211-225.
6. Chao, C. Y. H., Wan, M. P., Morawska, L., Johnson, G. R., Ristovski, Z. D., Hargreaves, M., et al. (2009). Characterization of expiration air jets and droplet size distributions immediately at the mouth opening. *J. Aerosol Sci*, *40*(2), 122-133.
7. Effros, R. M., Hoagland, K. W., Bosbous, M., Castillo, D., Foss, B., Dunning, M., et al. (2002). Dilution of respiratory solutes in exhaled condensates. *Am. J. Respir. Crit. Care Med.*, *165*(5), 663-669.
8. Raphael, G. D., Jeney, E. V., Baraniuk, J. N., Kim, I., Meredith, S. D., & Kaliner, M. A. (1989). Pathophysiology of rhinitis. Lactoferrin and lysozyme in nasal secretions. *J. Clin. Invest.*, *84*(5), 1528-1535.
9. Seinfeld, J. H., & Pandis, S. N. (2006). *Atmospheric chemistry and physics - from air pollution to climate change* (2nd ed.). New York: John Wiley & Sons.
10. Shechmeister, I. L. (1950). Studies on the experimental epidemiology of respiratory infections: III. Certain aspects of the behavior of type A influenza virus as an air-borne cloud. *J. Infect. Dis.*, *87*(2), 128-132.
11. Hemmes, J., Winkler, K., & Kool, S. (1962). Virus survival as a seasonal factor in influenza and poliomyelitis. *Antonie Van Leeuwenhoek*, *28*(1), 221-233.
12. Harper, G. J. (1961). Airborne micro-organisms: Survival tests with four viruses. *J Hyg*, *59*, 479-486.
13. Schaffer, F. L., Soergel, M. E., & Straube, D. C. (1976). Survival of airborne influenza virus: Effects of propagating host, relative humidity, and composition of spray fluids.

- Arch. Virol*, 51(4), 263-273.
14. Shaman, J., & Kohn, M. (2009). Absolute humidity modulates influenza survival, transmission, and seasonality. *Proc Natl Acad Sci USA*, 106(9), 3243-3248.
  15. Loudon, R. G., & Roberts, R. M. (1967). Droplet expulsion from the respiratory tract. *Am. Rev. Respir. Dis.*, 95(3), 435-442.
  16. Papineni, R. S., & Rosenthal, F. S. (1997). The size distribution of droplets in the exhaled breath of healthy human subjects. *J. Aerosol Med.*, 10(2), 105-116.
  17. Yang, S., Lee, G. W. M., Chen, C.-M., Wu, C.-C., & Yu, K.-P. (2007). The size and concentration of droplets generated by coughing in human subjects. *J. Aerosol Med.*, 20(4), 484-494.
  18. Morawska, L., Johnson, G. R., Ristovski, Z. D., Hargreaves, M., Mengersen, K., Corbett, S., et al. (2009). Size distribution and sites of origin of droplets expelled from the human respiratory tract during expiratory activities. *J. Aerosol Sci*, 40(3), 256-269.
  19. Xie, X., Li, Y., Sun, H., & Liu, L. (2009). Exhaled droplets due to talking and coughing. *J. R. Soc. Interface*, 6(Suppl 6), S703-S714.
  20. Duguid, J. P. (1946). The size and the duration of air-carriage of respiratory droplets and droplet-nuclei. *J Hyg*, 44(6), 471-479.
  21. Tang, J. W. T., Tambyah, P. A., Lai, F. Y. L., Lee, H. K., Lee, C. K., Loh, T. P., et al. (2010). Differing symptom patterns in early pandemic vs seasonal influenza infections. *Arch. Intern. Med.*, 170(10), 861-867.
  22. Nicas, M., Nazaroff, W. W., & Hubbard, A. (2005). Toward understanding the risk of secondary airborne infection: Emission of respirable pathogens. *J Occup Environ Hyg*, 2(3), 143-154.
  23. Mikhailov, E., Vlasenko, S., Niessner, R., & Poschl, U. (2004). Interaction of aerosol particles composed of protein and salts with water vapor: Hygroscopic growth and microstructural rearrangement. *Atmos. Chem. Phys.*, 4, 323-350.
  24. Posada, J. A., Redrow, J., & Celik, I. (2010). A mathematical model for predicting the viability of airborne viruses. *J. Virol. Methods*, 164(1-2), 88-95.
  25. Tang, I. N., Tridico, A. C., & Fung, K. H. (1997). Thermodynamic and optical properties of sea salt aerosols. *J. Geophys. Res.*, 102(D19), 23269-23275.
  26. Bagger, H., Fuglsang, C., & Westh, P. (2006). Hydration of a glycoprotein: Relative water affinity of peptide and glycan moieties. *Eur. Biophys. J.*, 35(4), 367-371.
  27. Jensen, M. M. (1964). Inactivation of airborne viruses by ultraviolet irradiation. *Appl. Microbiol.*, 12, 418-420.

28. Yamamoto, N., Shendell, D. G., Winer, A. M., & Zhang, J. (2010). Residential air exchange rates in three major US metropolitan areas: Results from the relationship among indoor, outdoor, and personal air study 1999–2001. *Indoor Air*, 20(1), 85-90.
29. Tompkins, J. A., White, J. A., Bozer, Y. A., & Tanchoco, J. M. A. (2010). *Facilities planning* (4th ed.): John Wiley & Sons, Inc.
30. Myatt, T. A., Kaufman, M. H., Allen, J. G., MacIntosh, D. L., Fabian, M. P., & McDevitt, J. J. (2010). Modeling the airborne survival of influenza virus in a residential setting: The impacts of home humidification. *Environ Health*, 9, 55.
31. Blachere, F. M., Lindsley, W. G., Pearce, T. A., Anderson, S. E., Fisher, M., Khakoo, R., et al. (2009). Measurement of airborne influenza virus in a hospital emergency department. *Clin. Infect. Dis.*, 48(4), 438-440.
32. Lindsley, W. G., Blachere, F. M., Davis, K. A., Pearce, T. A., Fisher, M. A., Khakoo, R., et al. (2010). Distribution of airborne influenza virus and respiratory syncytial virus in an urgent care medical clinic. *Clin. Infect. Dis.*, 50(5), 693-698.
33. Yang, W., Elankumaran, S., & Marr, L. C. (2011). Concentrations and size distributions of airborne influenza A viruses measured indoors at a health centre, a day-care centre, and on aeroplanes. *J R Soc Interface*, 8(61), 1176-1184.
34. 2007 California mechanical code (part 4, title 24, California code of regulations) (2007).
35. McDevitt, J., Rudnick, S., First, M., & Spengler, J. (2010). Role of absolute humidity in the inactivation of influenza viruses on stainless steel surfaces at elevated temperatures. *Appl. Environ. Microbiol.*, 76(12), 3943-3947.
36. Brown, J. D., Goekjian, G., Poulson, R., Valeika, S., & Stallknecht, D. E. (2009). Avian influenza virus in water: Infectivity is dependent on pH, salinity and temperature. *Vet. Microbiol.*, 136(1-2), 20-26.
37. Parker, E. R., Dunham, W. B., & MacNeal, W. J. (1944). Resistance of the Melbourne strain of influenza virus to desiccation. *J. Lab. Clin. Med.*, 29, 37-42.
38. Thomas, Y., Vogel, G., Wunderli, W., Suter, P., Witschi, M., Koch, D., et al. (2008). Survival of influenza virus on banknotes. *Appl. Environ. Microbiol.*, 74(10), 3002-3007.
39. Oberdorster, G., Oberdorster, E., & Oberdorster, J. (2005). Nanotoxicology: An emerging discipline evolving from studies of ultrafine particles. *Environ. Health Perspect.*, 113(7), 823-839.
40. Lowen, A. C., Steel, J., Mubareka, S., & Palese, P. (2008). High temperature (30 °C)

- blocks aerosol but not contact transmission of influenza virus. *J. Virol.*, 82(11), 5650-5652.
41. Lowen, A., & Palese, P. (2009). Transmission of influenza virus in temperate zones is predominantly by aerosol, in the tropics by contact: A hypothesis. *PLoS Curr*, 1, RRN1002.
  42. Fischer, H., & Widdicombe, J. H. (2006). Mechanisms of acid and base secretion by the airway epithelium. *J. Membr. Biol.*, 211(3), 139-150.
  43. Enberg, N., Alho, H., Loimaranta, V., & Lenander-Lumikari, M. (2001). Saliva flow rate, amylase activity, and protein and electrolyte concentrations in saliva after acute alcohol consumption. *Oral Surg. Oral Med. Oral Pathol. Oral Radiol. Endod.*, 92(3), 292-298.
  44. Michishige, F., Kanno, K., Yoshinaga, S., Hinode, D., Takehisa, Y., & Yasuoka, S. (2006). Effect of saliva collection method on the concentration of protein components in saliva. *J. Med. Invest.*, 53(1-2), 140-146.
  45. Lai, A. C. K., & Cheng, Y. C. (2007). Study of expiratory droplet dispersion and transport using a new eulerian modeling approach. *Atmos. Environ.*, 41(35), 7473-7484.
  46. Fabian, P., McDevitt, J. J., DeHaan, W. H., Fung, R. O. P., Cowling, B. J., Chan, K. H., et al. (2008). Influenza virus in human exhaled breath: An observational study. *PLoS ONE*, 3(7), e2691.
  47. Douglas Jr., R. G. (1975). Influenza in man. In E. D. Kilbourne (Ed.), *The influenza viruses and influenza* (pp. 395-447). New York: Academic Press.
  48. Lindsley, W. G., Blachere, F. M., Thewlis, R. E., Vishnu, A., Davis, K. A., Cao, G., et al. (2010). Measurements of airborne influenza virus in aerosol particles from human coughs. *PLoS ONE*, 5(11), e15100.
  49. Murphy, B. R., Rennels, M. B., Douglas, R. G., Jr., Betts, R. F., Couch, R. B., Cate, T. R., Jr., et al. (1980). Evaluation of influenza A/Hong Kong/123/77 (H1N1) ts-1A2 and cold-adapted recombinant viruses in seronegative adult volunteers. *Infect. Immun.*, 29(2), 348-355.
  50. Ward, C. L., Dempsey, M. H., Ring, C. J. A., Kempson, R. E., Zhang, L., Gor, D., et al. (2004). Design and performance testing of quantitative real time PCR assays for influenza A and B viral load measurement. *J. Clin. Virol.*, 29(3), 179-188.
  51. Hinds, W. C. (1999). *Aerosol technology* (2nd ed., pp. 75-110). New York: Wiley.

## 4 Relationship between Humidity and Influenza A Viability in Droplets and Implications for Influenza's Seasonality<sup>‡</sup>

Wan Yang<sup>1</sup>, Subbiah Elankumaran<sup>2</sup>, Linsey C. Marr<sup>1</sup>

<sup>1</sup>Department of Civil and Environmental Engineering, Virginia Tech, 418 Durham Hall, Blacksburg, Virginia 24061, USA

<sup>2</sup>Department of Biomedical Sciences and Pathobiology, Virginia-Maryland College of Veterinary Medicine, Virginia Tech, 1981 Kraft Drive, Blacksburg, Virginia 24060, USA

Corresponding author: Linsey C. Marr, 411 Durham Hall, Blacksburg, VA 24061, (540) 231-6071, (540) 231-7916, lmarr@vt.edu

Running Title: Humidity and influenza A viability

### **Abstract**

Humidity has been found to be associated with the incidence of influenza, but the mechanisms governing the relationship remain unclear. We measured the viability of influenza A virus in droplets consisting of various model media, chosen to isolate the effects of salts and proteins found in respiratory fluid, as well as in human mucus, at relative humidities (RH) ranging from 17% to 99%. In all media and mucus, viability was highest when RH was either close to 100% or below ~50%. At RHs between 50-84%, the relationship between viability and RH depended on droplet composition: in saline solutions with negligible proteins, viability decreased with decreasing RH; in saline solutions supplemented with proteins, viability did not change significantly with RH; and in mucus, viability increased dramatically with decreasing RH. Additionally, viral decay was shown to increase linearly with salt concentration in saline solutions but not when they were supplemented with proteins. There appear to be three regimes of virus viability in droplets, defined by humidity: physiological conditions (~100% RH), with high viability; concentrated conditions (~50% to near 100% RH), with lower viability; and dry conditions (<~50% RH), with high viability. Results in human mucus could help explain influenza's seasonality and global transmission patterns.

---

<sup>‡</sup>Submitted to *Journal of the Royal Society Interface*.

Key words: influenza virus; relative humidity; viability; mucus; evaporation; seasonality

## 4.1 Introduction

Annual influenza epidemics in the US result in an average of 610,660 life-years lost, 3.1 million hospitalization days, and 31.4 million outpatient visits, for a total economic burden of \$87.1 billion per year [1]. In temperate regions, influenza's incidence peaks during the wintertime [2-3], while in tropical regions, the disease's occurrence seems to coincide with the rainy season [4-6]. This distinct seasonal pattern has triggered intense interest. However, a consistent explanation for it remains lacking despite nearly a century of investigation [7-8].

Humidity has been identified as one factor that influences influenza's seasonality [9-10]. Previous studies have linked influenza's high incidence in temperate regions to low humidity in winter [11-13]. This connection is further supported by laboratory studies indicating that the virus survives better at low relative humidity (RH) [9; 14-16].

However, several important questions remain to be addressed. First of all, the connection between high influenza incidence and low humidity fails to explain the association of increased influenza activity in tropical areas during the rainy season when humidity is maximal. Secondly, although laboratory studies consistently showed a high survival rate for IAV at low RH (<50%), results were discordant at medium to high (~50% to ~90%) RH [8]. Of the four studies cited most often, Hemmes et al. [9] and Harper [14] found higher inactivation rates at both medium and high RH (referred to as H&H hereafter), while Shechmeister [16] and Schaffer et al. [15] reported the highest inactivation rates at medium RH and moderate ones at high RH (referred to as S&S hereafter). The relationship between the viability of IAV in airborne droplets and ambient RH remains poorly defined and poorly understood.

Another unanswered question surrounds the mechanism by which ambient RH might affect IAV in airborne respiratory droplets [10]. When released from the respiratory tract, where RH is ~100%, droplets experience rapid evaporation and shrinkage upon encountering the ambient atmosphere. Through application of a theoretically based model of droplet transformation [17], we showed that droplets shrink to 40-50% of their initial diameters at RH below 90%, as has been demonstrated previously [18-19]. The extent of evaporation is greater at lower RH.

As a result of evaporation, concentrations of solutes in the droplet increase by up to a factor of 15, and solutes such as salts (e.g., sodium chloride (NaCl)) that are harmless at physiological concentrations may therefore become harmful to the virus. For example, avian IAV has been reported to be stable in water at salinities below 20 g L<sup>-1</sup> but less stable at salinities greater than 25 g L<sup>-1</sup> [20]. Evaporation induces changes to IAV's microenvironment

inside a droplet that may affect the virus' viability, and the toxic effect of solutes may be enhanced at lower RH. However, the solutes in respiratory droplets also include a variety of inorganic salts and proteins [21-22], and their interactions at different RHs may complicate this picture under natural conditions.

We hypothesize that humidity mediates the survival of IAV in droplets by controlling the extent of evaporation and thus solute concentrations in the droplet and that solute concentrations in the droplet define the relationship between RH and IAV viability. We measured IAV viability in droplets at varying RH in four types of media with various combinations of inorganic salts and proteins and in human mucus. The experiment was designed to simulate what happens when respiratory droplets are expelled into ambient air and subjected to evaporation. Our results resolve the aforementioned discrepancy in laboratory studies. Based on our results and the thermodynamics of droplets, we propose a mechanistic explanation for the dependence of IAV's transmission on humidity. This mechanism consistently accounts for the disease's global transmission patterns in both temperate and tropical regions.

## **4.2 Materials and Methods**

### **4.2.1 Cells and Virus**

Madin-Darby canine kidney (MDCK) cells were maintained in DMEM supplemented with 5% FCS. The stock of the IAV A/PR/8/34 (H1N1) was prepared in 10-day-old specific pathogen-free embryonated hens' eggs. Virus stocks were stored as aliquots of allantoic fluid from infected embryos at -80 °C until use. The titer of the virus stock was determined to be  $1.78 \times 10^8$  median tissue culture infective dose (TCID<sub>50</sub>) mL<sup>-1</sup>. All virus titration experiments were performed in MDCK cells.

### **4.2.2 Mucus specimen**

Collection and use of human mucus was approved by the Institutional Review Board at Virginia Tech. A mucus specimen was collected from an infant 1 month of age in March 2011. The mucus specimen was allowed to desiccate in a sealed vial and was reconstructed by dissolution in MiliQ water (5% w/v). To preserve the mucus structure, we first attempted to sterilize the mucus specimen by filtration with a 0.45-µm pore size filter. The specimen was not filterable, indicating its large molecular size. Thus, the reconstructed mucus was sterilized by heating at 65 °C for 30 min and was checked for potential IAV contamination by TCID<sub>50</sub> assay. No IAV was detected, and the specimen was stored at 4 °C until use.

### **4.2.3 Control of RH in a desiccator**

Two Petri dishes filled with 20 mL of salt solution (either potassium acetate, potassium

carbonate, cobalt (II) chloride, or potassium chloride) or double distilled water were kept in a desiccator [23-24]. Air circulation inside the desiccator was enhanced by a fan to accelerate the establishment of equilibrium RH between the salt solution and the air inside the desiccator. Before each experiment began, the desiccator was conditioned to the desired RH. The desiccator had to be opened briefly to insert the samples, and the system reestablished equilibrium within ~10 min. The actual RH and temperature inside the desiccator were recorded at 1-min intervals during sampling with a temperature/humidity logger (OM-73, Omega Engineering, Inc., USA). RHs tested in model media included 17.5±1.0%, 27.6±0.9%, 42.0±0.8%, 44.1±1.2%, 50.2±0.7%, 59.5±1.1%, 76.1±0.7%, 84.1±0.8%, and 98.9±0.4%. RHs tested in mucus included 26.7±0.8%, 40.3±1.1%, 48.0±1.2%, 52.0±0.9%, 60.8±1.1%, 72.2±1.2%, 83.9±0.4%, and 99.1±0.4%.

#### **4.2.4 Exposure of IAV in droplets to various RH**

To simulate the transformation of respiratory droplets in the ambient atmosphere, we incubated droplets containing IAV at specific RHs in the range of 17% to 99% for 3 h at room temperature (20-24 °C). The droplets consisted of four different types of media (Table 4.1), chosen to isolate the effects of salt and/or protein concentrations on viability, or mucus. Phosphate buffered saline (PBS) and Dulbecco's modified Eagle medium (DMEM) were used as surrogates of media that contain inorganic salts at physiological levels but no or negligible amounts of proteins, respectively. The third and fourth types of media were PBS and DMEM supplemented with 5% fetal calf serum (FCS), a source of proteins.

Ten µL of stock PR/8 IAV was added into 90 µL of either PBS, PBS+5% FCS, DMEM, DMEM+5% FCS, or mucus as spiking solutions. The spiking solutions were distributed onto a 12-well cell culture plate, 1 µL per droplet, 10 droplets per well, and 3 replicates (i.e., 3 wells) for each medium. The plate was immediately placed into the desiccator and incubated at room temperature for 3 h for model media and 2 h for mucus. At the end of the period, the virus in each well was collected with 1 mL of DMEM supplemented with 1 µg mL<sup>-1</sup> TPCK trypsin (collection medium), by pipetting the medium ~10 times to rinse out any virus attached. The spiking solutions were stored on ice during the incubation period, and 10 µL of each spiking solution was supplemented with 990 µL of collection medium and used as control respectively. Samples and the corresponding controls were titrated at the same time by TCID<sub>50</sub> assay either immediately after collection or were stored at -80 °C until testing.

#### **4.2.5 Calculation of viral decay**

Percentage viability was calculated as

$$\% \text{ viability} = \frac{N_t}{N_0} \quad [1]$$

where  $N_t$  and  $N_0$  are, respectively, the final and initial titers of virus. The log decay rate was calculated as

$$\log \text{ decay} = \log\left(\frac{N_0}{N_t}\right) \quad [2]$$

$N_t$  was set to 1 for negative samples to avoid dividing by 0.

*Estimation of solute concentration in equilibrium.* The molality of NaCl in the resulting droplet at a specific RH was calculated using Microsoft Excel's solver tool according to an empirical relationship [25]:

$$RH = 1.0084 - 4.939 \times 10^{-2} m + 8.888 \times 10^{-3} m^2 - 2.157 \times 10^{-3} m^3 + 1.617 \times 10^{-4} m^4 - 1.990 \times 10^{-6} m^5 - 1.142 \times 10^{-7} m^6 \quad [3]$$

where  $m$  is the molality of NaCl (g (kg water)<sup>-1</sup>). The concentration of NaCl was then calculated based on  $m$ :

$$C_s = \frac{mM_s}{mv_s + 1} \quad [4]$$

where  $C_s$  is the concentration of solute in equilibrium;  $M_s$  is the molecular weight of NaCl (58.44 g mol<sup>-1</sup>);  $v_s$  is the molar volume of NaCl (2.7 × 10<sup>-2</sup> L mol<sup>-1</sup>); and the number 1 in the denominator represents the volume of 1 kg of water, i.e., 1 L.

## 4.3 Results

### 4.3.1 IAV viability in model media v. RH

As shown in Figure 4.1A and 4.1B, IAV viability in four model media containing various combinations of salts and proteins was highest at extremely high (~99%) and low (<50%) RH and minimal at medium (50 to 84%) RH. At ~99% RH, the viabilities ranged from 8% to 57%, namely, 36 ± 15% in PBS, 7.8 ± 0.27% in DMEM, 11 ± 4.1% in PBS+FCS, and 57 ± 11% in DMEM+FCS of input virus in different media. At ~84% RH, viabilities were much lower (~1-5%) but were of the same order of magnitude in all four media.

At RH between 50% and 84%, the trends in viability in the four media diverged dramatically, depending on whether the media contained proteins or not. The viability in PBS decreased with decreasing RH and reached a minimum at 50% RH. In DMEM, the trend was similar, but the minimum occurred at an RH of 60% (Figure 4.1A). In contrast, in PBS+FCS, viabilities did not change significantly over this range of RH, and in DMEM+FCS, viabilities increased slightly with decreasing RH (Figure 4.1B).

At RH below 50%, viabilities were higher in all types of media compared to those at medium RH, although viability in PBS alone was significantly lower than in the three other media, possibly due to the lack of proteins.

We repeated the experiment to confirm these results. The percent viabilities recovered varied slightly, but trends in viability versus RH were similar.

#### **4.3.2 IAV viability in mucus v. RH**

We tested the changes in viability of IAV spiked into human mucus at RH levels ranging from ~26 to 99%. As shown in Figure 4.1C, at ~99% RH, the viability of IAV was only  $1.7 \pm 0.26\%$ , an order of magnitude lower than recovered in model media. The finding that viability was highest at this extremely high RH was consistent with results in other media. At RH between ~50% and 84%, viabilities increased dramatically with decreasing RH. Only  $0.0027 \pm 0.0023\%$  was recovered at 84% RH, compared to  $1.5 \pm 1.4\%$  recovered at 48% RH, an increase of over two orders of magnitude. At RH below 48%, viabilities leveled off and remained around 1%. The relatively higher viabilities observed at RH below 50% were consistent with results in model media and those reported in the literature [26-27]. We repeated the experiment at four (27%, 60%, 84%, and 99%) of the six RHs, and the resulting viabilities followed the same trend as shown in Figure 4.1C. With spiking titers of  $5.1 \pm 2.6 \times 10^4$  TCID<sub>50</sub>, no viable IAV was detected in 5 out of 9 samples at ~84% RH.

#### **4.3.3 Relationship between viral decay and salt concentrations**

The relationship between viral decay rates and salt concentrations in the droplets is shown in Figure 2. Salts in the droplets were simplified as NaCl, and concentrations were estimated empirically [25]. The viral decay rate in PBS droplets increases linearly with NaCl concentration in the range of 25-510 g L<sup>-1</sup>, corresponding to 99-50% RH, respectively ( $R^2=0.97$ ). Concentrations are lower at high RH because there is less evaporation and vice versa. Likewise, the viral decay rate also increases linearly with NaCl concentration up to 420 g L<sup>-1</sup>, corresponding to 60% RH, in DMEM droplets ( $R^2=0.98$ ). In contrast, in media containing FCS, viral decay rates did not increase with elevated NaCl concentrations. Instead, they remained constant at concentrations above 200 g L<sup>-1</sup> up to 510 g L<sup>-1</sup>, corresponding to RHs ranging from 84% to 50%.

#### **4.3.4 Efflorescence**

At RH below ~50%, the relationship between NaCl concentration and IAV viability no longer holds. The NaCl concentration in a droplet reaches its solubility (310 g L<sup>-1</sup>) at 75% RH, and RH lower than 75%, evaporation is extensive enough to produce a supersaturated solution. The NaCl concentration can rise as high as 580 g L<sup>-1</sup> before the droplet crystallizes by means

of homogeneous nucleation [25; 28]. The critical RH at which a droplet crystallizes is termed the efflorescence RH (ERH), and it depends on the composition and size of the droplet [29].

We observed the droplets of each medium under a microscope immediately after incubation at different RHs and found that no crystals formed at  $RH > 60\%$ , while droplets of all media crystallized at an RH just below 50% (see Supplemental Material, Figure 4.1). Continuous observation under a microscope at  $\sim 50\%$  RH indicated that the droplets of all media crystallized within  $\sim 10$  min. This observation confirms that the droplets crystallized at low RH. Crystallization in DMEM at a lower NaCl concentration (corresponding to higher RH) than in PBS, due to a different ERH, could explain the lower decay rate in DMEM at a concentration of  $510 \text{ g L}^{-1}$  (50% RH).

#### **4.4 Discussion**

##### **4.4.1 Hypothesis to explain the relationship between RH and viability in laboratory studies**

We hypothesize that RH influences the viability of IAV in a respiratory droplet by controlling the extent of evaporation and thus the final concentrations of solutes that comprise IAV's microenvironment. Upon droplet evaporation, the elevated salt concentrations that result are likely to be toxic to the virus, but at RH less than the ERH, the deleterious effects of dissolved salts are eliminated because the solution crystallizes. Furthermore, the chemical composition of a droplet may affect the extent and characteristics (e.g., ERH) of evaporation and thus may affect the relationship between viability and RH.

We postulate that there are three regimes governing viability of IAV in droplets, defined by ambient RH and shown in Figure 4.3: (1) physiological conditions ( $\sim 99$  to  $100\%$  RH), where solute concentrations remain at levels harmless to IAV and viability is maintained, (2) concentrated conditions ( $\sim 50$  to  $\sim 99\%$  RH), where evaporation leads to elevated salt concentrations that may be harmful to the virus, and (3) dry conditions ( $< 50\%$  RH), where solutes crystallize, all water is lost, and IAV viability is maintained. In a salt solution droplet, the minimum viability would be expected at RH just above the ERH of the salts contained in the droplet, when water is still present and solute concentrations are maximal. Therefore, the relationship between RH and IAV viability in such a droplet would be similar to that shown in Figure 4.3A. However, the presence of proteins in the droplet may alter this relationship. It is possible that the interaction between proteins, salts, and the virus mitigates the adverse effects of salts under concentrated conditions. Therefore, the virus would maintain high viability under physiological and dry conditions and moderate viability under concentrated conditions in a droplet composed of both salts and proteins (Figure 4.3B). In fact, viability

may increase with decreasing RH, as we found in DMEM+FCS and mucus, possibly due to protection provided by elevated concentrations of proteins [30-31].

Results from previous studies on the viability of Langat virus, a tick-borne flavivirus, support our hypothesis. Benbough [32] reported similar V-shaped curves of viability versus RH for Langat virus in aerosols composed of salt solutions. Of four RHs tested (i.e., ~25%, 50%, 70%, and 95%), the minimum viabilities were ~1% in NaCl and ~10% in KCl, both at ~50% RH, and zero in LiCl at RH<50%. Thus, the minimum viability of Langat virus in aerosols composed of an NaCl solution occurred at an RH close to the ERH of NaCl, which is  $43 \pm 3\%$  [29]. KCl has an ERH of 59% [29], and this RH was not tested, so it is unknown whether the virus' viability would have been lower at this RH. The ERH of LiCl, if it exists, is outside the range of RHs tested; its deliquescence RH is ~11% [24].

#### **4.4.2 Explanation of discordant findings in literature**

In reviewing the four aforementioned studies (H&H versus S&S), we noticed that the media used to produce airborne droplets containing IAV differed. All the media contained some salts; however, those in H&H contained substantially more proteins than did those in S&S (Table 4.1). We thus hypothesize that the conflicting results between S&S and H&H were due to the varying protein content of the media used in these studies. Our results with PBS and DMEM, media similar to those used in S&S in terms of composition of salts and proteins, showed similar trends to those reported in the two studies. Our results in PBS and DMEM supplemented with FCS, media similar to those in H&H, also showed similar trends in these two studies. In the former case, with salts only, the inactivation rate was maximal at medium RH, but in the latter, with proteins also, the inactivation rate was high at medium to high RH. None of the four studies tested the extremely high RH considered here.

As discussed earlier, the combination of increasing salt concentrations at lower RH and salt crystallization at the ERH may explain the trends observed in the two media with mainly salts (i.e., PBS and DMEM) and in S&S. The RH corresponding to the highest decay may differ between media, possibly due to different ERHs for media of different compositions [29]. The minimum viabilities occurred between 40-70% RH, mostly around 50% in Schaffer et al. [15] and 58-60% in Shechmeister [16]. Likewise, we found minimum viabilities at 50% in PBS and 60% in DMEM.

We estimated the concentration of salts in the droplet in equilibrium with a given RH, and showed that it was correlated with the viral decay (Figure 4.2) when the droplet contained mainly salts. To our knowledge, the relationship between decay of IAV and highly elevated solute concentrations resulting from evaporation of small droplets has never been

shown. In bulk media, supersaturated conditions cannot be achieved, and so the phenomenon observed here can only be demonstrated through methods that enable supersaturation.

Although it is still not clear how proteins in a droplet would interact with other components such as salts and/or the virus to mitigate the toxic effect of salts under concentrated conditions at medium RH, such an effect was shown in this study. Similar relationships were also reported in H&H, in which media containing proteins/peptones were used. In a study of aerosols composed of salts and proteins, the proteins were found to be enriched at the surface of the aerosols [33], possibly because of hydrophobic regions on protein surfaces. It is possible that proteins in aerosol droplets could become enriched around viruses and provide some protection against elevated salt concentrations. Although this hypothesis is highly speculative, it is supported by the fact that mucin glycoproteins usually serve as a barricade against potential pathogens including viruses and bacteria by specific or non-specific binding [30-31].

#### **4.4.3 Implications for influenza's occurrence patterns**

Respiratory tract mucus is a complicated combination of water (~95%), inorganic salts (~1%), and various macromolecular organic compounds including glycoproteins (i.e., mucins) and lipids [21-22; 34]. It has been shown to be protective for IAV at low RH [26-27]. However, the relationship between viability of IAV in mucus and RH is still not completely clear.

Our results show that the relationship in mucus bears some similarity to that in media with both salts and proteins, particularly DMEM+FCS. In both cases, viabilities were relatively higher at ~100% RH or RH<50%, and much lower at medium RH ranging from ~50-84%. However, the decrease in viability at RH ranging from 50-84% was more dramatic in mucus than in synthetic model media. During incubation of the virus in mucus, a slight change in RH from 52% to 48% reduced the viabilities by an order of magnitude, and at ~84% RH, the reductions in viabilities were over 500 times greater than at RH<50% and ~100%. In comparison, in model media, viabilities varied by only an order of magnitude over the same RH range, which is consistent with past studies [9; 14]. Thus, RH might have a greater effect on IAV's survival in mucus than has been demonstrated in past studies with synthetic media. Also, the viability of IAV was best preserved at ~100% RH, which, to our knowledge, has not been shown previously. These results underscore the potentially large impact of RH on the virus' survival in its natural aerosol carrier after being expelled from the human respiratory tract.

The relationship reported here in human mucus could help explain, at least in part, the transmission patterns of the disease. In temperate regions, wintertime heating reduces RH in

the indoor environment to low levels, usually <40% [35-36]. At such an RH, vigorous evaporation of respiratory droplets not only helps preserve the viability of IAV emitted by infected hosts but also enables the resulting aerosols to remain aloft longer because of their smaller size and lower settling velocities [17]. Thus, transmission of influenza in temperate regions could be enhanced in winter primarily via the aerosol route. In tropical regions, high temperatures may suppress transmission through the aerosol route [37-38], but during rainy seasons, temperatures are lower and RHs are close to 100%. Under such conditions, droplets do not shrink as much, only to 93% of their original diameters at 99% RH, and 76% at 98% RH [17], and they would be removed more quickly from the air by gravitational settling. However, submicron droplets, such as those exhaled in human breath [39] would remain aloft, and thanks to the lower temperatures and suitable RHs for survival, transmission by these submicron droplets via the aerosol route might still be effective. In addition, the contact transmission route, may be enhanced because it is insensitive to temperature [38; 40] and IAV is well preserved at ~100% RH, as shown in this study.

#### **4.4.4 Limitation and directions for future study**

In this study, droplets in 1  $\mu\text{L}$  volume, instead of smaller aerosols [41], were used to simulate the interplay of humidity, droplet evaporation, solute concentrations in the droplet, and virus viability. A respiratory droplet 20  $\mu\text{m}$  in diameter would evaporate to its final size, around half of its original diameter, within 1 s according to Nicas et al. [18]. The time needed for the droplets used in this study to dry out completely at ~50% RH was observed to be about 10 min, which is considerably longer than that for the aerosols. An uncertainty in extrapolating the results in this study to aerosols expelled from human respiratory tract thus resides in whether the dynamics of evaporation are critical for IAV decay. Harper [14] recovered 66-126% of IAV in aerosols 1 s after spraying, which indicates that the effect on viral decay due to evaporation within 1 s is limited. The relationships between IAV decay and RH in literature observed from exposing the virus in aerosols to varying RH conditions are thus mostly due to the effects of RH post evaporation.

To achieve the low RH in this study, the virus experienced a range of solute concentrations as the water evaporated over 10 min, including those concentrations corresponding to medium RH where viability is lower. Yet viability measured at 3 h was significantly higher at low RH than at medium RH. These results indicate that the brief exposure of the virus to solute concentrations corresponding to medium RH was not controlling, even though it may have had an influence. And even if it were critical, such an effect was controlled for when comparing viral decay in the same type of medium versus RH,

since all the droplets experienced a similar rate of evaporation. In addition, the droplets were incubated at a specific RH for up to 3 h to allow sufficient time for interplay of humidity and IAV after the initial evaporation process. Nevertheless, verifying these results in aerosols is warranted.

This study demonstrates the relationship between IAV viability and RH in both model media and human mucus, and we propose a mechanistic basis for this relationship based on the thermodynamics of droplets and the potential interplay between solutes and virus. However, it does not explain the mechanism by which salts affect IAV viability at a molecular level, nor does it explain how the presence of proteins alters the relationship. Furthermore, previous studies indicate that different viruses respond differently to changes in RH. For instance, poliovirus favors higher RH, in contrast to IAV that favors lower RH [9]. Hence, the relationship between virus and RH is probably a combined function of properties of the virus (e.g., surface proteins on the envelope and type of nucleic acid) and the interactions among the virus, solutes, and water molecules [42-43]. In addition, the relationship in mucus differed slightly from that observed in model media. Given the complex composition and unique nature of mucus, mechanisms governing the relationship in mucus might differ from those in model media.

#### **4.5 Conclusions**

Our results show that solutes in IAV-containing droplets can affect the relationship between virus viability and RH, and our hypothesis regarding the harmful effects of salts and protective effects of proteins explains seemingly contradictory results found previously [9; 14-16]. IAV viability in human mucus was relatively well preserved under both low and extremely high RH conditions (below 50% or ~100%, respectively) and decreased by one to two orders of magnitude at medium RHs (~50-84%). These results confirm the influence of RH on IAV's survival in its natural aerosol carrier. High viability at both low and extremely high RHs may help explain the higher incidence of influenza observed in temperate regions during wintertime and in tropical regions during the rainy season.

#### **Acknowledgments**

This research was partially supported by the National Science Foundation (CBET-0547107). W.Y. thanks Dr. Sandeep Kumar for providing help and advice with experiments.

## TABLES AND FIGURES

**Table 4.1 Media used in studies of influenza A virus viability versus RH**

Study	Media	Salt content	Protein content	Other components	Ref.
Hemmes et al. 1960	1 part allantoic fluid and one part 2% Difco peptone	$\sim 2.3 \text{ g L}^{-1}$ (0.4 g $\text{L}^{-1} \text{ K}^+$ , 0.9 g $\text{L}^{-1} \text{ Na}^+$ , 0.9 g $\text{L}^{-1} \text{ Cl}^-$ ) <sup>a</sup>	10 g $\text{L}^{-1}$ peptone	- <sup>b</sup>	[9; 44]
Harper 1961	Allantoic fluid diluted 1: 8 or 1:10 in casein McIlvaine's buffer (pH 7.2)	$\sim 2.2 \text{ g L}^{-1}$ (mainly $\text{Na}_2\text{HPO}_4$ ) <sup>a</sup>	$\sim 1.9 \text{ g L}^{-1}$ mainly casein	- <sup>b</sup>	[14; 45]
Shechmeister 1950	Allantoic fluid in 0.1 M Sorensen's phosphate buffer (pH 7.1)	19.6 g $\text{L}^{-1}$ (8.09 g $\text{L}^{-1} \text{ NaH}_2\text{PO}_4$ , 9.51 g $\text{L}^{-1} \text{ Na}_2\text{HPO}_4$ )	$\sim 1 \text{ g L}^{-1}$ in allantoic fluid	- <sup>b</sup>	[16]
Schaffer et al. 1976	Minimum essential medium (MEM)	9.88 g $\text{L}^{-1}$ (6.8 g $\text{L}^{-1} \text{ NaCl}$ , 2.2 g $\text{L}^{-1} \text{ NaHCO}_3$ , and others)	0	amino acids, vitamins, glucose, others	[15; 44; 46]
	MEM+0.1% bovine serum albumen (BSA)	9.88 g $\text{L}^{-1}$	1 g $\text{L}^{-1}$	same as above	
This work	Allantoic fluid	$\sim 4.7 \text{ g L}^{-1}$ (0.8 g $\text{L}^{-1} \text{ K}^+$ , 1.8 g $\text{L}^{-1} \text{ Na}^+$ , 1.8 g $\text{L}^{-1} \text{ Cl}^-$ ) <sup>a</sup>	$\sim 1 \text{ g L}^{-1}$		
	Phosphate buffered saline (PBS) (pH 7.2)	9.55 g $\text{L}^{-1}$ (8 g $\text{L}^{-1} \text{ NaCl}$ , 0.2 g $\text{L}^{-1} \text{ KCl}$ , 1.15 g $\text{L}^{-1} \text{ Na}_2\text{HPO}_4$ , 0.2 g $\text{L}^{-1} \text{ KH}_2\text{PO}_4$ )	0	none	
	PBS+5% fetal calf serum (FCS)	same as above	$\sim 3.5 \text{ g L}^{-1}$	others from FCS	
	DMEM	10.92 g $\text{L}^{-1}$ (6.4 g $\text{L}^{-1} \text{ NaCl}$ , 3.7 g $\text{L}^{-1} \text{ NaHCO}_3$ )	0.42 g $\text{L}^{-1}$	amino acids, vitamins, glucose, others	
	DMEM+5%FCS	same as above	$\sim 3.9 \text{ g L}^{-1}$	same as above	

<sup>a</sup>Estimated; <sup>b</sup>Detailed composition of allantoic fluid is unknown.

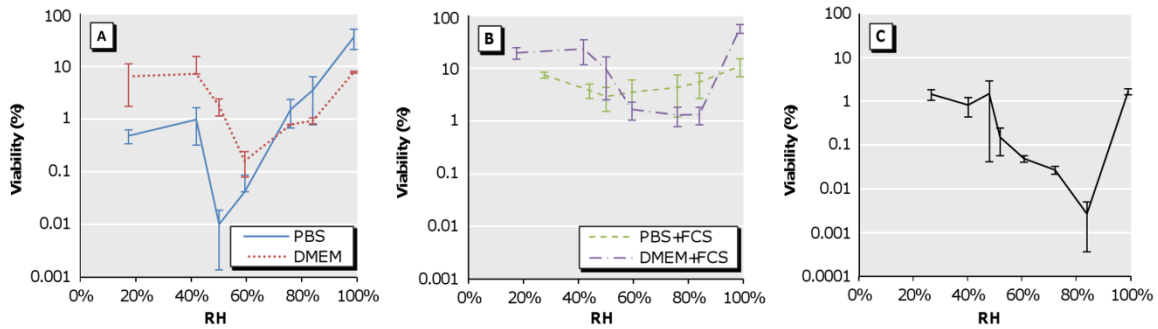


**Figure 4.1** Relationship between IAV viability and RH in (A) media with mainly salts, (B) media with salts plus proteins, and (C) mucus. Error bars denote standard deviations.

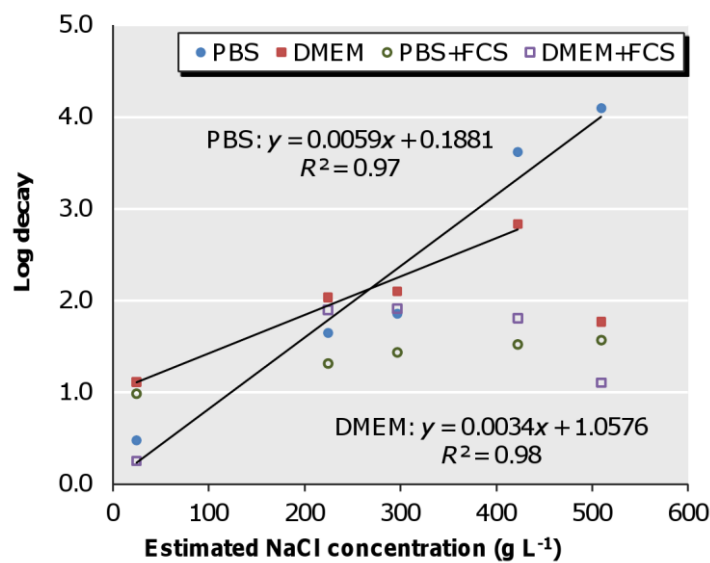


**Figure 4.2** Viral decay over 3 h versus NaCl concentration in droplets consisting of four types of media.

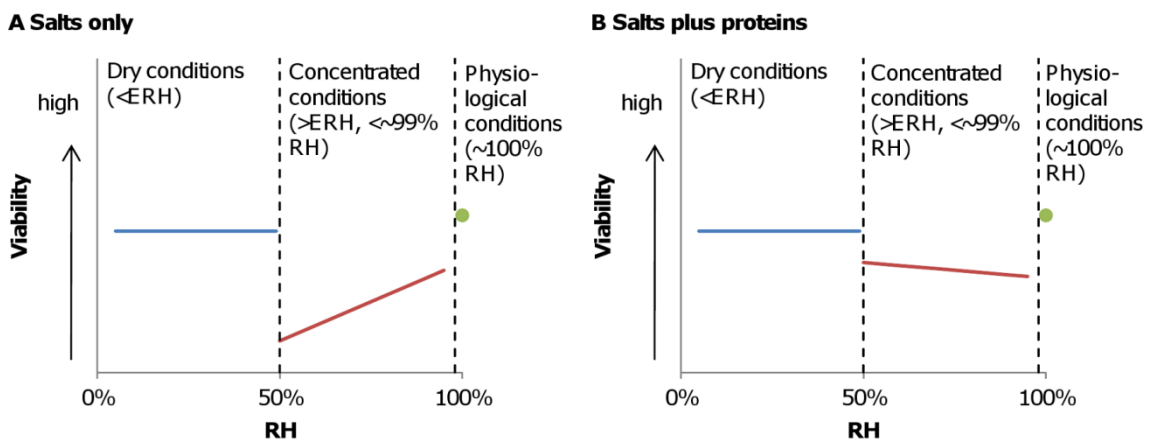


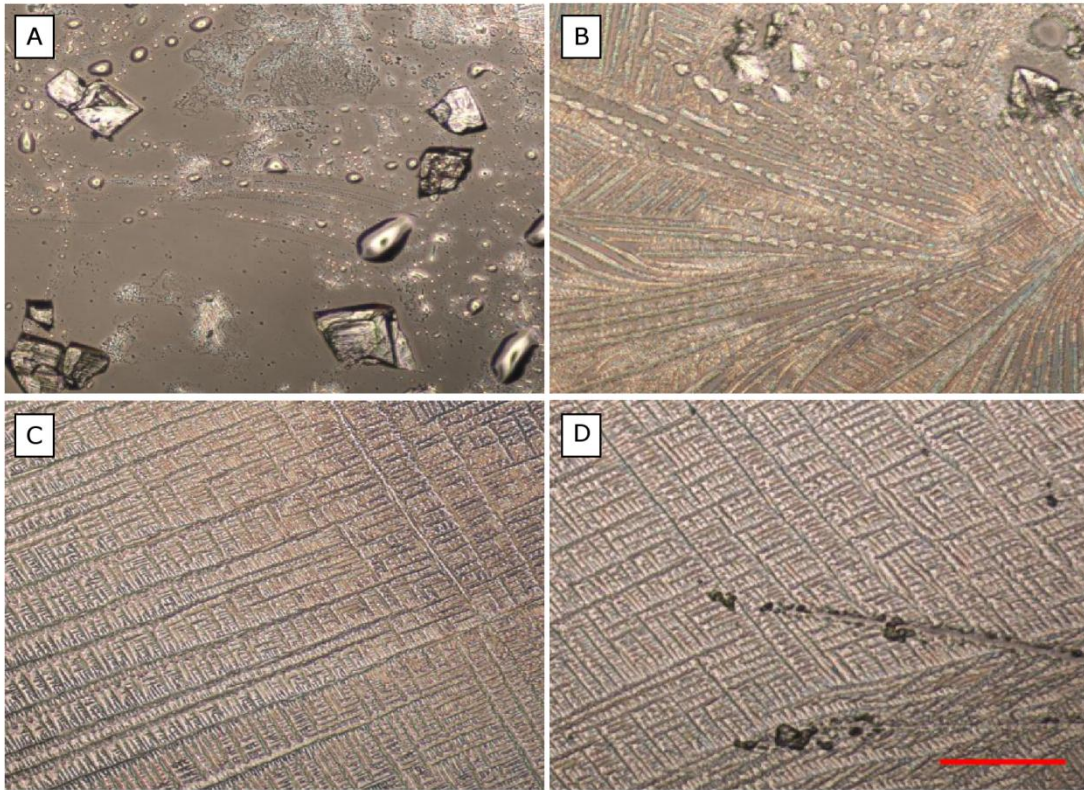
**Figure 4.3** Hypothesized relationship between IAV viability and RH in (A) droplets containing salts only and (B) droplets containing salts plus proteins.

## Supplemental Material

### **Observation of transformation of droplets under varying RH levels.**

Droplets of PBS, PBS+5% FCS, DMEM, or DMEM+5% FCS (all without addition of IAV) in 1  $\mu\text{L}$  volumes were distributed on a 12-well cell culture plate and incubated under different RH levels as described above. Plates were taken from the incubator and observed under an inverse light microscope (100X) immediately. Photos were taken with a camera (Nikon) connected to the microscope. To determine the time needed for a droplet of 1  $\mu\text{L}$  to dry out, droplets of PBS, PBS+5% FCS, DMEM, or DMEM+5% FCS were distributed on a glass slide, left under the microscope and observed continuously until the droplet crystallized. The ambient RH was recorded to be  $49.4 \pm 0.2\%$ .

No crystals were found when  $\text{RH} > 60\%$ , for all four types of media. All media crystallized at an RH around 50%. The images of crystals formed in the media are shown in Supplemental Material, Figure 4.1. At  $\sim 50\%$  RH, all media crystallized within 10 min.



**Supplemental Material, Figure 4.1 Crystals of the four media: (A) PBS, (B) PBS+FCS, (C) DMEM, (D) DMEM+FCS. Light microscope, 100X magnified; scale bar = 20  $\mu\text{m}$ .**

## References

1. Molinari, N.-A. M., Ortega-Sanchez, I. R., Messonnier, M. L., Thompson, W. W., Wortley, P. M., Weintraub, E., et al. (2007). The annual impact of seasonal influenza in the US: Measuring disease burden and costs. *Vaccine*, *25*(27), 5086-5096.
2. Viboud, C., Bjrnstad, O. N., Smith, D. L., Simonsen, L., Miller, M. A., & B.T, G. (2006). Synchrony, waves, and spatial hierarchies in the spread of influenza. *Science*, *312*(5772), 447-451.
3. Alonso, W. J., Viboud, C., Simonsen, L., Hirano, E. W., Daufenbach, L. Z., & Miller, M. A. (2007). Seasonality of influenza in Brazil: A traveling wave from the Amazon to the subtropics. *Am. J. Epidemiol.*, *165*(12), 1434-1442.
4. Dosseh, A., Ndiaye, K., Spiegel, A., Sagna, M., & Mathiot, C. (2000). Epidemiological and virological influenza survey in Dakar, Senegal: 1996-1998. *Am. J. Trop. Med. Hyg.*, *62*(5), 639-643.
5. Shek, L. P., & Lee, B. W. (2003). Epidemiology and seasonality of respiratory tract virus infections in the tropics. *Paediatr Respir Rev*, *4*(2), 105-111.
6. Moura, F. E., Perdigao, A. C., & Siqueira, M. M. (2009). Seasonality of influenza in the tropics: A distinct pattern in northeastern Brazil. *Am. J. Trop. Med. Hyg.*, *81*(1), 180-183.
7. Dushoff, J., Plotkin, J. B., Levin, S. A., & Earn, D. J. D. (2004). Dynamical resonance can account for seasonality of influenza epidemics. *Proc. Natl. Acad. Sci. U. S. A.*, *101*(48), 16915-16916.
8. Tamerius, J., Nelson, M., Zhou, S., Viboud, C., Miller, M., & Alonso, W. (2011). Global influenza seasonality: Reconciling patterns across temperate and tropical regions. *Environ. Health Perspect.*, *119*(4), 439-445.
9. Hemmes, J. H., Winkler, K. C., & Kool, S. M. (1960). Virus survival as a seasonal factor in influenza and poliomyelitis. *Nature*, *188*, 430-431.
10. Shaman, J., & Kohn, M. (2009). Absolute humidity modulates influenza survival, transmission, and seasonality. *Proc Natl Acad Sci USA*, *106*(9), 3243-3248.
11. Shaman, J., Pitzer, V. E., Viboud, C., Grenfell, B. T., & Lipsitch, M. (2010). Absolute humidity and the seasonal onset of influenza in the continental United States. *PLoS Biol*, *8*(2), e1000316.
12. Soebiyanto, R. P., Adimi, F., & Kiang, R. K. (2010). Modeling and predicting seasonal influenza transmission in warm regions using climatological parameters. *PLoS ONE*, *5*(3).

13. Tang, J. W., Lai, F. Y. L., Nymadawa, P., Deng, Y. M., Ratnamohan, M., Petric, M., et al. (2010). Comparison of the incidence of influenza in relation to climate factors during 2000-2007 in five countries. *J. Med. Virol.*, 82(11), 1958-1965.
14. Harper, G. J. (1961). Airborne micro-organisms: Survival tests with four viruses. *J Hyg*, 59, 479-486.
15. Schaffer, F. L., Soergel, M. E., & Straube, D. C. (1976). Survival of airborne influenza virus: Effects of propagating host, relative humidity, and composition of spray fluids. *Arch. Virol*, 51(4), 263-273.
16. Shechmeister, I. L. (1950). Studies on the experimental epidemiology of respiratory infections: III. Certain aspects of the behavior of type A influenza virus as an air-borne cloud. *J. Infect. Dis.*, 87(2), 128-132.
17. Yang, W., & Marr, L. C. (2011). Dynamics of airborne influenza A viruses indoors and dependence on humidity. *Plos One*, 6(6), e21481.
18. Nicas, M., Nazaroff, W. W., & Hubbard, A. (2005). Toward understanding the risk of secondary airborne infection: Emission of respirable pathogens. *J Occup Environ Hyg*, 2(3), 143-154.
19. Parienta, D., Morawska, L., Johnson, G. R., Ristovski, Z. D., Hargreaves, M., Mengersen, K., et al. (2011). Theoretical analysis of the motion and evaporation of exhaled respiratory droplets of mixed composition. *J. Aerosol Sci*, 42(1), 1-10.
20. Brown, J. D., Goekjian, G., Poulson, R., Valeika, S., & Stallknecht, D. E. (2009). Avian influenza virus in water: Infectivity is dependent on pH, salinity and temperature. *Vet. Microbiol.*, 136(1-2), 20-26.
21. Effros, R. M., Hoagland, K. W., Bosbous, M., Castillo, D., Foss, B., Dunning, M., et al. (2002). Dilution of respiratory solutes in exhaled condensates. *Am. J. Respir. Crit. Care Med.*, 165(5), 663-669.
22. Raphael, G. D., Jeney, E. V., Baraniuk, J. N., Kim, I., Meredith, S. D., & Kaliner, M. A. (1989). Pathophysiology of rhinitis. Lactoferrin and lysozyme in nasal secretions. *J. Clin. Invest.*, 84(5), 1528-1535.
23. Buckland, F. E., & Tyrrell, D. A. J. (1962). Loss of infectivity on drying various viruses. *Nature*, 195(4846), 1063-1064.
24. Greenspan, L. (1977). Humidity fixed points of binary saturated aqueous solutions. *J. Res. Natl. Bur. Stand. Sec. A*, 81A(1), 89-96.
25. Cohen, M. D., Flagan, R. C., & Seinfeld, J. H. (1987). Studies of concentrated electrolyte solutions using the electrodynamic balance. 1. Water activities for single-electrolyte

- solutions. *J. Phys. Chem.*, 91(17), 4563-4574.
26. Parker, E. R., Dunham, W. B., & MacNeal, W. J. (1944). Resistance of the Melbourne strain of influenza virus to desiccation. *J. Lab. Clin. Med.*, 29, 37-42.
  27. Thomas, Y., Vogel, G., Wunderli, W., Suter, P., Witschi, M., Koch, D., et al. (2008). Survival of influenza virus on banknotes. *Appl. Environ. Microbiol.*, 74(10), 3002-3007.
  28. Tang, I. N., Munkelwitz, H. R., & Wang, N. (1986). Water activity measurements with single suspended droplets: The NaCl-H<sub>2</sub>O and KCl-H<sub>2</sub>O systems. *J. Colloid Interface Sci.*, 114(2), 409-415.
  29. Martin, S. T. (2000). Phase transitions of aqueous atmospheric particles. *Chem. Rev.*, 100(9), 3403-3454.
  30. McGuckin, M. A., Lind é, S. K., Sutton, P., & Florin, T. H. (2011). Mucin dynamics and enteric pathogens. *Nat Rev Micro*, 9(4), 265-278.
  31. Thornton, D. J., Rousseau, K., & McGuckin, M. A. (2008). Structure and function of the polymeric mucins in airways mucus. *Annu. Rev. Physiol.*, 70, 459-486.
  32. Benbough, J. E. (1971). Some factors affecting the survival of airborne viruses. *J. Gen. Virol.*, 10(3), 209-220.
  33. Mikhailov, E., Vlasenko, S., Niessner, R., & Poschl, U. (2004). Interaction of aerosol particles composed of protein and salts with water vapor: Hygroscopic growth and microstructural rearrangement. *Atmos. Chem. Phys.*, 4, 323-350.
  34. Bansil, R., & Turner, B. S. (2006). Mucin structure, aggregation, physiological functions and biomedical applications. *Curr. Opin. Colloid Interface Sci.*, 11(2-3), 164-170.
  35. Engvall, K., Wickman, P., & Norb äck, D. (2005). Sick building syndrome and perceived indoor environment in relation to energy saving by reduced ventilation flow during heating season: A 1 year intervention study in dwellings. *Indoor Air*, 15(2), 120-126.
  36. Yang, W., Elankumaran, S., & Marr, L. C. (2011). Concentrations and size distributions of airborne influenza A viruses measured indoors at a health centre, a day-care centre, and on aeroplanes. *J R Soc Interface*, 8(61), 1176-1184.
  37. Lowen, A. C., Mubareka, S., Steel, J., & Palese, P. (2007). Influenza virus transmission is dependent on relative humidity and temperature. *PLoS Pathog*, 3(10), e151.
  38. Lowen, A. C., Steel, J., Mubareka, S., & Palese, P. (2008). High temperature (30 °C) blocks aerosol but not contact transmission of influenza virus. *J. Virol.*, 82(11), 5650-5652.
  39. Fabian, P., McDevitt, J. J., DeHaan, W. H., Fung, R. O. P., Cowling, B. J., Chan, K. H., et

- al. (2008). Influenza virus in human exhaled breath: An observational study. *PLoS ONE*, 3(7), e2691.
40. Lowen, A., & Palese, P. (2009). Transmission of influenza virus in temperate zones is predominantly by aerosol, in the tropics by contact: A hypothesis. *PLoS Curr*, 1, RRN1002.
41. Duguid, J. P. (1946). The size and the duration of air-carriage of respiratory droplets and droplet-nuclei. *J Hyg*, 44(6), 471-479.
42. De Jong, J. C., Trouwborst, T., & Winkler, K. C. (1973). The mechanism of virus decay in aerosols. In J. F. P. Hers, Winkler KC (Ed.), *Airborne transmission and airborne infection* (pp. 124-130). New York-Toronto: John Wiley & Sons.
43. Trouwborst, T., & De Jong, J. C. (1973). Surface inactivation, an important mechanism of aerosol inactivation for viruses, inactivated at high relative humidity. In J. F. P. Hers, Winkler KC (Ed.), *Airborne transmission and airborne infection* (pp. 137-140). New York-Toronto: John Wiley & Sons.
44. Stewart, M. E., & Terepka, A. R. (1969). Transport functions of the chick chorio-allantoic membrane. I. Normal histology and evidence for active electrolyte transport from the allantoic fluid, *in vivo*. *Exp. Cell Res.*, 58(1), 93-106.
45. McIlvaine, T. C. (1921). A buffer solution for colorimetric comparison. *J. Biol. Chem.*, 49(1), 183-186.
46. Sigma-Aldrich. (2012). Minimum essential medium eagle (MEM). Retrieved 02/09, 2012, from <http://www.sigmaaldrich.com/img/assets/11020/MEM.pdf>

## 5 Conclusions

### 5.1 Summary of results

This dissertation features three main components: measurement of airborne influenza A virus (IAV) in indoor environments, modeling of the dynamics of IAV-laden aerosols, and investigation of the correlation between relative humidity (RH) and viability of IAV in droplets. Through these studies, we have shown how environmental factors affect airborne concentrations of IAV and have identified the possible governing mechanisms for the relationship between RH and influenza transmission. The major results are novel data on the concentrations of IAVs and size distributions of their carrier aerosols in indoor air, new quantitative understanding of how RH affects concentrations of viable IAV in indoor air, and a proposed mechanistic basis for the dependence of influenza transmission on RH.

Measurements of airborne IAV in a health center, a daycare facility, and airplanes show that IAV is present in air at levels sufficient to induce infection. During the 2009-2010 flu season, 50% of the samples collected (8/16) contained IAV with concentrations ranging from 5800 to 37,000 genome copies  $\text{m}^{-3}$  air. On average, 64% of the viruses were found to be associated with particles smaller than 2.5  $\mu\text{m}$ , which can remain airborne for hours and deposit readily in the respiratory system if inhaled. These concentrations correspond to  $35.4 \pm 21.0$  medium tissue culture infective doses (TCID<sub>50</sub>)  $\text{m}^{-3}$  air and inhalation doses of  $30 \pm 18$ ,  $236 \pm 140$ , and  $708 \pm 419$  TCID<sub>50</sub> over 1 h, 8 h, and 24 h, respectively [1]. These doses are adequate to induce infection, compared to the human infectious dose 50% (ID<sub>50</sub>) by aerosols of 0.6-3 TCID<sub>50</sub> [2].

Our models on the size distribution and dynamics of IAV-laden droplets emitted from a cough in typical residential and public settings provide insight into the mechanisms by which humidity might influence aerosol transmission. We have shown that IAV-laden aerosols shrink to 40-50% of their original diameters at RHs between 10% and 90%, due to evaporation. We have further incorporated these results into a mass balance model that considers removal by gravitational settling, ventilation, and virus inactivation. The predicted concentration of infectious IAV in air is 2.4 times higher at 10% RH than at 90% RH after 10 min in a residential setting, and this ratio grows over time. The model indicates that settling is important for removal of large droplets containing large amounts of IAV, while ventilation and inactivation are relatively more important for removal of IAV associated with droplets  $< 5 \mu\text{m}$ . Based on results published in the literature [3], we have shown that the inactivation rate increases linearly with RH over the range of 10-90%, and that at 90% RH, inactivation can

remove up to 28% of IAV in 10 min. These results suggest that humidity could mediate the aerosol transmission of IAV by influencing both droplet size and IAV inactivation. They provide a mechanistic connection between low humidity and influenza's seasonality in temperate regions [4-5]. They also suggest that maintaining a reasonably high indoor RH (~50-60%) and ventilation rate may help reduce the chances of IAV infection.

Our measurements of the viability of IAV in droplets composed of varying levels of salts and proteins indicate that viability is a function of RH and the solute composition of the droplet. At RH levels above the efflorescence RH (ERH) of the droplet, the point at which salts crystallize and all water is lost, viability decreases with decreasing RH in droplets composed of saline solutions with negligible proteins and is minimal at an RH just above the ERH. Depending on the composition of the droplet, the precise ERH could vary, but it typically falls around 50% RH. In droplets supplemented with proteins, viability does not change significantly with RH above the ERH, probably due to protection provided by proteins. In both cases, viability remains high at RHs either close to ~100% or <ERH. Additionally, we have shown that viral decay increases linearly with salt concentration in saline solutions but not when they are supplemented with proteins. These results explain the conflicting findings in the literature [3; 6-8].

We have confirmed the influence of RH on IAV's survival in its natural carrier medium, namely, mucus. Results show that IAV viability in human mucus is relatively well preserved under both low and extremely high RH conditions (below 50% or ~100%, respectively), and decreases by one to two orders of magnitude at medium RH levels (~50-84%) compared to the more extreme conditions. The high viability at both low and saturated RHs may help explain the high incidence of influenza observed in the temperate regions during winter and in the tropics during the rainy season, respectively.

## **5.2 Implications**

Several implications for the inter-host dynamics of IAV and prevention of influenza follow from our study. Through measurement of airborne IAV indoors, we have shown that airborne transmission of IAV is feasible. IAVs are associated with droplets small enough (<2.5  $\mu\text{m}$ ) to remain suspended for hours and to efficiently penetrate the human respiratory tract. The concentrations found indoors even under normal ventilation conditions are high enough to induce infection. Prevention measures thus should take the airborne route into account.

Our model on the fate and transport of IAV-laden droplets shows that concentrations of infectious IAV in indoor air can be at least partially regulated by controlling RH and ventilation. Maintaining high air exchange rates in public spaces with a high risk of infection

(e.g., hospitals and classrooms) and an RH above ~50% can help reduce concentrations of airborne infectious IAV and thus reduce the chances of infection.

Our study on the relationship between RH and viability of IAV in droplets introduces a new paradigm to explain the seasonality of influenza and seemingly conflicting results in the literature. We hypothesize that RH influences the viability of IAV in a respiratory droplet by controlling the extent of evaporation and thus the concentrations of solutes in the droplet, which in turn affect the virus' viability. Three regimes appear to govern the relationship, defined by ambient RH: physiological conditions (~100% RH) with high viability, concentrated conditions (~50% to near 100% RH) with lower viability that depends on solute concentrations in the droplet, and dry conditions (<~50% RH) with high viability. These regimes may be governed by the interplay of the solutes (salts versus proteins) and the virus in response to RH.

Humidity has been found to be associated with the incidence of influenza, yet a consistent account for its differing seasonal patterns in temperate and tropical regions remains lacking. We have shown that IAV viability in mucus droplets is relatively well preserved at RH close to 100% or below 50% and that it decreases dramatically with increasing RH at the range of 50-84%. These results could help explain, at least in part, transmission patterns of influenza. In temperate regions, wintertime heating reduces RH in the indoor environment to low levels, usually <40% [9-10]. At such an RH, vigorous evaporation of respiratory droplets not only helps maintain the viability of IAV emitted from infected hosts but also enables the resulting aerosols to remain aloft longer because of their smaller size and slower settling velocities [11]. Thus, transmission of influenza in temperate regions could be enhanced in winter primarily via the aerosol route. In tropical regions, high temperature may suppress transmission through the aerosol route [5; 12], but during rainy seasons, temperature is relatively lower and RH is close to 100%. Under such conditions, the droplets do not shrink as much, only to 93% of their original diameters at 99% RH, and 76% at 98% RH [11], thus they would be removed more quickly from the air due to gravitational settling. However, submicron aerosols, such as those exhaled in human breath [13], would remain aloft, and thanks to the relatively lower temperature and suitable RH for survival, transmission via these aerosols through the aerosol route might still be effective. In addition, the contact transmission route may be enhanced because it is insensitive to temperature [4; 12] and IAV is well preserved at ~100% RH, as shown in our study.

### **5.3 Recommendations for future study**

#### **5.3.1 Expand the detection of airborne IAV in more inter-host environments**

Due to challenges in detecting airborne viruses at low levels, our survey of IAV in indoor air was limited to places where concentrations were more likely to be elevated, either because of the presence of infected individuals (e.g., hospitals and day care centers) or a high density of people (e.g., airplanes). As measurement methods with better sensitivity become more readily available in the future, the prevalence of IAV should be investigated in places such as schools, offices, and residences, to study the possibility of airborne transmission in these indoor environments. The prevalence of IAV could also be studied in outdoor air to investigate the potential for long-range transmission [14].

### **5.3.2 Simulate the dynamics of airborne IAV with multiple modeling techniques**

More sophisticated modeling techniques could be incorporated into the study of transmission dynamics. Computational fluid dynamics (CFD) combined with the biological characteristics of IAV can be utilized to better simulate the fate and transport of IAV emitted from infected individuals in indoor environments and to investigate the source and spread of the disease [15]. Stochastic theories such as the Markov chain model can be applied to study the risk of infection [16].

### **5.3.3 Explore how RH affects IAV viability at the molecular level**

Chapter 4 presents the relationship between IAV viability and RH in droplets of both model media and human mucus, and we propose a mechanism to explain this relationship based on the thermodynamics of the droplet and the potential interplay between solutes and the virus. However, the study does not address how salts affect IAV viability at a molecular level, nor does it explain how the presence of proteins alters the relationship. In addition, the relationship in mucus differs slightly from that observed in model media. Given the complex composition and unique nature of mucus, mechanisms governing the relationship in mucus might differ from those in model media.

Previous studies indicate that different viruses respond differently to changes in RH. For instance, poliovirus favors higher RH, in contrast to IAV, which favors lower RH [6]. Hence, the relationship between a virus and RH is probably a combined function of properties of the virus (e.g., surface proteins on the envelope and type of nucleic acid) and interactions among the virus, solutes, and water molecules [17-18]. A more in-depth investigation is warranted.

Possible mechanisms may include but are not limited to (1) changes in mucus structure following evaporation, resulting in protection or inactivation of IAV to varying degrees, (2) enrichment of proteins present in mucus at the virus envelope, providing protection to the virus, (3) salting-out of proteins, causing the virus to precipitate from a

concentrated salt solution, or (4) a combination of these mechanisms. These hypotheses could be tested by studying the response of IAV viability to changes in RH in media chosen to demonstrate the effects of different solutes or the changes in the medium's structure following evaporation. Visualization techniques (e.g., scanning electronic microscopy and fluorescence microscopy) could be applied to observe the structure of dried mucus and the distribution of IAV and components such as proteins with the assistance of proper staining of IAV and proteins. Studies on the loss in function of the virus' envelope (including the hemagglutinin proteins and the lipid bilayer) and the viral genome after exposure to varying RHs could confirm whether damage to the virus occurs.

#### **5.3.4 Study the airborne transmission route for IAV holistically**

The efficiency of airborne transmission is affected by a combination of the characteristics of the virus, properties of the virus carrier aerosol (e.g., its size and composition), the environment, and the host immune response. These factors are interdependent. Therefore, a complete understanding of the airborne transmission route will require investigation into all these factors.

The size of IAV carrier aerosol not only determines how long it can remain suspended, but also where in the respiratory system it would deposit. It can be shown that the most efficient deposition in the head airways (87%) is achieved by aerosols 6.1  $\mu\text{m}$  in diameter, while the most efficient deposition in the alveolar region (13%) is achieved by aerosols 1.4  $\mu\text{m}$  in diameter [19]. In turn, where the aerosol deposits within the respiratory system could influence whether and how effectively the virus can initiate an infection. On the one hand, the target cells for IAV are distributed heterogeneously in different regions within the human respiratory tract [20]. On the other, the airway clearance mechanisms differ in different regions within the respiratory system [21]. A successful infection is determined by both the availability of susceptible and permissible cells (i.e., cells that the virus can enter and replicate in) and the host's immune response. Yet it is still unclear which part of the respiratory tract is the most susceptible target site for influenza infection. Investigation with size-fractionized aerosols may provide clues to questions such as "which size is the most efficient in initiating an infection?" and "which site in the respiratory system is most susceptible to infection?"

In addition, it is possible that the site of infection could affect the efficiency of airborne transmission. Infection in different regions in the respiratory system could result in the generation of virus-laden aerosols of different sizes and compositions, due to differences in geometry and physiological conditions in various regions within the respiratory system (e.g., mucus secretion, cilia movement, presence of immune cells, airway clearance mechanisms).

The aerosols generated thereby could bear different transmission efficiencies, which may affect the next transmission cycle. Hence, the transmissibility of IAV and the site of infection from where the aerosols are generated may be interdependent. To provide insight into this potential correlation, a systematic investigation is warranted. It should take the virus-laden aerosols' size distribution, infectivity, and the corresponding site of emission into account simultaneously. Animal models such as ferrets could be used for such research.

Finally, environmental factors such as humidity and temperature may affect both the virus and the host. For instance, humidity has been shown in this study to affect both the size transformation of the carrier aerosol and the viability of IAV in it. It could also play a role on the host's susceptibility to infection [5]. Assessment of the effect of environmental factors should thus take both the pathogen and the host into account.

## References

1. U.S. EPA. (1994). *Methods for derivation of inhalation reference concentrations and application of inhalation dosimetry*.
2. Alford, R. H., Kasel, J. A., Gerone, P. J., & Knight, V. (1966). Human influenza resulting from aerosol inhalation. *Proc. Soc. Exp. Biol. Med.*, 122(3), 800-804.
3. Harper, G. J. (1961). Airborne micro-organisms: Survival tests with four viruses. *J Hyg*, 59, 479-486.
4. Lowen, A., & Palese, P. (2009). Transmission of influenza virus in temperate zones is predominantly by aerosol, in the tropics by contact: A hypothesis. *PLoS Curr*, 1, RRN1002.
5. Lowen, A. C., Mubareka, S., Steel, J., & Palese, P. (2007). Influenza virus transmission is dependent on relative humidity and temperature. *PLoS Pathog*, 3(10), e151.
6. Hemmes, J. H., Winkler, K. C., & Kool, S. M. (1960). Virus survival as a seasonal factor in influenza and poliomyelitis. *Nature*, 188, 430-431.
7. Schaffer, F. L., Soergel, M. E., & Straube, D. C. (1976). Survival of airborne influenza virus: Effects of propagating host, relative humidity, and composition of spray fluids. *Arch. Virol*, 51(4), 263-273.
8. Shechmeister, I. L. (1950). Studies on the experimental epidemiology of respiratory infections: III. Certain aspects of the behavior of type A influenza virus as an air-borne cloud. *J. Infect. Dis.*, 87(2), 128-132.
9. Engvall, K., Wickman, P., & Norbäck, D. (2005). Sick building syndrome and perceived indoor environment in relation to energy saving by reduced ventilation flow during heating season: A 1 year intervention study in dwellings. *Indoor Air*, 15(2), 120-126.
10. Yang, W., Elankumaran, S., & Marr, L. C. (2011). Concentrations and size distributions of airborne influenza A viruses measured indoors at a health centre, a day-care centre, and on aeroplanes. *J R Soc Interface*, 8(61), 1176-1184.
11. Yang, W., & Marr, L. C. (2011). Dynamics of airborne influenza A viruses indoors and dependence on humidity. *PLoS ONE*, 6(6), e21481.
12. Lowen, A. C., Steel, J., Mubareka, S., & Palese, P. (2008). High temperature (30 °C) blocks aerosol but not contact transmission of influenza virus. *J. Virol.*, 82(11), 5650-5652.
13. Fabian, P., McDevitt, J. J., DeHaan, W. H., Fung, R. O. P., Cowling, B. J., Chan, K. H., et al. (2008). Influenza virus in human exhaled breath: An observational study. *PLoS ONE*, 3(7), e2691.

14. Chen, P.-S., Tsai, F. T., Lin, C. K., Yang, C.-Y., Chan, C.-C., Young, C.-Y., et al. (2010). Ambient influenza and avian influenza virus during dust storm days and background days. *Environ. Health Perspect.*, 118(9).
15. Yu, I. T. S., Li, Y., Wong, T. W., Tam, W., Chan, A. T., Lee, J. H. W., et al. (2004). Evidence of airborne transmission of the severe acute respiratory syndrome virus. *N. Engl. J. Med.*, 350(17), 1731-1739.
16. Nicas, M., & Sun, G. (2006). An integrated model of infection risk in a health-care environment. *Risk Anal.*, 26(4), 1085-1096.
17. De Jong, J. C., Trouwborst, T., & Winkler, K. C. (1973). The mechanism of virus decay in aerosols. In J. F. P. Hers, Winkler KC (Ed.), *Airborne transmission and airborne infection* (pp. 124-130). New York-Toronto: John Wiley & Sons.
18. Trouwborst, T., & De Jong, J. C. (1973). Surface inactivation, an important mechanism of aerosol inactivation for viruses, inactivated at high relative humidity. In J. F. P. Hers, Winkler KC (Ed.), *Airborne transmission and airborne infection* (pp. 137-140). New York-Toronto: John Wiley & Sons.
19. Hinds, W. C. (1999). *Aerosol technology*. New York: John Wiley and Sons, Inc.
20. Nicholls, J., Bourne, A., Chen, H., Guan, Y., & Peiris, J. M. (2007). Sialic acid receptor detection in the human respiratory tract: Evidence for widespread distribution of potential binding sites for human and avian influenza viruses. *Respiratory Research*, 8(1), 73.
21. Oberdorster, G. (1993). Lung dosimetry - pulmonary clearance of inhaled particles. *Aerosol Sci. Technol.*, 18(3), 279-289.